Check for updates

ADVANCED MATERIALS TECHNOLOGIES
www.advmattechnol.de

Wireless Power and Data Transfer Technologies for Flexible Bionic and Bioelectronic Interfaces: Materials and Applications

Massimo Mariello and Christopher M. Proctor*

The next-generation bionics and, more specifically, wearable and implantable bioelectronics require wireless, battery-free, long-term operation and seamless bio-integration. Design considerations, materials choice, and implementation of efficient architectures have become crucial for the fabrication and deployment of wireless devices, especially if they are flexible or soft. Wireless power and data transfer represent key elements for the development of robust, efficient, and reliable systems for health monitoring, advanced disease diagnosis and treatment, personalized medicine. Here, the recent advances in materials and technologies used for wireless energy sourcing and telemetry in bio-integrated flexible bionic and bioelectronic systems are reviewed. The study tackles different challenges related to mechanical compliance, low thickness, small footprint, biocompatibility, biodegradability, and in vivo implementation. The work also delves into the main figures of merit that are mostly adopted to quantify the wireless power/data transfer performances. Lastly, the pivotal applications of wearable and implantable wireless bionics/bioelectronics are summarized, such as electrical stimulation/recording, real-time monitoring of physiological parameters, light delivery trough optical interfaces, electromechanical stimulation via ultrasounds, highlighting their potential for future implementation and the challenges related to their commercialization.

1. Introduction

The integration of electronics with biological systems has catalyzed profound advancements in healthcare and technology, revolutionizing the landscape of medical diagnostics, therapeutics, and human-machine interfaces.[1–3] Flexible bionics, wearable devices, and implantable bioelectronics represent key pillars of this burgeoning field. From prosthetic limbs with biomimetic motion capabilities to flexible neural interfaces enabling precise neurostimulation, these technologies hold promise for restoring lost functionality and augmenting human abilities. Wearable devices, whether integrated into clothing, adhered to the skin, or worn as accessories, have emerged as indispensable tools for health monitoring, fitness tracking, and real-time feedback in everyday activities. Meanwhile, implantable bioelectronics, by directly interfacing with neural circuits or physiological pathways, offer targeted therapies for neurological disorders, chronic pain management, monitoring of biological processes,[4–7] with unparalleled specificity and efficacy, ease of use, and portability.[8]

However, the clinical translation of all these devices has long been hindered by the limitations of traditional tethered systems, including infection risks, immune responses, tissue damage, and restricted mobility. Traditional wired systems, composed of physical tethers such as electrical wiring,[9] fluidic channels,[10–12] or optical-fiber cables,[13–18] have been commonly used in medical systems due to their simplicity and functional maturity, besides their accessibility and commercial availability. However, they pose challenges related to mechanical inconsistency with soft living tissue,[19–24] restricted operational modes, and impaired anatomical versatility,[25,26] in particular when interfacing with mobile body areas like the spinal cord, peripheral nerves, joints, etc., carrying risks of infections, venous obstructions, and tissue perforation.[27–31] The necessity for fixation to stable anatomical structures or specialized orthoses poses inherent limitations, compounded by micrometer-scale motions induced by tether forces during natural movements and cable manipulations. These dynamics can induce tension and stress, and thus tissue damage and artifacts, diminishing chronic stability and signal fidelity. Moreover, advanced interfaces demanding multichannel operations may prompt unrestrained animals to attempt cable removal or disconnection, further complicating experimental protocols.[32–35]

M. Mariello, C. M. Proctor
Institute of Biomedical Engineering (IBME)
Department of Engineering Science
University of Oxford
Old Road Campus, Headington, Oxford OX3 7DQ, UK
E-mail: massimo.mariello@eng.ox.ac.uk

The ORCID identification number(s) for the author(s) of this article can be found under https://doi.org/10.1002/admt.202400797

© 2024 The Author(s). Advanced Materials Technologies published by Wiley-VCH GmbH. This is an open access article under the terms of the Creative Commons Attribution License, which permits use, distribution and reproduction in any medium, provided the original work is properly cited.

DOI: 10.1002/admt.202400797



Figure 1. Bio-integrated wireless power and data transfer technologies for flexible bionics, wearable and implantable bioelectronics. Four main categories can be distinguished: wireless extrinsic power transfer, wireless intrinsic power transfer, wireless data transfer, and wireless data interrogation. These are described in detail in Sections 2–4. The images are representative examples of devices used for these categories (original production of the authors).

Recent advancements in soft materials have shown promise in addressing these challenges by allowing better conformity with tissue, reducing inflammatory responses,[36–38] and mitigating motion artifacts.[39] The advent and use of bioresorbable materials[40–43] is also particularly relevant to eliminating the need for surgical removal procedures and mitigating infection risks.

In parallel, researchers have embarked on a quest to develop wireless power and data transfer technologies tailored to the unique requirements of flexible bionics and bioelectronics. By harnessing principles of electromagnetic induction, resonant coupling, or ultrasonic transmission, these wireless solutions eliminate the need for physical connections and offer safe, efficient, and reliable means of energizing and communicating with electronic systems embedded within or in close proximity to biological tissues. Therefore, they provide more robust, enduring, and high-fidelity interfaces, fostering experimental reproducibility, enhancing mobility, comfort, and functionality, reducing subject and environmental interference,[44] and minimizing requirements for supporting equipment and interface hardware.[45–50] Moreover, they enable greater freedom of movement and flexibility in device placement, allowing for optimal positioning without constraint and intimate integration with curved or irregular anatomical surfaces. In addition to powering devices, wireless technologies facilitate bidirectional communication between implants and external control systems, enabling real-time monitoring, adjustment, and data logging. By establishing robust and low-latency data links, these wireless interfaces enable seamless interaction between the biological and electronic components of hybrid systems, fostering closed-loop control and adaptive functionality. Furthermore, by integrating wireless power and data transfer capabilities into these flexible substrates, researchers have unlocked new possibilities for unobtrusive and long-term integration of electronic devices with the human body.

In this review, we aim to provide an in-depth exploration of the state-of-the-art in wireless powering and telemetry for flexible bionics and wearable/implantable bioelectronics. We delve into the underlying principles of wireless energy transmission and harvesting (**Figure 1**), examine the design considerations for integrating wireless interfaces into bioelectronic systems, provide useful figures of merit, and discuss the latest advancements and emerging applications in the field. Through a critical analysis of current research trends and future prospects, we seek to elucidate the transformative potential of wireless technologies to lay the groundwork for future advances in healthcare, biotechnology, and human augmentation.

© 2024 The Author(s). Advanced Materials Technologies published by Wiley-VCH GmbH

2365709x, 0, Downloaded from https://onlinelibrary.wiley.com/doi/10.1002/admt.202400797 by University Of Oxford, Wiley Online Library on [19/11/2024]. See the Terms and Conditions (https://onlinelibrary.wiley.com/terms-and-conditions) on Wiley Online Library for rules of use; OA articles are governed by the applicable Creative Commons License

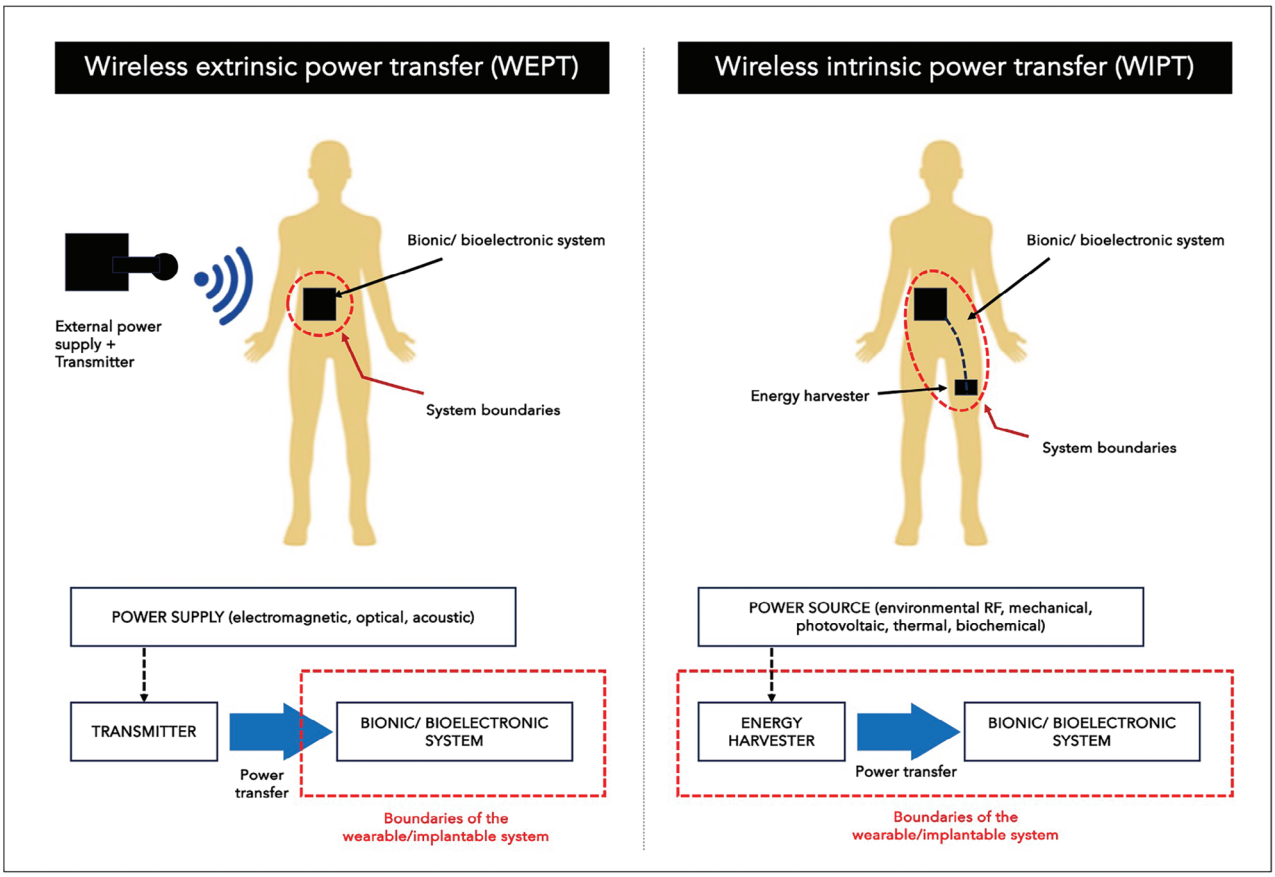


Figure 2. Difference between wireless extrinsic power transfer (WEPT) and wireless intrinsic power transfer (WIPT).

2. Wireless Powering

If not externally powered via cables and wires, bionic devices and bioelectronic implants generally receive their energy supply from integrated electrochemical power sources (batteries) which can satisfy the power requirements of sophisticated devices.[44,51] However, batteries present several drawbacks, including a limited lifetime, the need of frequent replacements and reinstallations, a non-negligible environmental impact, and a remarkable hindrance. In fact, their sizes are usually larger than 2–3 cm^3, occupying a large portion of the device volume and weight.[52,53] Tethered and battery-powered approaches thus present clear limitations to the potential utility of bionics and bioelectronics. Wireless powering (or wireless power transfer, WPT) provides an efficient solution to transfer energy to the system without any physical connection from the outer environment but only through i) a transmitter connected to an external power source or ii) an integrated energy scavenger/harvester within the system itself (**Figure 2**). The first approach is known as wireless extrinsic power transfer (WEPT), or remote powering: a transmitter serves as a contactless bridge between the device and the external power supply and it can be based on different working principles, such as radio-frequency (RF) energy transfer[54–56] (capacitive coupling, inductive coupling), ultrasound energy transfer,[57,58] optical/photonic energy transfer.[59,60] This strategy offers a wide range of available power but it relies on external systems that can provide the requested energy (signal generator, sourcemeters, AC/DC power generators, etc.) and depends on the specific power-consumption requirements[61,62] and device location,[63,64] especially for implantable devices. The dependence on an external source can also be an advantage since it can provide a reliable and constant power supply, decoupling the device operation from the subject (patient, animal, etc.) and guaranteeing a robust operation for multimodal physiological recording,[65,66] optofluidic neuromodulation[51,67,68] and close-loop-system operations.[69–72]

The second approach is called wireless intrinsic power transfer (WIPT) or self-powering: it is based on the integration of an energy harvester and consists of scavenging energy directly from the environment or the human/animal body according to different available mechanisms (piezoelectric, triboelectric, electromagnetic, electrostatic, etc.). For instance, harvesters can extract kinetic energy from heartbeat,[73,74] lung, diaphragm[75–78] or visceral motions,[79] chemical energy from blood sugar or other biofluids,[80–83] thermal energy from body heat.[84,85] Differently from WEPT, WIPT is independent from external components (i.e., power supplies that do not belong to the system) and offers wider design tunability.[86] However, it provides lower output power levels compared to WEPT and the associated energy sources are often intermittent (not continuously constant), compromising the overall device operation. **Table 1** summarizes advantages and drawbacks of all the techniques of wireless powering described hereafter.

© 2024 The Author(s). Advanced Materials Technologies published by Wiley-VCH GmbH

2365709x, 0, Downloaded from https://onlinelibrary.wiley.com/doi/10.1002/admt.202400797 by University Of Oxford, Wiley Online Library on [19/11/2024]. See the Terms and Conditions (https://onlinelibrary.wiley.com/terms-and-conditions) on Wiley Online Library for rules of use; OA articles are governed by the applicable Creative Commons License

Table 1. Techniques and operation modes for wireless powering with indication of the advantages, limitations, operation conditions and miniaturization scale.

Technique	Type	Operating frequencies	Operation distance (from energy source)	Efficiency/Power density/Data transfer rate	Advantages	Disadvantages	Refs.
Wireless powering							
Wireless extrinsic power transfer (WEPT)							
Far-field RF power transfer (FFPT)	EM-R	420 MHz – 2.5 GHz	cm – m	Medium/n/a	• Long-range transmission capabilities • Wide range of usable frequencies	• Constraints on antenna shape/size • Sensitivity to tissue properties • Susceptible to interference	[63,99,130]
Near-field magnetic resonant coupling (NFMRC)	EM-NR	100 kHz – 200 MHz	mm – cm	High/n/a	• Higher efficiency than FFPT • Less susceptible to interference and to coil misalignments	• Constraints on coil size • Device overheating, tissue damage	[121,133]
Inductive coupling power transfer (ICPT)	EM-NR	2 kHz – 460 MHz	mm – cm	Medium-high/n/a	• Higher efficiency than FFPT • Suitable for very short range • Simple circuitry and low cost	• Sensitivity to coil misalignment • Device overheating, tissue damage	[117,118,120]
Capacitive coupling power transfer (CCPT)	EM-NR	100 kHz – 10 MHz	mm – cm	Medium/n/a	• Lower SAR than ICPT • Simple circuitry and low cost	• Susceptible to electrical interference • Efficiency decreases with distance (limited to very short range)	[146–148,151]
Optic/Photonic power transfer (OPT)	NEM-O	350 THz – 750 THz	>m	Medium/n/a	• Highly directional • Immune to electromagnetic interference	• Tissue opacity, scattering • Thermal effects • Requires line of sight	[202,265]
Ultrasound power transfer (UPT)	NEM-A	20 kHz – ≈2 GHz	cm	Medium-low/n/a	• Potential for high efficiency • Safer for tissues than FFPT, ICPT, CCPT	• Tissue ultrasound absorption • Sensitivity to receiver misalignments	[57,158,259]

(*Continued*)

© 2024 The Author(s). Advanced Materials Technologies published by Wiley-VCH GmbH

2365709x, 0, Downloaded from https://onlinelibrary.wiley.com/doi/10.1002/admt.202400797 by University Of Oxford, Wiley Online Library on [19/11/2024]. See the Terms and Conditions (https://onlinelibrary.wiley.com/terms-and-conditions) on Wiley Online Library for rules of use; OA articles are governed by the applicable Creative Commons License

Table 1. (Continued)

Technique	Type	Operating frequencies	Operation distance (from energy source)	Efficiency/Power density/Data transfer rate	Advantages	Disadvantages	Refs.
Wireless intrinsic power transfer (WIPT)							
RF energy harvesting (RF-WIPT)	EM	100 kHz – 10 GHz	cm – m	Medium/ 0.01–0.1 μW cm^{-2}	• Does not require light or body motion and continuously available	• Low output power • Distance dependence	[266–268]
Mechanical (kinetic) energy harvesting (KE-WIPT)	NEM-EMc EM	Hz (motions)	mm – cm	High/ 0.25–29.2 mW cm^{-2}	• Does not require RF waves or light	• Intermittency • Require body activity	[76,78,162,269]
Photovoltaic energy harvesting (PE-WIPT)	NEM-O	n/a	>m	>Medium-high/ 35 μW cm^{-2}	• Lightweight and flexible (perovskites)	• Require light • Poor stability • Toxicity for perovskite materials	[99,203,204,207]
Thermal energy harvesting (TE-WIPT)	NEM-T	n/a	mm – cm	Medium/ ≈100 μW cm^{-2}	• Cost-effectiveness • Does not require light or body motion	• Low power source	[84,210–212,216,219,220]
Biochemical energy harvesting (BE-WIPT)	NEM-Bc	n/a	mm – cm	High/3.7 mW cm^{-2}	• Does not require RF waves, light or body activity	• Challenging fabrication • The analyte concentration influences the power density	[80,83,221,222]
Wireless data communication (telemetry)							
Wireless data transfer (WDT)							
Bluetooth-Low-Energy (BLE)	EM-R	2.4 GHz (ISM Band)	cm – m (up to 30 m)	High/125 kbps, 500 kbps, 1–2 Mbps	• Low power consumption • Low cost • Wide range of supported devices • Good data transfer rates	• Limited range (up to 100 m) • Susceptible to interference from other wireless devices • Security concerns	[270,271]

(*Continued*)

© 2024 The Author(s). Advanced Materials Technologies published by Wiley-VCH GmbH

2365709x, 0, Downloaded from https://onlinelibrary.wiley.com/doi/10.1002/admt.202400797 by University Of Oxford, Wiley Online Library on [19/11/2024]. See the Terms and Conditions (https://onlinelibrary.wiley.com/terms-and-conditions) on Wiley Online Library for rules of use; OA articles are governed by the applicable Creative Commons License

Table 1. (Continued)

Technique	Type	Operating frequencies	Operation distance (from energy source)	Efficiency/Power density/Data transfer rate	Advantages	Disadvantages	Refs.
Wi-Fi	EM-R	2.4 GHz, 5–6 GHz	m	High/600 Mbps, 1.3 Gbps	• High data rates • Wide availability and compatibility with many existing devices and infrastructures • Established standards ensure reliability and interoperability.	• High power consumption, limitation for battery-operated bioelectronics • Prone to interference from other electronic devices, especially in the 2.4 GHz band. • Penetration limits: higher frequencies (e.g., 5 GHz) have lower penetration through biological tissues and obstacles.	[272,273]
ZigBee	EM-R	868 MHz, 915 MHz, 2.4 GHz	m	High/250 kbps	• Low power consumption • Supports mesh networks, enhancing reliability and range through multiple hops • Can handle a large number of devices in a network • Resilient to interference due to its mesh network topology	• Low data rates: not suitable for applications requiring high data throughput • Shorter range compared to Wi-Fi, especially in non-line-of-sight conditions • Less widespread than Wi-Fi, potentially requiring additional infrastructure or gateways.	[272,274,275]

(*Continued*)

© 2024 The Author(s). Advanced Materials Technologies published by Wiley-VCH GmbH

2365709x, 0, Downloaded from https://onlinelibrary.wiley.com/doi/10.1002/admt.202400797 by University Of Oxford, Wiley Online Library on [19/11/2024]. See the Terms and Conditions (https://onlinelibrary.wiley.com/terms-and-conditions) on Wiley Online Library for rules of use; OA articles are governed by the applicable Creative Commons License

Table 1. (Continued)

Technique	Type	Operating frequencies	Operation distance (from energy source)	Efficiency/Power density/Data transfer rate	Advantages	Disadvantages	Refs.
Near-field communication (NFC)	EM-NR	13.56 MHz	cm (up to 10 cm)	Medium/424 kbps	• Very short range (up to 10 cm), providing high security • Simple to use (touch-based) • Low power consumption • Less tissue absorption than Bluetooth	• Very short-range limits applications • Low data transfer rates	[123,238]
RF Identification (RFID)	EM-R	LF: 125–134 kHz HF: 13.56 MHz UHF: 860–960 MHz	cm – m (up to 3 m)	Medium-high/ 0.1–424 kbps	• No line-of-sight requirement • Can operate over longer distances compared to NFC • Cost-effective for mass deployment	• Limited data transfer rates • Susceptible to interference • Security concerns	[101,240,241,276]
Infrared radiation (IR)	NEM-O	300 GHz – 430 THz	cm – m (up to 5 m)	Medium/1–100 Mbps	• No interference with RF devices • High security due to line-of-sight requirement	• Limited range (typically up to a few meters) • Line-of-sight requirement • Limited data transfer rates	[277,278]
Ultrasound	NEM-A	20 kHz – ≈2 GHz	cm	Medium/1–10 Mbps	• Works well in noisy environments • High accuracy in distance measurement • Low power consumption	• Limited range (typically up to a few meters) • Susceptible to interference from background noise • Relatively complex implementation	[259]
Wireless data interrogation (WDI)							
LC systems	EM-R/NR	Various, depending on the circuit designs	cm	Medium-high	• High sensitivity and selectivity • Low power consumption • Relatively simple implementation • Cost-effective	• Limited range • Susceptible to interference from environmental factors • Limited data transfer rates	[248,250]

(*Continued*)

© 2024 The Author(s). Advanced Materials Technologies published by Wiley-VCH GmbH

2365709x, 0, Downloaded from https://onlinelibrary.wiley.com/doi/10.1002/admt.202400797 by University Of Oxford, Wiley Online Library on [19/11/2024]. See the Terms and Conditions (https://onlinelibrary.wiley.com/terms-and-conditions) on Wiley Online Library for rules of use; OA articles are governed by the applicable Creative Commons License

Table 1. (Continued)

Technique	Type	Operating frequencies	Operation distance (from energy source)	Efficiency/Power density/Data transfer rate	Advantages	Disadvantages	Refs.
Ultrasound-based systems	NEM-A	Various, depending on the system designs	cm	Medium	• High accuracy in distance measurement • Works well in noisy environments • Low power consumption	• Limited range • Susceptible to interference from background noise • Complex implementation	[254,259,264]
Active responders	EM	Various, depending on the circuit designs	cm	Medium-high	• Can actively respond to interrogation signals • Higher data transfer rates compared to passive systems • Suitable for real-time tracking applications	• Higher power consumption compared to passive systems • Costlier due to additional components and complexity • Limited lifespan of active devices	[94]

Nomenclature: EM: electromagnetic; R: radiative; NR: non-radiative; NEM: non-electromagnetic; NEM-O: non-electromagnetic, optical; NEM-A: non-electromagnetic, acoustic; NEM-T: non-electromagnetic, thermal; NEM-Bc: non-electromagnetic, biochemical; NEM-EMc: non-electromagnetic, electromechanical. LF: low-frequency; HF: high-frequency; UHF: ultra-high frequency.

© 2024 The Author(s). Advanced Materials Technologies published by Wiley-VCH GmbH

2365709x, 0, Downloaded from https://onlinelibrary.wiley.com/doi/10.1002/admt.202400797 by University Of Oxford, Wiley Online Library on [19/11/2024]. See the Terms and Conditions (https://onlinelibrary.wiley.com/terms-and-conditions) on Wiley Online Library for rules of use; OA articles are governed by the applicable Creative Commons License

2.1. Wireless Extrinsic Power Transfer (WEPT)

WEPT is the most established method of wireless powering that can replace chemical batteries. It has been applied to medical devices but also to RFID tags for tracking items or food products, as well as to cellphone charging, space satellite communication, etc. Significant amounts of power (up to ≈500 mW)[87] can be reliably transmitted, with versatile design and deployment options. WEPT can be classified into different categories based on the specific working mechanism adopted to transfer electrical energy without any contact or intermediate media (wires, cables, etc.): (i) far-field RF power transfer (FFPT),[88] (ii) near-field (NF) magnetic resonant coupling (NFMRC)[54] and inductive coupling power transfer (ICPT),[89] (iv) optic/photonic radiation,[59] (v) ultrasonic stimulation.[58] These strategies differ in terms of proximity to the device location,[56,90,91] output transferrable power and in-depth resolution: a comparison of these techniques is illustrated in **Figure** 3A,B. It should be noted that due to the lack of a single universal metric for properly comparing different WEPT technologies based on different mechanisms (as well as for WIPT and WDC), it is extremely difficult and not straightforward to make a reasonable comparison in an attempt to understand their potential for operating in bionic and bioelectronic flexible systems. To sum up this complexity, we proposed radar charts where desired performance of key properties for these technologies are reported at the extremity of each axis. Polygons covering larger surfaces should in principle represent the most appropriate technology to be used in bionic and bioelectronic systems. They are plotted taking into account our estimation of where the current limits for each feature lie, therefore each polygon represents our estimated limit for the set of chosen criteria and not the space that any particular device would occupy. Hence, we expect any epitome of a wireless devices based on one specific technology to fall within the corresponding polygon. We also highlight that these charts incorporate criteria that are difficult to objectively estimate, very heterogeneous and different for each technology. For instance, collecting scientific evidences for quantitatively evaluating the lifetime and reliability of each mechanism remains presently complex. Therefore, the criteria reported have been qualitatively ranked based on authors' estimation after having comprehensively studied the available literature, including previous review works,[63,92–94] and it represents a dynamic picture of the current development status.

2.1.1. Far-Field RF Power Transfer (FFPT)

RF radiation falls in the frequency range of 3 kHz – 300 GHz, covering also the microwave spectrum (300 MHz – 300 GHz).[95] This WEPT technique relies on the emission of RF radiation (frequency 420 MHz–2.5 GHz, wavelength: 0.1–1 m) by a transmission antenna (transmitter), the reception of the same radiation by a harvesting antenna (receiver) and its rectification into direct current (AC/DC conversion)[96] (Figure 3C). FFPT has potential for applications in long-distance (≈ meters) transmission and in implantable optoelectronic systems for modulating spinal cord and peripheral nerves. In particular, far-field (FF) electromagnetic transmission is exploited at distances $d \geq d_F = 2D^2/\lambda$, where D is the largest antenna dimension, λ is the wavelength and d_F is the Fraunhofer distance (Fraunhofer region).[97] In this region, the amplitudes of the electric and magnetic fields fall off as $1/r$ (r distance from the antenna). Specialized antenna designs enable efficient power delivery over short distances in laboratory-scale setups and the use of stretchable electronics facilitates the creation of compact and lightweight devices capable of accommodating anatomical variations.[88] Although advanced antenna designs allow for multimodal operation, motion tracking and increased harvesting efficiency,[55,88] FFPT suffers from a heavy dependence on the angle between transmission and receiving antennas, requiring careful antenna design and deployment strategies. In fact, there is a trade-off between angular acceptance and antenna gain.[98–100] Additionally, environmental obstructions, especially conductive and high-refractive-index dielectric materials, can interfere with high-frequency (0.5-2.5 GHz) RF transmission, reflecting RF waves. The interference between reflected and incident RF waves is detrimental, leading to spatial variations in power density and potential hotspots or dead zones.[101] To address these challenges, one strategy involves using an RF cavity to resonate electromagnetic fields within the animal's body, though this may result in high specific absorption rates (SARs).[56,102] SAR levels can reach up to 6.2 W kg^{-1} due to power absorption by biological tissues, potentially causing heating that could affect or be toxic for biological activities.[103–105] This absorption effect also limits the amount of power that can be safely delivered to fully implanted devices. FFPT typically operates at higher power levels compared to other technologies (e.g. near-field wireless power transfer): the power requirements for FFPT can vary depending on factors such as the distance between the transmitter and receiver, the efficiency of the antenna system, and the desired power output at the receiver. In general, FFPT systems can deliver power ranging from microwatts (μW) to watts (W), with some advanced systems capable of delivering even higher power levels. The current requirements depend on the power output and voltage levels required by the receiving device: typically, the current levels can range from milliamps (mA) to amps (A), with higher currents associated with higher power output requirements. The efficiency of the FFPT system, including any rectification circuitry and voltage regulation components, also influences the current drawn by the receiving device. Overall, FFPT offers the advantage of longer-range power transmission compared to near-field technologies, making them suitable for applications such as wireless charging of electronic devices, powering sensors in remote locations and enabling wireless communication networks. However, optimizing the power and current requirements for specific applications is essential to ensure efficient power transfer and reliable operation of the receiving devices. A similar configuration for FFPT is also used for RF energy harvesting, i.e., to passive capture environmental RF waves to energize low-power electronic devices (see section 2.2).[106–109]

2.1.2. Near-Field Magnetic Resonant Coupling (NFMRC)

Near-field magnetic resonant coupling, initially pioneered by Nikola Tesla,[110,111] utilizes non-radiative electromagnetic energy within a short range from the transmitter, relying on induc-

© 2024 The Author(s). Advanced Materials Technologies published by Wiley-VCH GmbH

2365709x, 0, Downloaded from https://onlinelibrary.wiley.com/doi/10.1002/admt.202400797 by University Of Oxford, Wiley Online Library on [19/11/2024]. See the Terms and Conditions (https://onlinelibrary.wiley.com/terms-and-conditions) on Wiley Online Library for rules of use; OA articles are governed by the applicable Creative Commons License

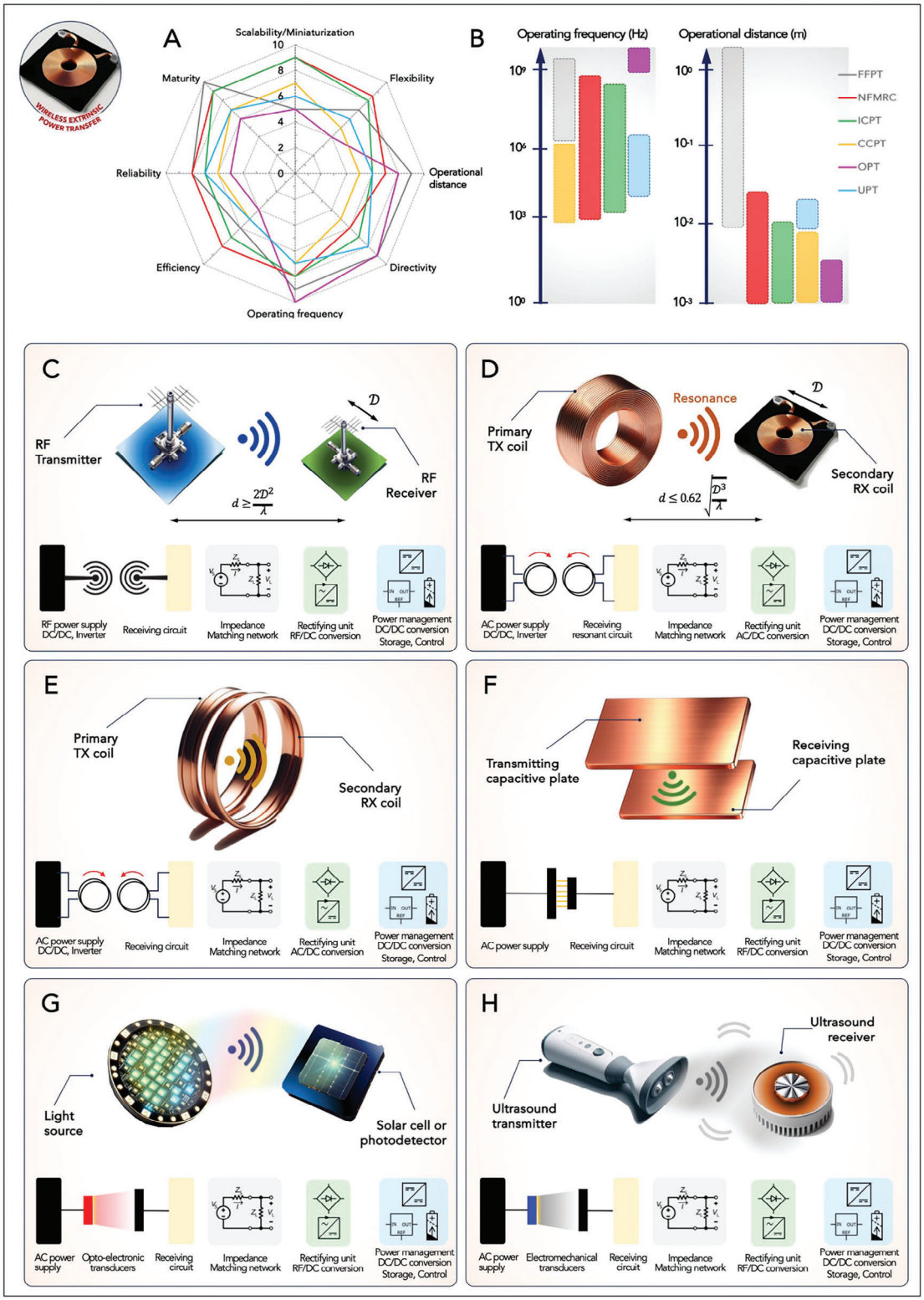


Figure 3. Schematic illustrations of the main categories of wireless extrinsic power transfer (WEPT) with an estimated comparison based on different features (A) and on operational distance and frequency (B): far-field RF power transfer (FFPT, C), near-field magnetic resonant coupling (NFMRC, D) and inductive coupling (ICPT, E), capacitive coupling power transfer (CCPT, F), optic/photonic power transfer (OPT, G), ultrasound (acoustic) power transfer (UPT, H). The radar chart in A provides a qualitative estimation, based on literature review for biomedical devices, for the following technical features of WEPT: operational distance, operating frequency, efficiency and directivity (ratio of the power transferred in a given direction to the power averaged over all directions), reliability, maturity, scalability/miniaturization and flexibility.

© 2024 The Author(s). Advanced Materials Technologies published by Wiley-VCH GmbH

2365709x, 0, Downloaded from https://onlinelibrary.wiley.com/doi/10.1002/admt.202400797 by University Of Oxford, Wiley Online Library on [19/11/2024]. See the Terms and Conditions (https://onlinelibrary.wiley.com/terms-and-conditions) on Wiley Online Library for rules of use; OA articles are governed by the applicable Creative Commons License

tive coupling between transmitting (primary) and receiving (secondary) coils[112–114] (Figure 3D). In particular, non-radiative near-field effects can be exploited (reactive near-field region) at distances $d \leq 0.62\sqrt{D^3/\lambda}$ (Rayleigh region).[97] For smaller antennas, the previous condition can be approximated to $d \lesssim \lambda/2\pi$. The first coil (transmitter, TX) will have an oscillating current applied to it, creating a varying magnetic field in the second coil (receiver, RX), generating an electromagnetic field (EMF) on it that can be used to power the medical device.

In the Rayleigh region predicting and measuring the relationship between the strengths and phases of the electric and magnetic fields is often intricate and challenging (their amplitudes generally fall off as $1/r^3$). Consequently, determining the true power density in this area poses difficulties. Electromagnetic waves are not only radiated outward into far space but also exhibit a reactive component in the EMF. Thus, the strength, direction, and phase of the electric and magnetic fields surrounding the antenna are sensitive to electromagnetic absorption and re-emission in this zone, and they adjust accordingly. In contrast, absorption far away from the antenna has minimal impact on the fields nearby and does not prompt any feedback in the transmitter. Within the reactive region, a certain amount of energy, if not absorbed by a receiver, is retained and stored very close to the antenna's surface, and it oscillates back and forth between the antenna and the reactive near field through electromagnetic radiation, gradually altering electrostatic and magnetostatic effects. The reactive component of the near field can lead to ambiguous or indeterminate results during measurements in this area. In contrast, the radiative near field (Fresnel region),[115] lacks reactive field components from the source antenna thus, the available energy in this region consists entirely of radiant energy and the field amplitudes fall off as $1/r^2$. Nevertheless, being in the near field, unexpected or adverse conditions are possible, especially when a metal object is in the surroundings, becoming a secondary radiating antenna surface.

NFMRC has found widespread applications, including wireless charging for electric vehicles and consumer electronics.[116–118] However, challenges arise with alignment sensitivity and limited transfer range, particularly for implantable devices.[112] Efficiency and distance limitations (within few cm) can be overcome by employing high quality factor resonators tuned for strong magnetic coupling.[119,120] NFMRC operates within frequencies ranging from approximately 100 kHz to 200 MHz,[121,122] and due to its non-radiative nature, it exhibits insensitivity to dielectric environments and obstacles, making it suitable for complex surroundings. Additionally, power can be successfully transferred even when the space between two resonators is obstructed.[119] Frequencies around 13.56 MHz ($\lambda \approx 12$ m) are particularly attractive due to their minimal tissue absorption,[123,124] large penetration depths, minimized biological effects, alignment with NFC standards[125] and compatibility with wireless data transmission using NFC protocols.[126,127] Furthermore, in experimental setups for wearable and implantable electronics,[128,129] where a primary coil is wrapped around a test arena and a secondary coil is integrated into the device,[54,66,90] power transfer efficiency (with delivery of up to tens of mW) remains consistent across different orientations of secondary coils and is minimally sensitive to the coils' shape.[66,90,130,131] Lower NFMRC frequencies require larger receiving coils, while higher frequencies can support improved device efficiency with reduced sizes and miniaturized form factors.[119,132,133] NFMRC enables an easy adaptation of the device geometry to accommodate various anatomical structures and viscoelastic properties of biological tissues, compatibly with fabrication methods of flexible printed circuit boards (FPCB). The method, being operational at lower frequencies than FFPT, also ensures lower tissue absorption during long-term operation, enabling its implementation in various wireless, battery-free, and fully implantable devices for biomedical applications, e.g. optogenetic stimulation or physiological monitoring of neural activity.[54,67,89,112,123,134]

NFMRC efficiency depends on the coupling coefficient and Q-factors of the coils,[112,135] posing challenges for ultraminiaturized implants. The coupling coefficient for two inductively coupled coils (not at resonance) is defined in Section 5,[136] and at resonance it is expressed as $\kappa_L(f_R) = M_{12}/\sqrt{L_1 L_2}$ where L_1,L_2 are the self-inductances of the individual coils; M_{12} is their mutual inductance; f_R is the resonance frequency. The Q-factor of a coil is defined as $Q_i = 2\pi f_i L_i/R_i$, where f_i,L_i,R_i are the resonance frequency, self-inductance and resistance of the *ith* coil.

The maximum achievable efficiency (η_{opt}) for two inductively coupled coils is defined as follows, respectively:[119,137]

$$\eta_{opt} = \frac{U^2}{\left(1+\sqrt{1+U^2}\right)^2} \tag{1}$$

where $U = \kappa\sqrt{Q_1 Q_2}$ is the coupling efficiency. The previous parameters decrease with increasing the coil size and with the distance and lateral misalignment between the coils.[112,138] Q-factors also increase with decreasing coils' electrical resistance.[88,90] Optimizing coil designs and coupling schemes is crucial, particularly for small animals, where enclosing the test arena with primary coils is feasible.[89] Similar cages or test arenas for large animals (pigs or non-human primates) are less effective because it is more challenging to maintain a uniform magnetic flux density over the area. In conclusion, despite challenges, NFMRC remains the most widely adopted method for wireless and battery-free devices, and in particular flexible bioelectronic implants in small animal models. In fact, NFMRC is generally used for short distances, typically within a few centimeters (cm) to a few meters (m). The power levels can range from milliwatts (mW) to several watts (W), depending on the application. For example, for charging small electronic devices like smartphones or wearables, power levels around 5 W may be sufficient. Typically, the current levels can range from hundreds of milliamps (mA) to several amps (A).

Noteworthy, NFMRC is a variant of inductive coupling power transfer (ICPT)[89] (Figure 3E): they both involve the wireless transfer of power using magnetic fields and the mutual induction between two coils, but in NFMRC the coils are tuned to resonate at the same frequency. This resonance enhances the transfer of power between the coils, enabling more efficient power transfer over slightly longer distances compared to traditional inductive coupling.[117] As a result, ICPT is effective over very short distances, typically not beyond few millimeters (mm) to centimeters (cm). NFMRC, instead, allows for more extended TX-RX distances, typically up to a few meters (m), and offers greater tol-

© 2024 The Author(s). Advanced Materials Technologies published by Wiley-VCH GmbH

2365709x, 0, Downloaded from https://onlinelibrary.wiley.com/doi/10.1002/admt.202400797 by University Of Oxford, Wiley Online Library on [19/11/2024]. See the Terms and Conditions (https://onlinelibrary.wiley.com/terms-and-conditions) on Wiley Online Library for rules of use; OA articles are governed by the applicable Creative Commons License

erance to spatial variations and positioning errors.[139] To reduce the RX coil impedance, the simplest strategy is to place a capacitor in series/parallel to the coil, causing them to resonate at the frequency used to excite the TX coil. The RX coil can also be optimized to self-resonate at a specific frequency by controlling its self-capacitance.[119,140] Examples of non-resonant ICPT systems for wearable/implantable bioelectronics can be found in literature, as well with various approaches to enhance the ICPT efficacy by using ferrite cores,[141] increasing the number of TX coils,[142] adjusting dynamically a matching network based on efficiency drops due to coil misalignment,[143] or modifying the shape of the RX coil.[144,145]

2.1.3. Capacitive Coupling Power Transfer (CCPT)

Capacitive coupling power transfer (CCPT), operates on a different principle than ICPT or NFMRC. In fact, electrical energy is transferred through the electric field between two capacitive plates or electrodes, rather than though the magnetic field. The working principle involves creating a capacitor by embedding a metal plate beneath biological tissue to receive power (RX), with another metal plate positioned atop the body to transfer energy (TX), thereby forming an electric field between them, with the biological tissue serving as the dielectric layer (Figure 3F). Similarly to ICPT, the coupling coefficient for CCPT ($\kappa_C = C_{12}/\sqrt{C_1 C_2}$, where C_1,C_2,C_{12} are respectively the capacitances and mutual capacitance of the two plates or resonators) decays with the distance between the two plates or resonators, and it is given by the following expression.[146] High-frequency signals across a capacitor result in low impedance, facilitating the transfer of most power to the other side. Utilizing high-frequency signals enables energy transmission through the skin. Research efforts have focused on developing flexible capacitive coupling implantable devices to better conform to the skin, thus enhancing performance.[147–150] Although still in the nascent stages of research for medical device applications, CCPT presents several advantages compared to ICPT. Due to the confinement of electric fields between capacitive plates, it exhibits lower EMI than ICPT. Additionally, being capacitive-based, it demonstrates higher efficiency at higher frequencies owing to its lower impedance. Furthermore, its SAR values are notably lower than those of ICPT.[120,151–153] Despite these advantages, CCPT is primarily suitable for implants near the skin due to dielectric losses.

The power and current requirements for capacitive coupling power transfer can vary depending on several factors, including the capacitance of the coupling plates, the voltage applied across them, and the distance between the plates. Typically, the CCPT efficiency tends to be lower compared to ICPT or NFMRC, especially over longer distances. This is because the electric field strength decreases rapidly with distance, leading to reduced efficiency and power transfer capabilities. In terms of current requirements, they are influenced by the voltage applied across the capacitive plates and the impedance of the load. While CCPT can be suitable for short-range power transfer applications where physical contact or close proximity between the coupling plates is feasible, its power and current requirements may not be as practical for longer-range or high-power applications compared to other wireless power transfer methods.[154,155]

2.1.4. Optic/Photonic Power Transfer (OPT)

Optic/photonic power transfer (OPT) is a WEPT method that utilizes electromagnetic radiation in the form of visible and near-infrared (NIR) light to transfer optical power and convert it to electrical power (Figure 3G). It is usually achieved with optoelectronic devices, such as solar cells[99,156] or photodetectors[60] that convert the optical power coming from an external source into an electrical signal that drives optoelectrodes (μ-LEDs) or wireless optogenetic devices. For example, Lee et al.[59] presented the technology for a tetherless optoelectronic neural interface integrating 180 nm complementary metal–oxide–semiconductor (CMOS) circuits, to amplify and encode neural signals, with an AlGaAs photodiode transitioning between photovoltaic modes for power harvesting (with a power density of ≈12 mW cm^{-2} on a diode area of ≈50 × 80 μm) and LED modes for data communication (near-infrared emission) with external systems. This ASIC device enables the development of small implants (4.7 × 10^{-3} mm^3) with low power consumption (1 μW), without a tether or a bulky RF coil, serving as potential foundations for electrophysiological recording or stimulation at high spatial resolution and specific discrete sites within single neurons or muscle fibers.

Although these technologies enable various possibility of integration of optical devices into intelligent wireless platforms, the main concerns regard the total power requirements[63] that need to account for the low efficiencies of optical emitters and power losses due to absorption or scattering by biological tissues as well as the device positioning (in the case of solar cells).

2.1.5. Ultrasound (Acoustic) Power Transfer (UPT)

UPT transfers power by propagating energy as sound or vibration waves to a receiver which converts the it to useful electrical energy (Figure 3H). The proposal to utilize acoustic waves for energy transmission was initially introduced by Cochran et al.[157] in 1985. Subsequently, numerous devices have been developed to harness this energy source. Ultrasound (20 kHz – ≈2 GHz) offers lower tissue absorption compared to electromagnetic radiation and outperforms inductive coupling, particularly with smaller implants or greater reading distances. It offers as well a higher approved safe dose (730 mW cm^{-2})[138,158] and it is suitable for devices intended for tissues with lower SAR limits, such as deep brain implants. Due to the substantial disparity in speed between light and sound (× 10^5 difference), acoustic waves exhibit much smaller wavelengths (0.3–0.7 mm for medical imaging ultrasound) at the same frequency, enabling the design of compact transmitters and receivers with high spatial resolution.[159] Typically, UPT is employed for low-power implants and as an energy harvester, with a predominant focus on external transmitters to ensure reliable power delivery to the device.[158] The UPT operation consists of the wireless (contactless) interaction between a transmitter (primary side) and a receiver (secondary side). The transmitter utilizes a specified amount of energy, primarily in the form of electrical power, via a converter, and applies its effects by inducing vibration in the active region.[160] This process can be described as efficient electrical-to-mechanical conversion. The vibration promptly induces resonance within the surrounding medium and propagates in all directions, whether through

© 2024 The Author(s). Advanced Materials Technologies published by Wiley-VCH GmbH

2365709x, 0, Downloaded from https://onlinelibrary.wiley.com/doi/10.1002/admt.202400797 by University Of Oxford, Wiley Online Library on [19/11/2024]. See the Terms and Conditions (https://onlinelibrary.wiley.com/terms-and-conditions) on Wiley Online Library for rules of use; OA articles are governed by the applicable Creative Commons License

air for open environments or through materials in other scenarios, depending on the specific circumstances (e.g. metals, biological tissues, liquids, etc.). The propagated energy is subsequently captured by a receiving transducer and converted into usable electrical power. Most devices leverage the piezoelectric properties of materials to capture ultrasound energy.[161–164] The propagation of acoustic waves induces mechanical stresses within the material, thereby generating energy via the piezoelectric effect. Seo et al.[58] proposed a miniaturized implantable ultrasonic backscattering sensor, comprising a piezocrystal, a transistor, and a pair of electrodes, that facilitates the wireless recording of electromyogram (EMG) and electroneurogram (ENG) data. Zhang et al.[165] devised a deep brain stimulation device utilizing the piezoelectric effect to harness ultrasound energy with high power density, achieving up to 1.1 W cm^{-2} in vitro. Furthermore, the absence of metal dependence in ultrasound systems allows for the exploration of alternative material classes. Islam et al.[166] developed a stent that collects ultrasound energy by replacing the metal component with piezoelectrics, demonstrating that custom geometric patterns can enhance energy collection through increased surface vibrations. Hinchet et al.[167] utilized ultrasound to displace a triboelectric generator's membrane, generating power. Triboelectric ultrasound devices have also been integrated into flexible PCBs, offering significant improvements in performance. Recently, there has been increasing interest in utilizing triboelectric nanogenerators for power transmission via ultrasound waves, with developments such as injectable and biodegradable devices showcased by Xiao et al.[168] Examples of wireless neural stimulators powered and controlled through ultrasounds can also be found in literature.[169,170]

A general drawback of UPT is the reduced coupling efficiency with slight misalignments between the external transmitter and the receiver, owing to the directional propagation of ultrasonic waves. Additionally, the ultrasonic attenuation is a key efficiency-reducer due to scattering and absorption of ultrasound waves, influenced by tissue types and ultrasonic frequencies: in fact, highly absorbing bone tissue may induce significant heating effects, while low ultrasonic frequencies can induce cavitation.[171] To solve this issue, beam-steering strategies can potentially be adopted with miniaturized and wearable transducer arrays controlled by specific algorithms.[172] Moreover, the tissue-air interface introduces a remarkable acoustic impedance that reduces the efficiency; thus, skin contact and wearability of the transmitting transducer is essential but the large size of commercially available transducers poses challenges for practical use in awake and freely behaving small animals. Another limitation lies in the materials choice: most of the high-performance inorganic piezoelectric crystals are brittle, high-mass density, rigid and planar, thus they cannot provide the proper mechanical compliance with human or animal bodies. The typical acoustic-to-electrical conversion efficiency is of 2%[138] and it can reach a maximum of ≈25% under perfect alignment.[57]

2.2. Wireless Intrinsic Power Transfer (WIPT)

WIPT consists of powering the devices through energy scavenged internally to the wireless architecture and available in the device's environment. Energy sources can be the moving body (joints' motion, muscle contraction, respiration, heartbeat, etc.) or other types, such as light (photovoltaic energy) or biochemical energy. Therefore, WIPT can be classified in terms of the type of energy that is harvested, collected and converted into electrical energy useful to power the devices: (i) mechanical (kinetic) energy (KE-WIPT); (ii) thermal energy (TE-WIPT); (iii) biochemical energy (BE-WIPT); (iv) photovoltaic energy (PE-WIPT); (v) mechanical (acoustic) energy (AE-WIPT). Moreover, the same energy may be harvested through different fundamental mechanisms. For instance, kinetic energy can be scavenged using (a) piezoelectric, (b) triboelectric, or (b) electromagnetic energy-harvesters or nanogenerators. Thermal energy, instead, is generally converted through (a) thermoelectric or (b) pyroelectric generators, which offer a good power budget, especially when used at subdermal locations. The highest amount of harvestable energy can be transferred through photovoltaic harvesters, which however have several drawbacks in terms of in-depth detection limit and intermittent powering. Electromechanical harvesters offer a wider variability of possible locations on and inside the body and they can rely on a continuous generation, especially for those applied onto non-voluntary (autonomic) muscles (e.g. myocardium surface, respiratory and gastrointestinal muscles)[76–79,173,174] without the need for separate power supplies.[86] Electromagnetic generators offer higher electrical currents and lower voltages, compared to triboelectric nanogenerators. Additionally, they differ in terms of operating conditions, the electromagnetic generators preferring high frequencies. Piezoelectric generators generally require more space, unless they are in the shape of microscale nanogenerators, and they usually provide more power than triboelectric harvesters, with the same sizes. In Table 1 the pros and cons of the different WIPT strategies are outlined and summarized, whereas **Figure 4A,B** shows a comparison based on the reviewed literature. As stated for WEPT, different technical features are used to compare the technologies based on qualitative estimations relying on previous literature. For instance, the ease of miniaturization is one of these criteria: electromagnetic transducers that scavenge kinetic energy through electromagnetic induction are more difficult to be miniaturized than triboelectric or piezoelectric energy harvesters. In fact, their power output is proportional to the square of the coil area, of the magnet-coil relative speed and of the operation frequency, thus it is dramatically reduced for small-scale generators.[162,175–177] The radar chart in Figure 4A also includes a feature related to the materials choice which refers to the different range of available materials that can be adopted for a specific energy harvesting technology: piezoelectric and triboelectric harvesters offer wider ranges of materials compared to thermoelectric, pyroelectric or electromagnetic generators.

2.2.1. RF Energy Harvesting (RF-WIPT)

RF energy harvesting (RF-WIPT) involves the process of passively capturing and converting RF radiation into usable electrical power (Figure 4C). Similarly to a system for FFPT, an average setup consists of a receiving antenna, a matching circuit, a rectifier, a power management unit (PMU), and a load. RF energy harvesting typically exploits frequencies ranging from a few hundred megahertz (MHz) to several gigahertz (GHz). In particular,

© 2024 The Author(s). Advanced Materials Technologies published by Wiley-VCH GmbH

2365709x, 0, Downloaded from https://onlinelibrary.wiley.com/doi/10.1002/admt.202400797 by University Of Oxford, Wiley Online Library on [19/11/2024]. See the Terms and Conditions (https://onlinelibrary.wiley.com/terms-and-conditions) on Wiley Online Library for rules of use; OA articles are governed by the applicable Creative Commons License

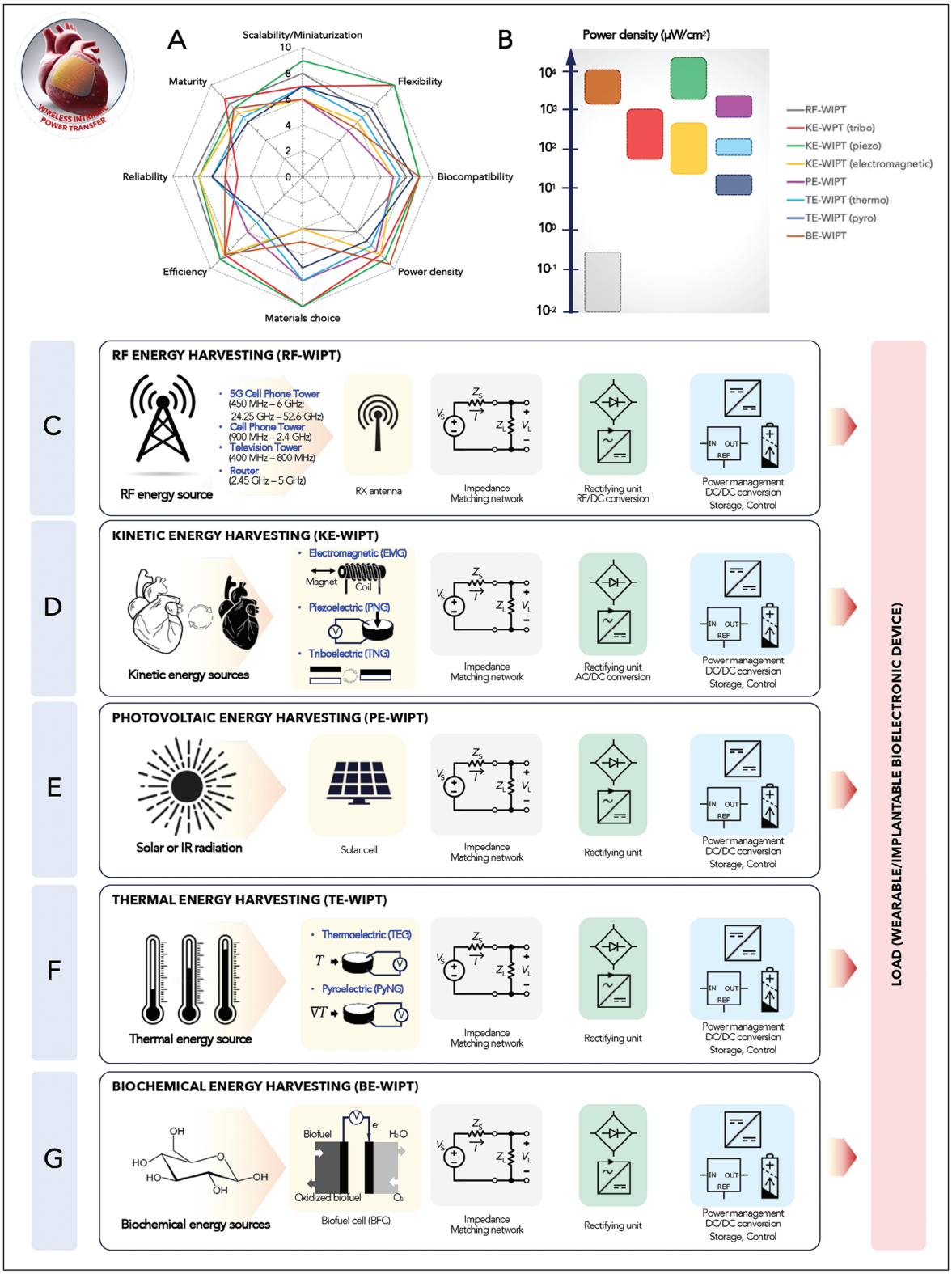


Figure 4. Schematic illustrations of the main categories of wireless intrinsic power transfer (WIPT) with an estimated comparison based on different features (A) and on power density (B): RF energy harvesting (RF-WIPT, C), mechanical (kinetic) energy harvesting (KE-WIPT, D), photovoltaic energy harvesting (PE-WIPT, E), thermal energy harvesting (TE-WIPT, F), biochemical energy harvesting (BE-WIPT, G). The radar chart in A provides a qualitative estimation, based on literature review for biomedical devices, for the following technical features of WIPT: efficiency, power density, technological maturity, reliability, ease of scalability/miniaturization, flexibility and biocompatibility.

© 2024 The Author(s). Advanced Materials Technologies published by Wiley-VCH GmbH

2365709x, 0, Downloaded from https://onlinelibrary.wiley.com/doi/10.1002/admt.202400797 by University Of Oxford, Wiley Online Library on [19/11/2024]. See the Terms and Conditions (https://onlinelibrary.wiley.com/terms-and-conditions) on Wiley Online Library for rules of use; OA articles are governed by the applicable Creative Commons License

frequencies within the ISM (Industrial, Scientific, and Medical) bands,[178] such as 433 MHz, 900 MHz, 2.4 GHz, and 5.8 GHz, are commonly utilized. These frequencies are unlicensed and widely available for use, making them suitable for RF energy harvesting applications. Moreover, the proliferation of wireless communication technologies, such as Wi-Fi, Bluetooth, ZigBee and RFID, has led to an abundance of RF signals in the environment, providing ample opportunities for energy harvesting. Additionally, RF-WIPT can also leverage ambient RF sources, such as broadcast radio and television signals, cellular networks, and microwave communication systems. By harnessing these RF signals, energy harvesting devices can generate power to supplement or even replace traditional battery sources in a variety of applications, including wireless sensors, IoT (Internet of Things) devices, wearable electronics, and autonomous systems.[179] Furthermore, advancements in RF harvesting technologies, such as efficient rectifying antennas, metamaterials, and impedance matching techniques, continue to improve the efficiency and effectiveness of RF-WIPT systems. The amount of received power (P_R) that can be harvested depends on the transmitted power (P_T), the RF signal's wavelength (λ), the distance (d) between the RF power source and the harvesting node, according to the Friis equation:[115,180]

$$P_R = \frac{G_R G_T \lambda^2}{(4\pi d)^2 L} P_T \tag{2}$$

where G_R, G_T are the transmitter and receiver gains of the antenna, L is the path loss factor.

A key parameter to quantify the loss in the signal strength is the free-space path loss ($\mathcal{P}_L$), computed as[181] $\mathcal{P}_L\,(dB) = 32.44 + 20\log_{10}(f \cdot d) - G_T - G_R$. The power conversion efficiency (η_{PCE}) of the RF energy harvesting module is thus given by the ratio between the converted DC power (P_{DC}) and the incident RF power at the antenna (P_{IN}):[182]

$$\eta_{PCE} = \frac{P_{DC}}{P_{IN}} = \frac{V_{DC}^2}{R_{load}} \cdot \frac{1}{\mathcal{P}_L} \tag{3}$$

Noteworthy, FFPT and RF-WIPT are both methods used to harness electromagnetic energy, particularly in the RF range, but they serve different purposes and operate under different principles.[106–109] RF WEPT is used to wirelessly transmit electrical power from an RF power source to a receiver device over relatively long distance (e.g. FFPT), and it is adopted in applications such as wireless charging of electronic devices, powering remote sensors, and providing energy to IoT devices without the need for physical connections. Thus, the source of RF energy is provided with an external tool (signal generator, function generator, power supply, etc.) and the energy transfer is intentional towards the targeted application.[106] The effectiveness of the power transfer depends on the input power, which can be set with the external power supply. Dedicated power sources with high power and beamforming capabilities can result in higher RF power density levels: FFPT systems can generate higher power densities compared with RF-WIPT systems.[106,107] Additionally, the end-to-end efficiency of an FFPT system is defined as the product of each subsystem's efficiency, e.g. transmit efficiency, free-space propagation (channel) efficiency and the power receiver efficiency.

RF-WIPT is used instead to capture ambient RF energy and convert it into usable electrical power. The source of RF energy is therefore provided by the environment, it is existing and opportunistic, and it would be otherwise wasted and not utilized by the end users.[106,108] Accordingly, the effectiveness of the energy harvesting depends on the available power levels in the environment. For instance, in cities, ambient RF energy is pervasive, which comes from digital TV (DTV) towers (with signals usually below 800 MHz), Wi-Fi hotspots (either at 2.4 GHz or 5 GHz), or cellular 4G/5G networks, which offer ambient RF energy sub-2.7 GHz or sub-6 GHz.[106] Differently from an FFPT system, a basic RF-WIPT system consists only of a rectified antenna (rectenna, comprising an antenna, an impedance matching network and a rectifier) and a power management unit. To increase the harvested power level of RF-WIPT systems, multiband and broadband rectifiers have been investigated in various frequency bands.[106] RF-WIPT is employed in low-power electronic devices and sensor networks to supplement or replace batteries, i.e. to enable battery-free operation for wireless sensors, RFID tags, wearable electronics. In summary, FFPT is focused on actively transmitting electrical power wirelessly from a transmitter to a receiver, while RF-WIPT involves passively capturing and converting ambient RF energy into usable electrical power for low-power electronic devices.

2.2.2. Mechanical (kinetic) Energy Harvesting (KE-WIPT)

The human/animal body generates various sources of kinematic energy, conveyed through muscle contractions and extensions, pressure, blood flow, etc. Different methods exist to convert kinetic energy into electrical energy: the main options are (i) electromagnetic generators (EGs), (ii) piezoelectric nanogenerators (PNGs), (iii) triboelectric nanogenerators (TNGs), and their hybrid combinations (Figure 4D). Electromagnetic induction, the basic principle of EGs, involves the movement of a magnet inside a copper coil to create a change in magnetic flux and generate a potential. While less explored in implantable devices literature due to the requirement of a moving part, electromagnetic induction has been successful in collecting power from heart motion. For example, Yang et al.[183] presented a device utilizing a stack of permanent magnets suspended between flexures and positioned inside a copper coil. They implanted it into a pig's right ventricular cavity, demonstrating a generated mean output power of 0.78 and 1.7 μW at a heart rate of 84 and 160 bpm, respectively. PNGs utilize mechanical vibrations within the body to induce the piezoelectric effect in the harvester.[176,184–187] For instance, Zhang et al.[188] utilized a poly(vinilydene fluoride) (PVDF) strip wrapped around the ascending aorta to convert pulsatile expansion into electrical energy, yielding up to 681 nW. Xu et al.[189] devised a Kirigami-based stretchable PNG with an intersegment electrode design capable of generating up to a maximum of 228 nW. TNGs are based on the triboelectric effect, according to which the contact or friction between two dissimilar materials induces a charge redistribution on the materials' surfaces which can be collected into an external circuit and generate AC current and voltage. Literature on TNGs is very vast and comprehensive reviews describe in details the mechanisms and operating modes of TNGs:[162,190–195] their application into flexible wearable

© 2024 The Author(s). Advanced Materials Technologies published by Wiley-VCH GmbH

2365709x, 0, Downloaded from https://onlinelibrary.wiley.com/doi/10.1002/admt.202400797 by University Of Oxford, Wiley Online Library on [19/11/2024]. See the Terms and Conditions (https://onlinelibrary.wiley.com/terms-and-conditions) on Wiley Online Library for rules of use; OA articles are governed by the applicable Creative Commons License

and implantable bioelectronics has been accelerated in the recent years.[79,196]

PNGs and TNGs offer distinct advantages and disadvantages compared to EGs, particularly concerning operational frequency, power outputs, current and voltage outputs, and suitability for wireless flexible bioelectronics applications. PNGs can operate at higher frequencies compared to EGs. Piezoelectric materials (described in more details in Section 6) respond well to mechanical vibrations, enabling them to harvest energy from various sources such as human motion, environmental vibrations, or acoustic waves.[162] This versatility in operational frequency allows PNGs to capture energy from a wide range of sources, making them suitable for diverse applications. Additionally, PNGs can generate relatively high-power outputs, especially when subjected to high-frequency mechanical stimuli. However, the current and voltage outputs of piezoelectric nanogenerators tend to be lower compared to EGs. Moreover, PNGs exhibit excellent flexibility and can be integrated into flexible and wearable devices, making them ideal for wireless flexible bioelectronics applications. On the other hand, TNGs harness energy from friction-induced electrification, thus they can operate at low frequencies and generate high power outputs, making them suitable for applications where mechanical vibrations are limited or unavailable. Furthermore, TNGs can produce both high current and voltage outputs simultaneously, which is advantageous for powering electronic devices directly without the need for additional voltage or current amplification circuits. Additionally, TNGs are highly flexible and can conform to irregular shapes and surfaces, allowing for seamless integration into wearable and implantable bioelectronics devices. However, one of the main disadvantages of TNGs is their reliance on external mechanical stimuli for energy harvesting, which may limit their effectiveness in certain environments or applications where consistent mechanical vibrations are lacking. The key drawbacks associated with PNGs and TNGs lie in their limited power availability and their pulsating, often intermittent, nature.[197] Devices relying on skeletal motion typically yield peak powers below 1 mW, and even lower after rectification. Power outputs in the range of tens of microwatts (with a power density of approximately 10–100 μW cm^{-2}) can be anticipated from visceral motions, which often fall short of meeting the power demands of microcontrollers, optoelectronic devices, microfluidic actuators, and wireless communication systems. As a result, current PNGs and TNGs are primarily applicable to passive devices with straightforward functionalities, such as generating pulsed voltages in pacemakers and providing instantaneous neural stimulation, tasks which necessitate peak powers in the tens of microwatts range. However, promising advancements in the materials, designs, architectures and hybrid combinations of PNGs and TNGs,[162,198–200] have boosted their use also in applications with higher power requirements.

2.2.3. Photovoltaic Energy Harvesting (PE-WIPT)

There has been significant interest in photovoltaic energy generation owing to the global surge in investment in renewable energy sources. This method of electrical energy generation has also been explored for powering wearable and implantable medical devices and holds significant promise for powering wireless flexible bioelectronics. Photovoltaic cells can be integrated into flexible and wearable substrates, allowing for seamless integration into clothing, accessories, or even directly onto the skin. Such devices can readily harness energy from external light sources, as multiple light sources are available in most environments (Figure 4E). However, photovoltaic generators cannot be deeply implanted into the body due to light absorption by biological tissue. Consequently, these devices are typically employed to power subcutaneous implants, although they still encounter challenges with low power capabilities, as much of the light received by the skin is reflected or absorbed. However, advancements in flexible and transparent photovoltaic materials enable their integration into implantable bioelectronics, providing a reliable power source for medical devices and sensors. Examples of photovoltaic energy harvesting can be found in previous works.[201–203] There are several challenges associated with the implementation of PE-WIPT for bioelectronics. One major challenge is achieving sufficient output power levels to meet the energy demands of bioelectronic devices. While photovoltaic cells can generate substantial power under optimal conditions, the efficiency of energy conversion may be limited, particularly in indoor or low-light environments. Generally, the efficiency of commercial Si-based photovoltaic cells ranges from around 15% to 22%.[204] However, research and development efforts have led to the creation of more efficient photovoltaic technologies such as multi-junction cells, which can achieve efficiencies of over 40% in laboratory settings.[204,205] Additionally, emerging technologies like perovskite solar cells show promising potential with reported efficiencies exceeding 25% in recent years.[206,207] Furthermore, the small form factor and flexible nature of wearable and implantable devices pose challenges for integrating photovoltaic cells with adequate surface area to capture sufficient light energy. Furthermore, the variability of ambient light conditions, including changes in intensity and spectral distribution, may affect the performance and reliability of photovoltaic energy harvesting systems. Another challenge is ensuring compatibility and biocompatibility of photovoltaic materials with the human body, particularly for implantable bioelectronics. Materials used in photovoltaic cells must be non-toxic and biocompatible to prevent adverse reactions or tissue damage. Additionally, the mechanical flexibility and durability of photovoltaic materials are essential for wearable and implantable applications to withstand bending, stretching, and other movements without degradation of performance.

We should highlight that OPT and PE-WIPT both involve converting light into electrical energy, but they differ significantly in their mechanisms, applications and design considerations. OPT is an active and directed method of energy transfer, usually over specific distances, using controlled light sources like lasers or LEDs.[208] Design focuses on optimizing the transfer of energy over a specific path and ensuring that the receiver is tuned to the wavelength of the light source. It can be highly efficient in converting transmitted light into electricity; however, the overall system efficiency depends on alignment, distance and environmental factors. It is particularly useful for remote, mobile, or inaccessible applications. On the other hand, PE-WIPT is a passive method that converts broad-spectrum unlight into electricity. Energy capture is diffuse, relying on the availability and intensity of sunlight, which can vary depending on time of day, weather

© 2024 The Author(s). Advanced Materials Technologies published by Wiley-VCH GmbH

2365709x, 0, Downloaded from https://onlinelibrary.wiley.com/doi/10.1002/admt.202400797 by University Of Oxford, Wiley Online Library on [19/11/2024]. See the Terms and Conditions (https://onlinelibrary.wiley.com/terms-and-conditions) on Wiley Online Library for rules of use; OA articles are governed by the applicable Creative Commons License

conditions, and geographic location.[203,209] The PE-WIPT systems are designed to capture a wide range of the solar spectrum to maximize energy conversion. However, solar cells have varying efficiencies across different wavelengths. The overall efficiency is also influenced by factors such as shading, angle of incidence, temperature, and the quality of the solar cells.

2.2.4. Thermal energy harvesting (TE-WIPT)

Thermal energy harvesting can be performed in two ways, i.e., through (i) thermoelectric generators or (ii) pyroelectric nanogenerators (Figure 4F). Thermoelectric generators (TEGs) have garnered significant research attention in recent years. These devices are capable of converting thermal energy from a temperature gradient into electrical energy using the properties of semiconductor and conductor materials.[84,85,210–212] This process exploits the Seebeck effect, where charge carriers migrate from the hot side to the cold end, creating an electrical potential between the two ends. Given the requirement for a temperature gradient, TEGs are particularly suitable for wearable devices that come into contact with both the cold external environment and the body. There is also potential for these devices to be used in subdermal implants to power implantable medical devices. The merit of the TEG approach lies in its direct utilization of the temperature difference intrinsically existing throughout the biological bodies where the TEGs are located.[213–215]

Differently from TEGs, pyroelectric nanogenerators (PyNGs) convert temperature fluctuations into electrical energy by inducing polarization changes in pyroelectric materials.[216] These materials exhibit a polar symmetry and generate electric charge in response to changes in temperature.[217] Baba et al.[218] examined the viability of PyNG as an energy source for self-sustaining wireless sensor nodes. Simulation results demonstrated that a transmission circuit with the device as the power source can transmit data at intervals of several minutes, even with slight temperature changes (e.g. 2 °C).

TEGs and PyNGs both convert thermal energy into electrical power, yet they operate on distinct principles, each offering unique advantages and disadvantages. One advantage of TEGs is their ability to generate power from relatively small temperature differentials, making them suitable for diverse applications. However, their efficiency is often limited, and they require stable temperature differentials to maintain optimal performance. On the other hand, PyNGs offer the advantage of higher efficiency compared to TEGs, especially in applications with fluctuating temperatures.[219,220] Additionally, they can be more compact and flexible, allowing for integration into wearable and implantable devices. Nevertheless, PyNGs typically require larger temperature changes to produce significant power outputs, limiting their effectiveness in environments with stable temperatures.

2.2.5. Biochemical Energy Harvesting (BE-WIPT)

The utilization of biofuel cells (BFCs) offers an alternative approach to harvesting energy from living organisms.[80,83,221–223] By leveraging redox reactions of energy-carrying substances, enzymatic fuel cells can generate electrical energy suitable for powering bionic and bioelectronic devices. In these biofuel cells, the biofuel serves as the anode, an oxidant is employed on the cathode, and oxidoreductases act as catalysts to facilitate the redox reaction, resulting in electron flow between the anode and cathode and subsequent electrical energy generation (Figure 4G). Biofuel cells exhibit power densities in the order of ~10 μW cm^{-2} and they provide a good energy conversion efficiency, making them suitable for powering a wide range of bioelectronics, including sensors, actuators, and medical devices. BFCs can utilize readily available biological fuels, such as glucose in bodily fluids, making them ideal for applications in healthcare monitoring and medical implants. Ongoing research endeavors concerning implantable biofuel cells across various host organisms (e.g., insects,[224] snails,[225] rats,[81,82] rabbits[226] and birds[227]) show promising signs. Furthermore, they offer the advantage of being environmentally friendly, producing minimal waste products and emitting no harmful byproducts during energy generation. However, challenges remain in optimizing the stability and longevity of biofuel cells, as well as in improving their power output to meet the energy demands of advanced bioelectronic devices.[73]

3. Wireless Data Communication (telemetry)

Wireless data communication (WDC), known as telemetry, stands as a cornerstone in the realm of flexible bionics and wearable/implantable bioelectronics, revolutionizing the landscape of healthcare and biotechnology.[94,228] In recent years, the convergence of advanced materials science, nanotechnology, and electronics technologies has spurred remarkable advancements in the development of WDC systems tailored for integration with flexible and wearable/implantable bioelectronics. WDC allows data collection directly from target organs or tissues, enabling seamless data exchange, real-time feedback mechanisms and uninterrupted, long-term monitoring irrespective of the patient's physiological condition.[229] Furthermore, as the demand for at-home monitoring solutions increases, there is a burgeoning requirement to acquire data from the patient's body without requiring intervention. To collect data wirelessly, the device can transmit its data or have them encoded in its physical state, which can be interrogated externally. To achieve a WDC strategy for the wearable/implantable device, there are two main categories: wireless data transfer (WDT) and wireless data interrogation (WDI). Choosing an efficient WDC strategy is paramount for ensuring dependable data transfer to external devices, particularly in the context of bioelectronic implants. Factors such as implantation depths, data rates, and accuracy must be taken into account. Data retrieval methods may involve interrogating device properties or employing active data transmission by the devices themselves. WDC techniques include near-field communication (NFC), Bluetooth, RFID, ISM bands, backscattering, infrared, and ultrasound transducers: they present both advantages and limitations (listed in Table 1), necessitating careful deliberation to make optimal design decisions.[230–233] **Figure 5A** shows a comparison of these techniques based on estimations of different features, including operational distance, operating frequency, communication efficiency, signal selectivity, as well as technological maturity, reliability, flexibility and scalability/miniaturization. A key parameter to make a reasonable comparison between these technologies is the data transfer rate which is rated in Figure 5B based on a comprehensive review of previous literature examples.

© 2024 The Author(s). Advanced Materials Technologies published by Wiley-VCH GmbH

2365709x, 0, Downloaded from https://onlinelibrary.wiley.com/doi/10.1002/admt.202400797 by University Of Oxford, Wiley Online Library on [19/11/2024]. See the Terms and Conditions (https://onlinelibrary.wiley.com/terms-and-conditions) on Wiley Online Library for rules of use; OA articles are governed by the applicable Creative Commons License

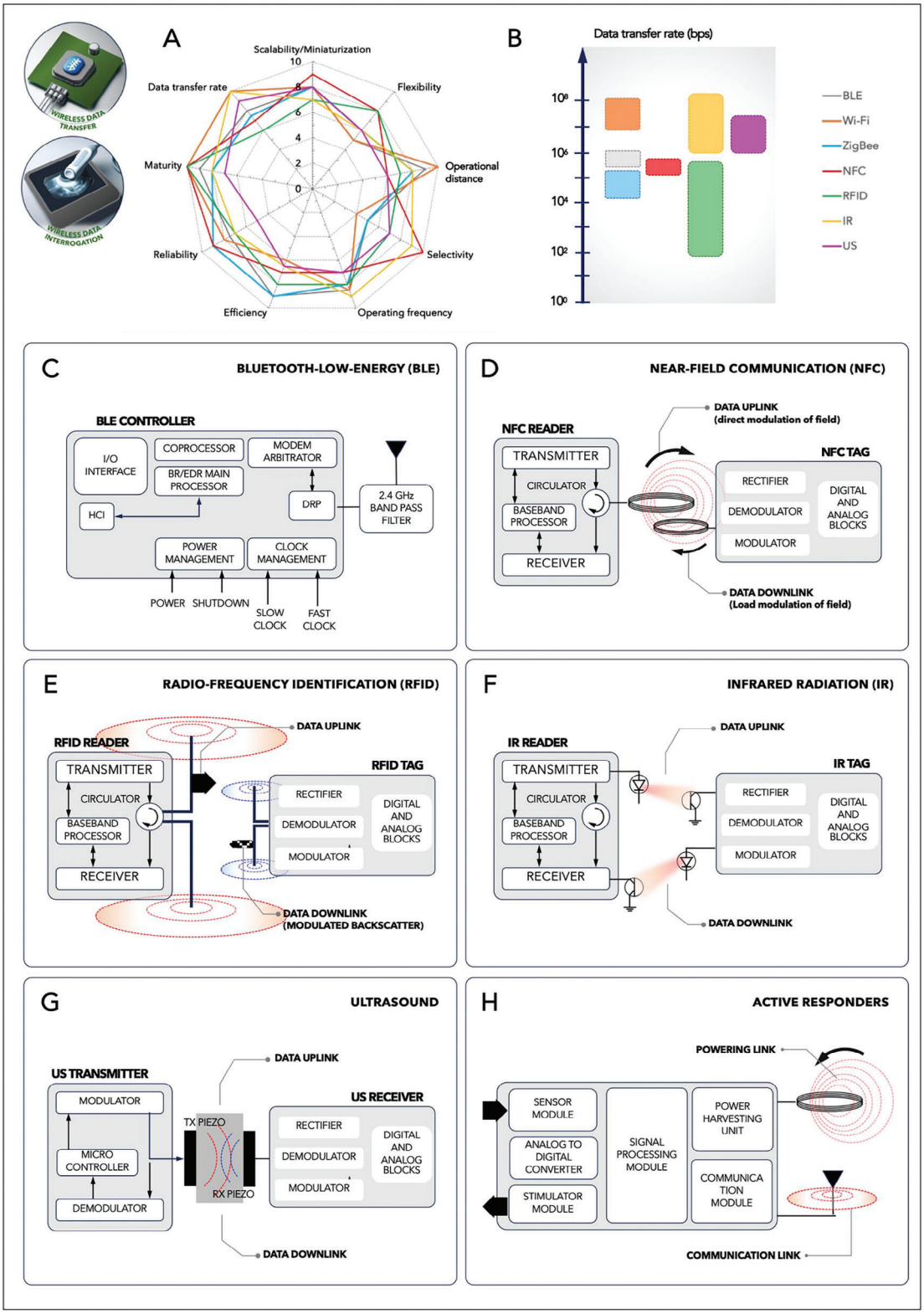


Figure 5. Schematic illustrations of the main categories of wireless data communication (WDC) with an estimated comparison on different features (A) and on data transfer rate (B): wireless data transfer (WDT), including BLE (C), NFC (D), RFID (E), IR (F) and ultrasounds (G); wireless data interrogation (WDI), including active responders (H). The radar chart in A provides a qualitative estimation, based on literature review for biomedical devices, for the following technical features of WDC: operational distance, operating frequency, efficiency, data transfer rate, selectivity, as well as technological maturity, reliability, flexibility and scalability/miniaturization.

© 2024 The Author(s). Advanced Materials Technologies published by Wiley-VCH GmbH

2365709x, 0, Downloaded from https://onlinelibrary.wiley.com/doi/10.1002/admt.202400797 by University Of Oxford, Wiley Online Library on [19/11/2024]. See the Terms and Conditions (https://onlinelibrary.wiley.com/terms-and-conditions) on Wiley Online Library for rules of use; OA articles are governed by the applicable Creative Commons License

3.1. Wireless Data Transfer (WDT)

In WDT the device must gather, encode, and dispatch data to an external device.[234] Employing established communication protocols like Bluetooth, ZigBee or Wi-Fi enhances compatibility with existing devices. However, the signal frequencies associated with these protocols, typically around 2.4 GHz, are notably attenuated by the body. Among the most established communication protocols, Bluetooth Low Energy (BLE), subset of Bluetooth v4.0, emerges as particularly well-suited for implantable devices (Figure 5C). This is attributed to its reduced power consumption, typically ranging between 0.01 and 0.5 W, with potential for even lower average power consumption down to a few μW if throughput is diminished.[235] Notably, BLE is compatible with most consumer devices and prominently with smartphones,[201] and it has been used for many wearable and implantable devices.[236] While BLE is optimized for low power consumption and short-range communication (10-100 m), making it ideal for portable, battery-powered devices where data rates are modest (≈1-2 Mbps), Wi-Fi provides high-speed data transfer (up to 1 Gbps or higher) and broad coverage, suitable for applications that require significant bandwidth, but with higher power consumption and more architectural complexity. ZigBee, instead, is focused on low-power, low-data-rate (20-250 kbps) communication, with the capability to support large scalable mesh networks, thus with more robustness and complexity than BLE (but simpler than Wi-Fi).[237]

Another established suite of communication protocols is NFC, which follows the same operating principle as NFMRC (Figure 5D). Operating through inductive coupling, NFC establishes a link between devices up to 4 cm apart, enabling bidirectional data transmission. Operating at a frequency of 13.56 MHz, NFC encounters less absorption by biological tissue compared to 2.4 GHz frequencies. Moreover, some NFC protocols are compatible with smartphones, particularly those employed for payment services. Lazaro et al.[238] investigated the feasibility of monitoring NFC implantable devices using a smartphone, and proposed a 3-coil system to enhance the readout distance. Gong et al.[239] enhanced NFC capabilities in a weak coupling regime by employing two different carrier frequencies and binary phase shift keying instead of load shifting keying.

Radio-Frequency Identification (RFID) represents another prevalent communication protocol utilized across various domains, including implantable medical devices, facilitating the creation of passive and active devices (Figure 5E). Passive RFID employs backscattering, where the signal is received, modulated, and reflected back to the reader.[240] One advantage of passive RFID is its extended readout distance: for instance, Zhang et al.[241] reported on an antenna measuring $\pi \times (6)^2 \times 1.27$ mm^3, which enabled readout distances as long as 87 cm.

Non-RF WDT methods include the utilization of IR (Figure 5F) or ultrasound (Figure 5G). Burton et al.[65] used an IR LED modulated using ON/OFF keying with a carrier frequency of 57 kHz, allowing for a data rate of 27 Hz. However, a significant portion of the transmitted light is absorbed by the body, with transmission rates in vivo varying from 53% in certain rat species to as low as 1% in others. For data transmission via ultrasound, Weber et al.[242] developed a device utilizing a piezoelectric transducer capable of transmitting data up to a depth of 12 cm, with the device measuring $1.7 \times 2.3 \times 7.8$ mm^3, demonstrating promise for deep implants.

3.2. Wireless Data Interrogation (WDI)

Instead of transmitting the collected data actively, devices can alter passively (without requiring power consumption) their physical state in a manner that allows external interrogation. The change can be related to a variation of resonance frequency in LC systems, a modification of its physical shape or acoustic absorption.

LC systems are composed of a capacitor (C) linked to an inductor (L), causing resonance at the frequency $f_{res} = 1/(2\pi\sqrt{LC})$. When an external inductor is coupled to the inductor, maximum transmission efficiency occurs when the signal frequency passing through the external inductor matches the resonance frequency. By conducting a frequency sweep and monitoring either the reflection coefficient or impedance, one can detect a peak to identify the resonance frequency of the implant externally. The resonance frequency can be correlated with the signal of interest using either a capacitive or inductive sensor (reader, interrogator), with the former being more commonly used.[243] The main drawbacks of LC systems lie in the weak coupling between coils and sensitivity to misalignment, thus it is crucial to optimize the design of the coils.[244–246] Square coils offer the highest inductance and, consequently, the highest quality factor for the same size, compared to circular, octagonal and 16-side coils.[246] To increase the efficiency, the coil resistance should be reduced by increasing the thickness,[247] whereas to increase the inductance ferrite cores can be used to enhance the magnetic coupling. To extend LC systems readout distances, repeaters (intermediate resonators) can significantly increase the performances without sensitivity decay or adjust the resonance frequency to match the sensor.[248,249] Another method to improve performances and increase readout distances is to use impedance matching techniques.[250] Achieving impedance matching between the antenna and the load is essential for maximizing data signal integrity. The use of impedance matching networks, such as L-section or pi-section networks,[251,252] helps match the impedance of the antenna to that of the interrogating circuit, minimizing signal reflections and losses. Another approach involves adjusting the physical properties of the antenna, such as its length or geometry, to achieve impedance matching with the LC circuit. Furthermore, techniques like impedance transformation using transformers or baluns can also be employed to match impedances between the antenna and the LC circuit.

As an alternative to LC systems, WDI can be performed utilizing ultrasound to assess the device's shape or acoustic properties. Typically, this is achieved using stretchable materials, fluids, or microbubbles. Compared to LC systems, these techniques offer advantages such as lower ultrasound absorption by biological tissue, enhanced efficiency for miniaturized devices, more cost-effective readout systems, and simpler fabrication procedures. Ultrasound-based communication systems typically involve modulating data onto ultrasound carrier waves, which are then transmitted through the air or other media to a receiving device. Upon reception, the data is demodulated and decoded

© 2024 The Author(s). Advanced Materials Technologies published by Wiley-VCH GmbH

2365709x, 0, Downloaded from https://onlinelibrary.wiley.com/doi/10.1002/admt.202400797 by University Of Oxford, Wiley Online Library on [19/11/2024]. See the Terms and Conditions (https://onlinelibrary.wiley.com/terms-and-conditions) on Wiley Online Library for rules of use; OA articles are governed by the applicable Creative Commons License

for further processing. Ultrasound-based WDI is particularly valuable in scenarios where RF communication is impractical or restricted, such as underwater communication, medical imaging, and industrial monitoring. Moreover, ultrasound waves can penetrate through solids and liquids, enabling communication through barriers that may obstruct other wireless technologies. An example of ultrasound-based WDI is to use a flexible material with a distinct acoustic impedance from the body which can be imaged to measure differences in shape and strains.[253,254]

Pressure sensors can also operate for WDI based on two main categories: microbubble and fluidic-based systems. In the first case, gas-filled microbubbles are injected into the tissue. Pressure variations may cause microbubbles to disappear, alter harmonic shifts, or change the amplitude of scattered echoes, with the latter method showing the most promise.[255] In the second case, external pressure changes the fluid level inside microchannels within the device, observable through ultrasound imaging.[230] This method offers greater sensitivity and is more suitable for long-term pressure monitoring compared to microbubbles.

In systems for ultrasonic WDI, transducers generate and receive ultrasonic waves, depending on their function: transmitters convert electricity into acoustic waves, receivers convert ultrasounds into electricity and transceiver both transmit and receive ultrasound. The ultrasonic power provided by the external transmitter is used to modify the properties (shape, acoustic impedance) of a transceiver or a receiver such that the signals are backscattered. Correct modulation allows for the provision of all power from the external transmitter, potentially reducing the size of the implantable devices significantly, offering a notable advantage and enabling ultra-small implants. However, drawbacks exist, including the backscatter temporal jitter effect, which directly impacts data retrieval. Additionally, effective operation necessitates efficient power coupling between the external and internal devices, restricting the transmission distance achievable with passive data telemetry. Consequently, this method is currently suitable only for shallow sub-cutaneous and sub-muscular communication scenarios. Ultrasound backscattering is a form of transmission onto which other modulation can be implemented.

On-Off Keying (OOK) stands out as the most commonly employed modulation technique due to its simplicity in implementation, requiring less sophisticated hardware. However, more intricate modulation schemes like Quadrature Amplitude Modulation (QAM), Quadrature Phase Shift Keying (QPSK), and Orthogonal Frequency Division Modulation (OFDM) have been reported to enhance data rates. Nevertheless, implementing these advanced schemes demands more complex hardware and software, particularly on the receiver side, potentially leading to increased power consumption. Omnidirectional transducers utilized for ultrasound in-body communication, such as sonomicrometry[256] and tube-, plate- or cube-shaped transducers operating in radial extension mode, have been integrated into active PCB circuitry.[58,257,258] Jiang et Wu[259] published a comprehensive review on emerging ultrasonic bioelectronics, enumerating different technologies and systems utilizing ultrasounds for power transfer and signal communication.

4. Simultaneous Wireless Power and Data Transfer (SWPDT)

When multiple sensors are implanted in the body, necessitating simultaneous sampling, new challenges arise as the transmitted data from each device must be discerned and must not overwrite each other and with the WPT module.[260] For instance, Lee et al.[261] presented a neural interface system that relies on a spatially-distributed network of wireless microscale implantable "Neurograin" sensors, providing a highly scalable, robust, and adaptive architecture. These individual neurograin chiplets incorporate a wireless link operating at around 1 GHz for energy harvesting and telemetry, alongside analog and digital electronics for neural signal amplification, on-chip storage, and networked communications at 10 Mbps employing a Time-Domain Multiple Access (TDMA) protocol. Each neurograin functions as a self-contained neural access channel: multiple implantable neurograins come together (up to 56) to form a fully wireless cortico-computer communication network, with each device having a unique identifier and with up to 1000 channels. Coordination of the implanted network is facilitated by a compact external RF transceiver and data processing hub known as the "Epidermal Skinpatch," designed to be wearable and compatible with clinical implant considerations. Feng et al.[262] introduced a robust wireless power transmission system enhanced by an EM lens and a novel method for data communication among distributed implantable medical devices. The proposed techniques addressed common issues associated with multiple implanted devices, including low power transfer efficiency through biological tissues, uneven power delivery to distributed devices, interference between simultaneous wireless power and data transmission, and intermodulation distortion between various data channels. Data communication was facilitated by a novel low-power backscatter-Code-Division Multiple Access (CDMA) scheme, allowing data transmission from multiple nodes simultaneously operating with the same carrier frequency (on the same channel) by reflecting power carriers to the primary side. Simultaneous communication between two nodes at a rate of 125 kbps with a power consumption of 1.05mW was demonstrated. Wang et al.[263] adopted the approach of integrating data communication links with the wireless power channel, encompassing both a downlink and an uplink, proposing a novel design for the uplink, based on a specialized tapped coil and a straightforward passive circuit for robust pulsed magnetic field generation. This potent field, oscillating at the resonant frequency identical to the WPT carrier, facilitates WDT over extended distances through the WPT channel. Hosur et al.[264] developed a hybrid sub-MHz magnetic-ultrasonic interrogation method, named MagSonic, utilizing a single magnetoelectric transducer embedded within the implant. They demonstrated the reception of wireless power through magnetic field and simultaneous uplink data transmission using ultrasounds. At a depth of 40 mm, the MagSonic link achieves a 100 kbps uplink data rate with a bit error rate of $\leq 10^{-5}$, employing 190 pJ/bit transmitted energy and delivering 8 mW of power in tissue. Most commonly, power and communication links are carried out with physically separated antennas. In such systems, called active responders (Figure 5H), a wireless power harvesting unit receives and stores power sent from an external transmitter, distributing it to other modules (sensor module, analog-to-digital

© 2024 The Author(s). Advanced Materials Technologies published by Wiley-VCH GmbH

2365709x, 0, Downloaded from https://onlinelibrary.wiley.com/doi/10.1002/admt.202400797 by University Of Oxford, Wiley Online Library on [19/11/2024]. See the Terms and Conditions (https://onlinelibrary.wiley.com/terms-and-conditions) on Wiley Online Library for rules of use; OA articles are governed by the applicable Creative Commons License

converter, data storage module, etc.). Then, based on the requests from the external unit, data communication are transmitted to the external reader through a separate antenna.[94]

5. Technical Constraints and Figures of Merit

5.1. Design Requirements

WEPT, WIPT and WDC systems have several design requirements, which depend on the application mode (wearable, implantable, etc.), the target tissues and the final purpose (sensing, stimulation, etc.). Besides technical constraints related to the minimum power consumption for supplying the devices or for data transmission, biological constraints also play an important role, to a higher extent for implantable biomedical devices. These requirements can be summarized in the following points: (i) biocompatibility and bio-integration, (ii) geometry and dimensional parameters, (iii) biomechanical matching, (iv) durability and isolation, (v) application modalities, (vi) specific absorption rate (SAR) limits. Operation frequencies, power levels and operational distances are summarized in Table 1.

5.1.1. Biocompatibility and Bio-Integration

The reactions of a bio-tissue after being in contact with a foreign device (especially an implant) can range from minor immune responses with the buildup of defensive cells around the device to significant disruptions in the function of nearby organs.[279] Foreign-body responses (FBR) can degrade the performances, sensitivity and efficiency of bionic and bioelectronic interfaces.[280,281] Ensuring the safety and compatibility of wearable and implantable systems is thus paramount and selecting materials that establish a secure interface between the device and the tissue is a critical aspect of the design. The chemical affinity between the constituent materials and the surrounding tissue (surface chemistry) plays a key role in their interaction.[282] Studies have found that surface functionalization with carboxyl groups,[283] anti-fouling coatings[284] and smoother surface morphologies[285,286] promote better tissue integration and reduce inflammatory responses.

5.1.2. Geometry and Dimensional Parameters

The miniaturization scale and dimensional limitations are fundamental elements in the advancement of wireless systems for bionics and bioelectronics. Their shape must be carefully tailored to fit anatomical structures and physiological dynamics, ensuring comfort and optimal performance. Miniaturization is essential for reducing device size and weight, minimizing tissue disruption, invasiveness and biocompatibility issues. Furthermore, dimensional constraints dictate the spatial boundaries imposed by anatomical regions or implant sites, necessitating compact and streamlined designs to navigate confined spaces or accommodate intricate tissue geometries (e.g. epidermal,[125] subdermal,[201] epidural,[287] subdural,[288] epicardial,[289] endocardial,[290] etc.). Advanced fabrication methods such as microfabrication, 3D printing, and nanotechnology offer precise control over device dimensions, enabling the creation of ultra-compact and intricately structured bioelectronic systems. Miniaturization of the overall device design implies the size reduction of each single component, as well as the increase in the density of operations that can be achieved by the system. This is valid especially in neuroengineering, where smaller electrocorticography implants can detect electroneurogam (ENG) or electromyogram (EMG) signals from multiple sites through high-density electrode arrays[291] or neural dust ($0.8 \times 3 \times 1$ mm, device area of $0.21 cm^2$).[58] Examples of miniaturization can be found among ocular implants based on intelligent contact lenses or sensors to monitor intraocular pressure, with overall sub-mm^3 device volume.[143] However, reducing the dimensions of wireless circuits can modify their performances, especially at high frequencies (>2–3 GHz): most biomedical systems operate at lower frequencies (<10 MHz or in the UHF band, 300 MHz–3 GHz) where miniaturization can be more effective, achieving high wireless power transfer efficiency.[132,292] Wireless flexible antennas and coils have undergone significant miniaturization:[293] recent research has demonstrated antennas with volumes as small as $8.5 \times 8.5 \times 1.27$ mm^3, as proposed in a dual-band antenna design capable of receiving signals at 2.4 GHz and reflecting signals at 4.8 GHz.[294] Singh and Kaur[295] proposed a miniaturized skin implantable biocompatible microstrip antenna for biotelemetry applications at 2.4–2.48 GHz. The volume of the antenna is 42.68 mm^3 with dimensions $8.2 \times 6.94 \times 0.75$ mm^3 and it is functional at the ISM band,[178] which makes it best suitable for implantable devices. These advancements highlight the potential for further miniaturization in wireless antennas and coils for flexible bioelectronics, enabling seamless integration into wearable/implantable devices with reliable performance.[96,292,296–298]

5.1.3. Biomechanical Matching

Besides dimensional limitations, it is essential to tailor the design to conform to the tissue walls, ensuring compatibility and avoiding chronic inflammation or trauma.[299,23,300,301,125,88,90,100] The device's structure should in fact accommodate changes in tissue shape, necessitating mechanical properties that match those of the tissue,[279,302,303] e.g. following the compression-expansion cycles of blood vessels, contraction-release motions of the heart, frequent skin deformations or unusual movements of the spinal cord. The biomechanical mismatch may in fact induce large insertion-related lesions,[44,68,304] cell apoptosis and inflammation reactions,[32,33] to a higher extent if more rigid bioelectronic interfaces are employed.[25,305] Improved mechanical harmony and compliance between the biotic and abiotic interfaces, with minimally disruptive bio-integration,[23,306–309] can be achieved with soft/flexible materials and hybrid constructs of stiff materials[310] and soft supports[311] (e.g. nanowires, mesh structures, carbon nanomaterials,[312–314] nanoribbons,[315,316] conjugated polymers,[317–319] etc.), or through designs capable of stretching, twisting and deforming more complexly, such as buckling, serpentine patterns, origami, and textile designs.[320] Many research efforts have been made in the field of flexible and stretchable antennas, where interconnects can be designed with the shape of serpentine metal traces, ensuring high

© 2024 The Author(s). Advanced Materials Technologies published by Wiley-VCH GmbH

2365709x, 0, Downloaded from https://onlinelibrary.wiley.com/doi/10.1002/admt.202400797 by University Of Oxford, Wiley Online Library on [19/11/2024]. See the Terms and Conditions (https://onlinelibrary.wiley.com/terms-and-conditions) on Wiley Online Library for rules of use; OA articles are governed by the applicable Creative Commons License

conductivity and reliable operation even up to very high strains (≈300%,[321–323]), thus totally suitable for strains induced by natural biological motions (< 20–50%).[88,125] Soldering off-the-shelf electronic components (e.g. microcontrollers, RF switches, voltage regulators, oscillators, etc.) is the commonly adopted technique to fabricate flexible boards: although this increases the overall stiffness of the resulting systems, they can still support device-level deformability.[23,300,303]

5.1.4. Durability and Isolation

Durability and effective isolation are paramount considerations in the design and deployment of wireless wearable and implantable bioelectronic devices, ensuring longevity and optimal performance while safeguarding user safety.[4] These devices often operate in challenging physiological environments, subjected to mechanical stress, temperature fluctuations, and exposure to bodily fluids. Encapsulation serves as a crucial protective barrier, shielding sensitive electronic components from external influences and biological interactions, preserving device integrity and preventing corrosion or degradation.[324]

In wireless wearable devices, encapsulation plays a vital role in enhancing durability and resilience to external factors encountered during daily activities. Encapsulation ensures resistance to bending, stretching, and exposure to sweat or environmental moisture, prolonging device lifespan and maintaining accuracy and reliability of data acquisition. Similarly, in implantable bioelectronic devices, encapsulation serves as a barrier against physiological fluids, immune responses, and mechanical stresses encountered within the body. Furthermore, effective isolation through encapsulation minimizes electromagnetic interference (EMI) and cross-talk between electronic components, ensuring signal integrity and reliable wireless communication.[325] By enclosing antennas, transmitters, and receivers in electrically insulating materials, encapsulation prevents interference from external electromagnetic sources and reduces the risk of signal distortion or loss. Additionally, encapsulation materials with low dielectric constants facilitate efficient transmission and reception of electromagnetic signals, optimizing wireless connectivity and energy transfer in wearable and implantable bioelectronic devices.[326] The most common options for encapsulating wireless microfabricated bioelectronics include parylene C,[327] polyimide,[328] poly(dimethyl siloxane) (PDMS),[329] but more advanced ceramic oxides and nitrides can be used to enhance barrier properties,[330–332] as well as hybrid multilayer organic-inorganic structures.[333–336] Noteworthy, durability and long-term isolation is less crucial for temporary bioresorbable wireless bioelectronics.[40,337,338] Comprehensive reviews and works on encapsulation materials for flexible bioelectronics can be found in literature, and especially for wireless devices.[339–346]

5.1.5. Application Modalities

The design of flexible bionic and bioelectronic systems is closely correlated with the way they are going to be implemented and applied on the human or animal body. While wearable devices pose fewer challenges in terms of application protocols, implantable bioelectronics often require precise and validated procedures. The risks associated with complex surgical procedures to implant bioelectronics may often outweigh the benefits derived from the diagnostic insights provided by these devices. Therefore, it is imperative that researchers prioritize minimally invasive techniques and carefully weigh the advantages offered by the device when considering more invasive approaches. The device location, in fact, determines the application modality. In the context of implantable cardiovascular sensors, for instance, devices can be implanted on the sidewalls of the blood vessels externally or internally (intravascular), and this modifies completely the required implantation procedure (through intramuscular surgery with cuff configuration[347,348] or via catheters[247,349,350]). Moreover, incorporating diagnostic features into therapeutic implantable devices serves as a means to avoid unnecessary surgeries: in fact, sensors can assess the structural integrity of therapeutic devices or monitor post-surgery complications, e.g. detecting cracks, damages or loosening in metal/ceramic prostheses,[351] measuring joint contact forces and moments or strains in ligaments,[352] monitoring intraocular pressure during application of wireless smart contact lenses.[353,354]

5.1.6. Specific Absorption Rate (SAR) Limits

Specific absorption rate (SAR) limits serve as critical safety parameters for wearable and implantable bioelectronics, delineating the permissible levels of electromagnetic energy absorption by biological tissues. Some of the radiation energy carried both by the wireless power source and the handheld device, may be absorbed by the host tissue leading to an increase in the tissue temperature due to the power loss of dielectric polarization (related to vibrations of water molecules, free ions and other bound charges). SAR is a measure of the rate at which energy is absorbed per unit mass by a human body when exposed to an electromagnetic field, especially in the RF range (W kg^{-1}). The European Committee for Electrotechnical Standardization (CENELEC) defines it as the time derivative of the incremental energy (dE) absorbed by (dissipated in) an incremental mass (dm) contained in a volume element (dV) of given density (ρ, kg/m^3), i.e.:[355]

$$\mathrm{SAR} = \frac{d}{dt}\left(\frac{dE}{dm}\right) = \frac{d}{dt}\left(\frac{dE}{\rho dV}\right) \tag{4}$$

Its integral definition is:[356]

$$\mathrm{SAR} = \frac{1}{V}\int_{tissue} \frac{\sigma(\boldsymbol{r})\,|\boldsymbol{E}(\boldsymbol{r})|^2}{\rho(\boldsymbol{r})} d\boldsymbol{r} \tag{5}$$

where $\sigma(\boldsymbol{r})$ is the tissue electrical conductivity, $\boldsymbol{E}(\boldsymbol{r})$ is the RMS electric field, $\boldsymbol{r}$ is the space vector. Other definitions of SAR include the temperature increase in the tissue or the induced current density value in the body tissue (A/m^2).[355] This parameter represents a cornerstone in the development and deployment of wireless bionics and bioelectronics, given the intimate interaction of devices with the human/animal body, where they transmit data, receive power, or deliver therapeutic interventions. SAR is contingent upon various factors, including tissue properties and

© 2024 The Author(s). Advanced Materials Technologies published by Wiley-VCH GmbH

2365709x, 0, Downloaded from https://onlinelibrary.wiley.com/doi/10.1002/admt.202400797 by University Of Oxford, Wiley Online Library on [19/11/2024]. See the Terms and Conditions (https://onlinelibrary.wiley.com/terms-and-conditions) on Wiley Online Library for rules of use; OA articles are governed by the applicable Creative Commons License

the frequency of electromagnetic signals.[357,358] From a simplified model it can be shown that:[359–361]

$$SAR = \frac{\sigma A^2 f^2 B^2 D_c}{2\rho} \quad (6)$$

where A is the area crossed by the electromagnetic field; f is the RF frequency; B is the mean amplitude of the RF-pulse; D_c is the RF pulse duty cycle. Therefore, SAR is proportional to the tissue electrical conductivity, increases significantly with the body size, is proportional to the square of the RF frequency and its duty cycle.

Wearable and implantable bioelectronics must meticulously adhere to SAR constraints to prevent adverse effects such as tissue heating, which can lead to discomfort, tissue damage, or even organ dysfunction. The significance of SAR compliance is accentuated in implantable devices, where the proximity to vital organs and tissues necessitates stringent safety measures. For instance, devices implanted near sensitive areas such as the brain or the heart demand meticulous attention to SAR limits to mitigate the risk of thermal damage. Furthermore, the depth of implantation plays a pivotal role, as deeper placement increases the amount of tissue through which signals must traverse, consequently elevating SAR levels. In wearable bioelectronics, SAR considerations are paramount due to prolonged contact with the skin, necessitating designs that optimize energy transfer while remaining within SAR. Researchers and developers employ sophisticated techniques such as computational modeling, simulations, and experimental measurements to assess SAR levels and ensure compliance with safety standards. This is crucial to establish standardized protocols to streamline regulatory compliance and ensure the safe deployment of wearable and implantable bioelectronics in clinical and everyday settings. Integrating SAR considerations into the design and development process early on allows to prioritize user safety.[276]

5.2. Figures of Merit

The main figures of merit for quantifying the performance of WPT and WDC technologies in wearable and implantable bioelectronics encompass several key parameters. These include power transfer efficiency, which measures the proportion of transmitted power successfully received by the device and directly impacts its functionality and longevity. Communication range, bandwidth and reliability are also essential, ensuring seamless data transmission between devices and external sources over varying distances and environmental conditions. Furthermore, factors such as data transfer rate, latency, Q-factors and energy consumption play significant roles in determining the efficiency and responsiveness of communication protocols, particularly in real-time applications such as physiological monitoring or neural stimulation. Moreover, considerations of safety, including SAR and EMI, are paramount to prevent adverse effects on biological tissues. **Table 2** collects and describes the main parameters and figures of merit for WEPT, WIPT and WDC technologies, with the corresponding analytical expressions. References are indicated in the table for a more detailed list of parameters and figures of merit in literature, especially for specific energy harvesting mechanisms.

6. Materials for Wireless Bionics and Bioelectronics

Wireless flexible bionic systems rely on a vast range of suitable materials, both for the fabrication of the electrical interconnects and the realization of substrates and encapsulations.

Material choice plays a crucial role in the design and efficiency of WPT systems for biomedical devices. In such applications, materials must meet strict requirements related to biocompatibility, electrical properties, mechanical flexibility, and, in some cases, biodegradability. They must be non-toxic, non-inflammatory, conformable and safe for long-term exposure to body tissues and fluids. The materials should also ensure that the wireless power transfer system operates efficiently within the complex environment of the human body, which includes tissues of varying conductivity and permittivity.[296,297] Material choice significantly impacts the data transfer rate in WDC systems as well, by influencing factors such as signal attenuation, bandwidth, antenna efficiency, and noise. These factors, in turn, affect the overall performance of the wireless system, including the achievable data transfer rate.[393]

The materials used in antennas, coils, and interconnects in WPT systems need to have high electrical conductivity and appropriate dielectric properties to minimize energy loss and ensure efficient power transfer.[394] High dielectric materials with low loss, like ceramics, are ideal for components that require high capacitance with minimal energy dissipation, while low dielectric and low-loss materials, such as certain polymers and carbon-based materials, are better suited for applications requiring flexibility and minimal signal degradation. The dielectric loss is critical in determining how much energy is lost as heat, which can affect both the efficiency of WPT and the clarity of WDC signals. Materials with low dielectric loss are preferred for applications where maintaining signal integrity and minimizing energy loss are crucial.

Figure 6 illustrates the ranges of electrical conductivity and dielectric properties of materials used in WPT and WDC systems (i.e., dielectric constant (relative permittivity) and dielectric loss). We highlight that functional materials selected for specific WPT/WDC applications (optical, electromechanical, electrothermal, biochemical, etc.) should be also rated on the base of specific properties or figures of merit related to the corresponding energy-conversion mechanism (see Table 2), however this is out of the scope of this review. In this section, we present and describe the main categories of materials used to develop these systems, taking into account two main groups, i.e., biocompatible materials and bioresorbable materials. We further classify them based on their nature (metals, polymers, composites).

6.1. Biocompatible Materials

For a material to be deemed biocompatible, it must not induce an unacceptable level of harm to the host. Assessment of biocompatibility often revolves around scrutinizing a material's cytotoxicity or carcinogenic potential,[398] while in vivo implementation (especially for implantable devices) can reveal more intricate host reactions and FBR. These consist of releasing cytotoxic and neurotoxic biological factors into the peri-implant space, resulting in localized cell death,[399] chronic inflammation, tissue degeneration, fibrosis.[400] Moreover, the materials need to

© 2024 The Author(s). Advanced Materials Technologies published by Wiley-VCH GmbH

2365709x, 0, Downloaded from https://onlinelibrary.wiley.com/doi/10.1002/admt.202400797 by University Of Oxford, Wiley Online Library on [19/11/2024]. See the Terms and Conditions (https://onlinelibrary.wiley.com/terms-and-conditions) on Wiley Online Library for rules of use; OA articles are governed by the applicable Creative Commons License

Table 2. Figures of merit of WEPT, WIPT and WDC for flexible bionic and bioelectronic systems.

Figure of merit			Description	Notes	Ref.
Name	Unit	Symbol/Expression			
WIRELESS EXTRINSIC POWER TRANSFER (WEPT)					
Electromagnetic power transfer					
Specific absorption rate (SAR)	W kg^{-1}	$SAR = \frac{1}{V}\int \frac{\sigma(\mathbf{r})\lvert\mathbf{E}(\mathbf{r})\rvert^2}{\rho(\mathbf{r})} d\mathbf{r}$ $SAR = \frac{\sigma A^2 f^2 B^2 D_c}{2\rho}$	It is a measure of the rate at which energy is absorbed per unit mass by a tissue when exposed to an electromagnetic field, especially in the RF range.	σ: electrical conductivity of the tissue (S/m); E: RMS electric field; ρ: mass density of the tissue (kg/m^3); A: area crossed by the EM field; B: mean amplitude of the RF-pulse; f: RF frequency; D_c: RF pulse duty cycle.	[355,358]
Transmitting distance	m	d	It is the distance between the power source (transmitter) and the receiving circuit.		
Quality factor (Q-factor)	-	$Q = E_{stored}/E_{lost}$	It is the ratio of the energy stored in the resonator to the energy supplied to it, per cycle, to keep signal amplitude constant, at a frequency where the stored energy is constant with time.	E_{stored}: energy stored in the circuit per cycle E_{lost}: energy lost in the circuit per cycle	[362]
Q-factor for an RF resonant circuit (Bandpass Q-factor)	-	$Q = F_0/F_{-3dB}$	It measures the bandwith provided by the RF resonator.	F_0: centre frequency of the tuned circuit F_{-3dB}: frequency offset from the centre frequency when the response falls by -3dB	[363]
Q-factor for an inductor (coil) (Component Q-factor)	-	$Q = 2\pi f L/R$	It is the ratio of an inductor's inductive reactance to its resistance at a particular frequency.	L: self-inductance; R: resistance; f: operating RF frequency	[363]
Coupling coefficient for inductively coupled coils	-	$\kappa_L(f) = \frac{M_{12}}{\sqrt{L_1 L_2}} \cdot \frac{2}{\sqrt{(1+(f/f_1)^2)(1+(f/f_2)^2)}}$	It is a measure of how much power from the generated EM field is induced in the secondary coil. It is related to the reflected impedance from the secondary on the primary side.	L_1,L_2: self-inductances of the individual coils; M_{12}: their mutual inductance; $f_1 f_2$ are the resonance frequencies of the two coils (TX and RX circuits); f: operating RF frequency	[117,144]
Coupling coefficient for inductively coupled resonant coils	-	$\kappa_L(f_R) = \frac{M_{12}}{\sqrt{L_1 L_2}}$	It is a measure of how much power from the generated EM field is induced in the secondary coil, at resonance.	f_R: operating RF resonance frequency	[117,144]

(*Continued*)

© 2024 The Author(s). Advanced Materials Technologies published by Wiley-VCH GmbH

2365709x, 0, Downloaded from https://onlinelibrary.wiley.com/doi/10.1002/admt.202400797 by University Of Oxford, Wiley Online Library on [19/11/2024]. See the Terms and Conditions (https://onlinelibrary.wiley.com/terms-and-conditions) on Wiley Online Library for rules of use; OA articles are governed by the applicable Creative Commons License

Table 2. (Continued)

Figure of merit			Description	Notes	Ref.
Name	Unit	Symbol/Expression			
Coupling coefficient for capacitively coupled resonant plates	-	$\kappa_C(f_R) = \frac{C_{12}}{\sqrt{C_1 C_2}}$	It is a measure of how much power from the generated EM field is induced in the secondary capacitor plate, at resonance.	C_1,C_2: capacitances of the individual capacitors; C_{12}: mutual capacitance.	[146,151]
Coupling efficiency (dimensionless figure of merit)	-	$U = \kappa\sqrt{Q_1 Q_2}$	It is a more general parameter that measures how much efficient is the coupling between two coils or two capacitor plates.	κ: coupling coefficient; Q_1,Q_2: Q-factors for each coil/capacitor.	[93,119]
Optimal load factor for two coupled coils	-	$a_{max} = 2\pi f L_2/R_L$	It is similar to a quality factor but regarding the connection between the load and the receiver.	R_L: load resistance connected to the receiver.	[364]
Maximum achievable link efficiency (non-resonant)	-	$\eta_{opt,\ NR} = \frac{U^2}{2+U^2+2\sqrt{1+Q_2^2+U^2}}$	It is the maximum efficiency of an inductive coupling link, assuming ideal voltage source, optimized load and neglecting any losses in the tissue between the coils.		[364]
Maximum achievable link efficiency (resonant)	-	$\eta_{opt,R} = \frac{U^2}{(1+\sqrt{1+U^2})^2}$	It is the maximum efficiency of an inductive coupling link, assuming ideal voltage source, optimized load and neglecting any losses in the tissue between the coil. This parameter is valid also for CCPT.		[119,137,138,365]
Link efficiency	-	$\eta_{link} = \frac{P_2}{P_{IN}+P_2} = \frac{U^2}{1+U^2}$	It is the ratio between the power transferred to the receiver and the overall consumed power.	P_2: power transferred to the receiver $P_{IN} = P_1$: power consumed at the transmitter	[364]
Power transfer efficiency (PTE)	-	$\eta = PTE = \frac{P_2}{P_{IN}}$	It is the ratio between the power transferred to the receiver and the power consumed at the transmitter.		[364]
Power transfer efficiency (PTE) (2)	-	$\eta = PTE = \frac{\lvert S_{21}\rvert^2}{1-\lvert S_{11}\rvert^2}$	It is the power transfer efficiency seen in a two-port network model	S_{ij}: reflection parameters (transmitter, receiver)	[366]
Overall power transfer efficiency	-	$\eta_T = \frac{P_L}{P_{IN}}$	It is the ratio between the power transferred to the load (connected to the receiver) and the power at the transmitter.	P_L: power transferred to the load	[364]
Overall link efficiency	-	$\eta_T = \frac{P_L}{P_{IN}+P_2} = \frac{R_L}{R_2}\frac{U^2}{1+U^2}$	It is the ratio between the power transferred to the load (connected to the receiver) and the overall consumed power in the transmission.	R_2: resistance of the receiver.	[364]

(*Continued*)

© 2024 The Author(s). Advanced Materials Technologies published by Wiley-VCH GmbH

2365709x, 0, Downloaded from https://onlinelibrary.wiley.com/doi/10.1002/admt.202400797 by University Of Oxford, Wiley Online Library on [19/11/2024]. See the Terms and Conditions (https://onlinelibrary.wiley.com/terms-and-conditions) on Wiley Online Library for rules of use; OA articles are governed by the applicable Creative Commons License

Table 2. (Continued)

Figure of merit			Description	Notes	Ref.
Name	Unit	Symbol/Expression			
Loss fraction figure of merit	-	$FoM = \frac{(1-\eta_{ref})\eta_{SUT}}{\eta_{ref}(1-\eta_{SUT})}$	The efficiency is measured from the input of the transmit coil to the output of the receive coil, and does not include circuit losses.	η_{ref}: efficiency of power transfer of a reference system, depending on diameter of resonant coils, and distance between the coils; η_{SUT}: power transfer efficiency for the system-under-test (SUT)	[367]
Wireless power transfer efficiency	-	$\eta_{WPT} = \eta_{gen}\,\eta_{beam}\eta_{rec}$	It is a measure of the global wireless power transfer process, valid as well for non-electromagnetic mechanisms.	η_{gen}: efficiency for generation of the oscillation from DC current η_{rec}: efficiency for reception and rectification back to DC	[1]
Efficiency of beam propagation	-	$\eta_{beam} = \eta_{TX}\,\eta_{coll}\eta_{option}\eta_{transm}\eta_{RX}$	It is a measure of the efficiency related to the beam propagation subsystem, between the transmitter and the receiver.	η_{TX},η_{RX}: efficiency of the transmitter and receiver antennas; η_{option}: efficiency of all the optional components; η_{coll}: efficiency for the collection process, related to the spillover losses; η_{transm}: efficiency related to the absorption and scattering losses.	[1]
Figure of merit for beam propagation	-	$FO\,M_{beam} = 10\log(\frac{d^2}{(n+2)D\lambda}\eta_{beam})$ $FO\,M_{beam\,Alt} = 10\log(\frac{d^2}{(n+2)D\lambda})\cdot\eta_{beam}$	It is a generalized figure of merit taking into account the geometry and distance between the transmitter and receiver	d: transmitting distance; n: number of optional components in the system (focusing components, polarizers, transformers, etc.); D: largest dimension perpendicular to the axis of propagation; λ: wavelength.	[1]
Optic power transfer					
Photoelectric power efficiency	-	$\eta_{PV} = P_{OUT}/I_{SURF} = (I_{SC}V_{OC}\cdot FF)/I_{SURF}$	It is the ratio between the converted electrical power and the incident optical power on the receiver	P_{OUT}: output power; I_{SURF}: surface irradiation power (on the receiver); I_{SC}: short-circuit current; V_{OC}: open-circuit voltage; FF: fill factor.	[368,369]
Emitting side efficiency	-	$\eta_{emit} = \Phi/P_{IN}$	It is the efficiency of emission from the optical transmitter	Φ: power source's radiant flux; P_{IN}: electrical input power to the transmitter.	[370]
Ultrasound power transfer					
Incident ultrasonic power intensity	W/m^2	$I_P = \frac{p^2}{2\rho\nu}\,D_c$	It measures the power of the ultrasound waves per unit area	D_c: duty cycle of the ultrasound wave; ρ: density of the propagation medium; p: peak pressure of the ultrasound wave; ν: sound velocity in the medium.	[371]

(*Continued*)

© 2024 The Author(s). Advanced Materials Technologies published by Wiley-VCH GmbH

2365709x, 0, Downloaded from https://onlinelibrary.wiley.com/doi/10.1002/admt.202400797 by University Of Oxford, Wiley Online Library on [19/11/2024]. See the Terms and Conditions (https://onlinelibrary.wiley.com/terms-and-conditions) on Wiley Online Library for rules of use; OA articles are governed by the applicable Creative Commons License

Table 2. (Continued)

Figure of merit			Description	Notes	Ref.
Name	Unit	Symbol/Expression			
Rayleigh distance (separation between near-field and far-field region)	m	$RD = \frac{r_{TX}^2}{\nu} f_{exc}$	It gives the minimum distance at which an ultrasonic transducer should be placed to avoid near-field effects.	r_{TX}: radius of the transmitter; f_{exc}: excitation frequency provided by an external electrical generator	[372]
Ultrasound power efficiency	-	$\eta_{US} = P_{OUT}/I_p$	It is the ratio between the converted electrical power and the incident ultrasonic power on the receiver	P_{OUT}: output power.	[372]
Emission transfer function	N/V	$H_{TX} = F_{TX}/V_{ex}$	It is the ratio between the force at the front face of the emitter (transmitter) and the external voltage excited across the electrodes of the transmitter.	F_{TX}: force at the front face of the emitter; V_{ex}: external voltage excited at the emitter.	[373]
Reception transfer function	V/N	$H_{RX} = V_{RX}/F_{RX}$	It is the ratio between the voltage induced on the electrodes of the receiver and the force of the ultrasound waves on the front face of the receiver	F_{RX}: force at the front face of the receiver; V_{RX}: voltage induced at the receiver.	[373]
WIRELESS INTRINSIC POWER TRANSFER (WIPT)					
RF energy harvesting					
Harvested RF power	W	$P_R = \frac{G_R G_T \lambda^2}{(4\pi d)^2 L} P_T$	It is the power transferred at the receiver through the RF energy harvesting process.	P_T: transmitted power; λ: RF signal's wavelength; d: distance between the RF power source and the harvesting node; G_R, G_T: transmitter and receiver gains of the antenna; L: path loss factor	[115,180]
Free-space path loss	dB	$\mathcal{P}_L\,(dB) = 32.44 + 20\log_{10}(fd) - G_T - G_R$	It is a parameter to quantify the loss in the signal strength		[181]
Two-ray ground-reflection path loss	dB	$\mathcal{P}_L\,(dB) = \frac{d^2}{G h_T^2 h_R^2}$	The two-ray ground-reflection model is a multipath radio propagation model which predicts the path losses between the transmitter and the receiver when they are in line of sight (LOS)	d: horizontal distance between transmitter and receiver G: combined gain along the LOS path or the ground-reflected path h_T,h_R: heights of the transmitter and receiver	[356]
Power conversion efficiency	-	$\eta_{PCE} = \frac{P_{DC}}{P_{IN}} = \frac{V_{DC}^2}{R_{load}} \cdot \frac{1}{\mathcal{P}_L}$	It is the ratio between the converted DC power and the incident RF power at the antenna	P_{DC}: converted DC power P_{IN}: incident RF power at the receiver	[182]

(*Continued*)

© 2024 The Author(s). Advanced Materials Technologies published by Wiley-VCH GmbH

2365709x, 0, Downloaded from https://onlinelibrary.wiley.com/doi/10.1002/admt.202400797 by University Of Oxford, Wiley Online Library on [19/11/2024]. See the Terms and Conditions (https://onlinelibrary.wiley.com/terms-and-conditions) on Wiley Online Library for rules of use; OA articles are governed by the applicable Creative Commons License

Table 2. (Continued)

Figure of merit			Description	Notes	Ref.
Name	Unit	Symbol/Expression			
Kinetic energy harvesting (PNG)					
Electromechanical coupling coefficient	-	$k_{ij}^2 = d_{ij}^2/(\epsilon_{ii}^T s_{jj}^E)$	It is a measure of the conversion of mechanical energy into electrical energy in a piezoelectric material. It is defined also as the ratio between converted energy and supplied energy.	d_{ij}: piezoelectric coefficient. ϵ_{ii}^T: mechanical strain at constant stress. s_{jj}^E: elastic compliance at constant electric field.	[374,375]
Piezoelectric coefficients (product)	$(pm/N)^2$	$FOM = d_{ij} \cdot g_{ij}$	It is a measure of the piezoelectric performance of the energy harvesting system.	g_{ij}: voltage piezoelectric constants	[374,375]
Energy-conversion efficiency	-	$\eta = P_{out}/P_m$	It measures the efficiency of energy conversion of the PNG	P_{out}: output electrical power P_m: input mechanical power	[175]
Other specific figures of merit					[374–377]
Kinetic energy harvesting (TNG)					
Material figure of merit	$(\mu C/m)^2$	$FO\,M_M = \sigma_S^2$	It measures the triboelectrification capability of the materials	σ_S: surface charge density	[177,378,379]
Structural figure of merit	-	$FO\,M_S = \frac{2\epsilon_0}{\sigma_S^2}\frac{E_m}{Ax_{max}}$	It is a measure of the effectiveness of the design and architecture of the energy harvesting system.	E_m: output energy per cycle A: triboelectrification area x_{max}: maximum displacement	[177,378,379]
Performance figure of merit	$(\mu C/m)^2$	$FO\,M_P = FOM_M FO\,M_S = \frac{2\epsilon_0 E_m}{Ax_{max}}$	It is a measure of the full energy harvesting performance of the system.	-	[177,378,379]
Energy-conversion efficiency	-	$\eta = E_{out}/E_{in}$	It measures the efficiency of energy conversion of the TNG	E_{out}: output energy per cycle E_{in}: total energy per cycle (output + dissipation)	
Other specific figures of merit					[177,378,379]
Photovoltaic energy harvesting					
Power conversion efficiency	-	$\eta_{PV} = PCE = P_{OUT}/P_{IN} = (I_{SC}V_{OC} \cdot FF)/P_{IN}$	It is the ratio between the converted electrical power and the incident optical power on the solar cell	P_{OUT}: output power; P_{IN}: irradiated optical power; I_{SC}: short-circuit current; V_{OC}: open-circuit voltage; FF: fill factor.	[380,381]
Other specific figures of merit					[380,381]
Thermal energy harvesting					

(*Continued*)

© 2024 The Author(s). Advanced Materials Technologies published by Wiley-VCH GmbH

2365709x, 0, Downloaded from https://onlinelibrary.wiley.com/doi/10.1002/admt.202400797 by University Of Oxford, Wiley Online Library on [19/11/2024]. See the Terms and Conditions (https://onlinelibrary.wiley.com/terms-and-conditions) on Wiley Online Library for rules of use; OA articles are governed by the applicable Creative Commons License

Table 2. (Continued)

Figure of merit			Description	Notes	Ref.
Name	Unit	Symbol/Expression			
Maximum thermoelectric efficiency	-	$\eta_{max} = \frac{\Delta T}{T_h} \frac{\sqrt{1+Z\cdot T_{avg}}-1}{\sqrt{1+Z\cdot T_{avg}}+\frac{T_c}{T_h}}$	It is the product of the Carnot efficiency and a reduction factor depending on a material figure of merit. It represents the maximum achievable efficiency for a thermoelectric generator	ΔT: temperature difference between hot and cold sides; T_h,T_c, T_{avg}: temperatures at the hot, cold sides and their average $Z = S^2\,\rho^{-1}\kappa^{-1}$ material's figure of merit. S: Seeback coefficient; ρ: electrical resistivity; κ thermal conductivity	[382]
Dimensionless figure of merit	-	$ZT = S^2\,\rho^{-1}\kappa^{-1}T$	It is a measure of the effectiveness of a thermoelectric material		[383]
Performance figure of merit for PyNG	-	$F_E'' = \frac{p^2\Delta T}{c_E\epsilon_{33}}$	It is a measure of the energy harvesting capability of a pyroelectric material	p: pyroelectric coefficient ($mC/(m^2K)$); ϵ_{33}: permittivity of the pyroelectric material; c_E: specific heat capacity.	[384]
Other specific figures of merit					[385–387]
Biochemical energy harvesting					
Biofuel cell reaction efficiency	-	$\eta_{BFC} = -\frac{nFE_{cell}}{\Delta H}$	It is the ratio of electrical free energy to reaction enthalpy change represents the fuel cell's thermodynamic efficiency.	ΔH: enthalpy change during the redox reaction; n: number of electrons involved in the reaction; F: Faraday's constant; E_{cell}: cell's electrochemical potential.	[80,83,222]
Other specific figures of merit					[80,83,222]
WIRELESS DATA COMMUNICATION (WDC)					
Resonant frequency for LC systems	Hz	$f_{res} = \frac{1}{2\pi\sqrt{LC}}$	It is the resonance frequency of the LC systems	L: inductance; C: capacitance.	
Peak power gain of antenna	dB	$G_P = 10\log_{10}\frac{P_{out}(\theta,\phi)}{P_T} = 10\log_{10}(\frac{4\pi kA}{\lambda^2})$	It is the degree of directivity of an antenna's radiation pattern. It is equal to the product of the antenna's electrical efficiency and directivity.	$P_{out}(\theta,\phi)$: radiated power in a specific direction; P_T: power supplied to the antenna (sum of the radiated power and the ohmic losses in the antenna); k: dimensionless efficiency factor; A: physical aperture area; λ: signal wavelength	[115,180]

(*Continued*)

© 2024 The Author(s). Advanced Materials Technologies published by Wiley-VCH GmbH

2365709x, 0, Downloaded from https://onlinelibrary.wiley.com/doi/10.1002/admt.202400797 by University Of Oxford, Wiley Online Library on [19/11/2024]. See the Terms and Conditions (https://onlinelibrary.wiley.com/terms-and-conditions) on Wiley Online Library for rules of use; OA articles are governed by the applicable Creative Commons License

Table 2. (Continued)

Figure of merit			Description	Notes	Ref.
Name	Unit	Symbol/Expression			
Peak directivity gain of antenna	dB	$G_D = 10\log_{10}\frac{P_{out}(\theta,\phi)}{P_R}$	It is the degree of directivity of an antenna's radiation pattern. It is equal to the product of the antenna's electrical efficiency and directivity.	$P_{out}(\theta,\phi)$: radiated power in a specific direction; P_R: total radiated power; k: dimensionless efficiency factor; A: physical aperture area; λ: signal wavelength	[115, 180]
Frequency bandwidth (BW)	Hz	$BW = f_{max} - f_{min}$	It is the continuous range of frequencies within a WDC technique is operational. It refers to the maximum transfer capacity of a WDC network.	$f_{max} f_{min}$: maximum and minimum operating frequency	
Data transfer rate	bps	$DTR = BW \cdot MS \cdot BpS$	It relates to the speed of transmitting data through the wireless system	MS: modulation scheme (method used to encode digital data into analog signals or electromagnetic waves) BpS: number of bits per symbol (number of bits represented by each symbol transmitted by the modulation scheme)	[388]
Power supply voltage	V	-	It is the voltage used to supply power to the WDC system		
Power consumption	W	-	It is the power used to sustain the WDC system.		
Signal-to-noise ratio (SNR)	dB	$SNR = 20\log_{10}(\frac{V_{rms,\ signal}}{V_{rms,noise}})$	It is a measure that compares the level of the desired signal with the level of the background noise.	$V_{rms,\ signal}$: RMS voltage of the received signal $V_{rms,\ noise}$: RMS voltage of the signal without transmission	[257]
Bit error rate (BER)	-	$BER = \frac{1}{2}(1 - \sqrt{SNR/(1+SNR)})$	It is the number of bits received in error divided by the total number of bits transferred.		[257]
Data throughput (DT)	-	$DT = \frac{P_L(1-PER)}{T_p}$	It is a measure of the rate of data delivery over a communication channel in a communication network. It is a practical indication of how much data can be transferred from the transmitter to the receiver within a given time frame	P_L: payload length per packet; PER: packet error rate (given by the ration between the inappropriately received packets that the decoder cannot correct but detect, by the total number of the received packets); T_p: time spent on the data to be received at the receiver.	[257]
Other specific figures of merit					[389–392]

© 2024 The Author(s). Advanced Materials Technologies published by Wiley-VCH GmbH

2365709x, 0, Downloaded from https://onlinelibrary.wiley.com/doi/10.1002/admt.202400797 by University Of Oxford, Wiley Online Library on [19/11/2024]. See the Terms and Conditions (https://onlinelibrary.wiley.com/terms-and-conditions) on Wiley Online Library for rules of use; OA articles are governed by the applicable Creative Commons License

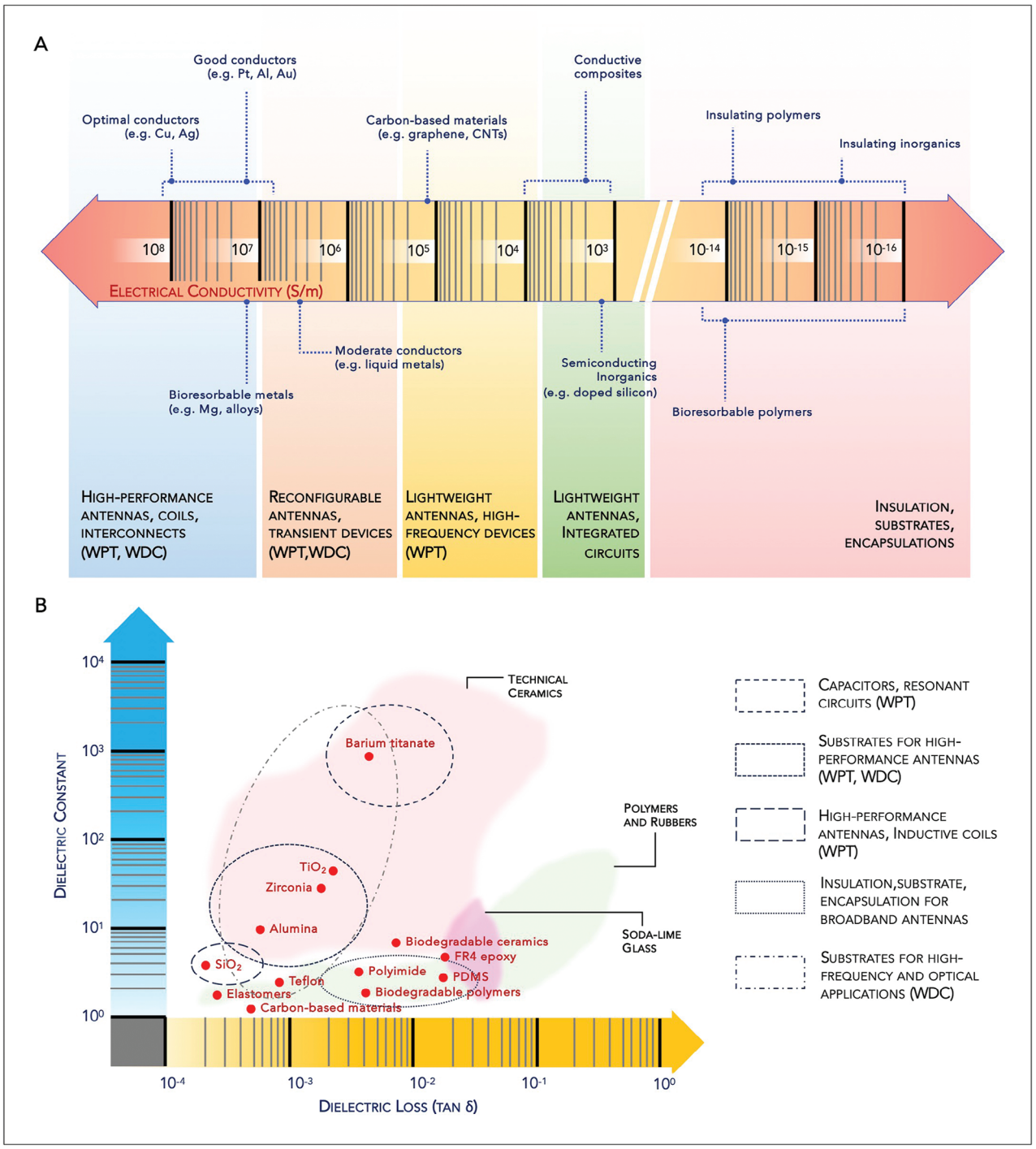


Figure 6. Scale bar (A) and graph (B) illustrating the ranges of electrical conductivity, dielectric constant (relative permittivity) and dielectric loss of the main materials categories used in WPT and WDC bionic and bioelectronic systems. Based on the values of these properties, materials can be used preferentially for WPT, WDC, high-frequency antennas, or for substrates and encapsulations.[395–397]

effectively accommodate change in morphology at the application site. According to Davis's law, soft tissues adapt structurally according to mechanical stresses applied to them:[401–403] thus, high-modulus materials may potentially cause degradation of the surrounding tissue, exacerbating adverse FBR.[23,324] Therefore, the crux lies not in creating biocompatible materials per se but in integrating biological and mechanical compatibility. Consequently, achieving physical softness becomes paramount, with characteristics such as toughness, flexural rigidity and elasticity playing crucial roles.[23,303,398,404,405] Native soft tissues typically exhibit Young's moduli ranging from 0.1 kPa to 1 MPa,[406,407] whereas gold film and bulk silicon have moduli of 69 GPa[408] and

© 2024 The Author(s). Advanced Materials Technologies published by Wiley-VCH GmbH

2365709x, 0, Downloaded from https://onlinelibrary.wiley.com/doi/10.1002/admt.202400797 by University Of Oxford, Wiley Online Library on [19/11/2024]. See the Terms and Conditions (https://onlinelibrary.wiley.com/terms-and-conditions) on Wiley Online Library for rules of use; OA articles are governed by the applicable Creative Commons License

130–188 GPa,[409] respectively. Consequently, various approaches have been explored to develop both intrinsically and extrinsically compliant materials, leveraging nanoscale and hierarchical structures, as well as controlled mechanical buckling. Thin-film metals and carbon-based materials possess robust electrical and mechanical properties, therefore, they are often chosen for the conductive tracks, electrodes and interconnects. Polymers and inorganic materials are generally used for substrates, encapsulations or specific functional layers (e.g. piezoelectric). Composites are used both as substrates and as conductive materials.

6.1.1. Thin-Film Metals and Metal Foils

Metals possess robust strength and electrical conductivity and are commonly employed in electrodes and interconnects. Nevertheless, most metals are unsuitable for direct contact to biotissues due to their potential cytotoxicity stemming from corrosion or leaching products, along with their limited ability to conform adequately.[324,410] Gold (Au), renowned for its high conductivity (4.11×10^7 S/m at 20 °C) and low cytotoxicity, finds popularity in biosignal sensors and in neural interfaces,[411] especially when it is processed with specialized structural designs to confer elasticity. Micro-cracked Au has been widely used for neural interfaces.[36,412,413]

Huang et al.[414] employed Au in a buckled nanotrough network to impart extrinsic stretchability and flexibility to typically inelastic gold on-skin electrodes. The fabrication of the buckled Au nanotrough network involves creating an interconnected Au nanofiber network transferred onto a pre-strained PDMS substrate and buckled upon release (sheet resistance of 29.4 Ω/□). Other methods to confer elasticity to gold electrodes rely on heat-pressing 2D gold nanosheets onto elastomeric substrates[415] or on introducing highly ordered pinhole microstructures in thin Au films to redistribute tensile stresses.[416] Sani et al.[417] used Au/Cu thin films to produce a wearable bioelectronic system to wirelessly and continuously monitor the physiological conditions of infected chronic wounds via a custom-developed multiplexed multimodal electrochemical biosensor array (**Figure** 7A).

Metal thin films (e.g., Au, Ag, Cu) are highly conductive, making them excellent choices for antennas and conductive traces in wireless systems. In fact, due to their high conductivity, metal thin films reduce resistive losses, improving impedance matching and enhancing antenna gain. This leads to more efficient power transfer for WPT and higher-quality signal transmission for WDC. Metal thin films can support wide bandwidths due to their excellent conductive properties, allowing for higher data transfer rates. For instance, Ag thin films are often used in high-frequency antennas for 5G communication systems, where they support high data rates due to their low loss and high conductivity.

Similar to thin films but thicker, metal foils (e.g., aluminum, copper) are also highly conductive and are used where more mechanical strength is needed. They provide excellent electrical performance with low resistance, making them suitable for large-area antennas and shielding applications. The thickness can help in better handling of higher power without significant losses. Compared to deposited thin films, they provide lower power consumption for WPT. Metal foils thus play a crucial role in the development of wireless bionic/bioelectronic systems, offering a range of advantageous properties for such applications.[418–420] For example, Cu foils are widely used in RFID tags and wireless charging coils due to their excellent conductivity and low cost. They are also used in antennas for Wi-Fi routers, supporting high data rates by ensuring minimal signal degradation. In fact, metal foils like copper offer low resistance and high conductivity, ensuring strong signal integrity over longer distances, which is important for maintaining high data rates. At higher frequencies, the skin effect (current flowing mostly on the surface) is significant, and thicker metal foils may suffer less from this, maintaining higher efficiency.

Commonly used metal foils include gold, platinum, titanium and steel due to their biocompatibility, which minimizes adverse reactions when in contact with biological tissues. Platinum (Pt) foils exhibit similar biocompatibility as gold and are often utilized in chronic implants for neural recording and stimulation. Titanium foils, renowned for their lightweight nature and corrosion resistance, find applications in flexible neural probes and sensing platforms. Steel, though less commonly associated with bioelectronic systems compared to other metals, still finds niche applications within this field. Specifically, stainless steel, renowned for its durability, corrosion resistance, and mechanical strength, can be employed in external casings or for stimulating electrodes.

6.1.2. Liquid Metals

Liquid metals, with their ability to flow and deform while maintaining good conductivity, present a new avenue for stretchable metals for wireless devices.[421,422] Gallium (Ga) and its alloys have recently garnered attention in liquid metal research due to their relatively low toxicity, vapor pressure, and viscosity.[423–426] For instance, Wu et al.[427] developed a liquid metal fiber sensor that mimics the structure of blood vessels to measure human body motion. This sensor was constructed using a superelastic biocompatible fiber channel infused with a low-toxicity liquid metal (EGaInSn). The liquid metal was capable of withstanding strains of up to 140% without losing conductivity.

Liquid metals like Ga alloys are highly conductive and can flow, allowing reconfigurable antennas that can change shape or adapt to different frequencies. In particular, they enable dynamic impedance matching and tunable antenna gain, which is useful in adaptive and reconfigurable wireless systems.[428–431] This tunability is crucial to optimize data rates for varying frequencies in WDC technologies. Xie et al.[100] provided a comprehensive overview of flexible and stretchable antennas based on liquid metals, for FFPT or NFC, where the key parameters, including operating frequency, Q factor, radiation pattern and reflection coefficient, remain stable across a range of mechanical deformations and cyclic loads.

The drawback of liquid metals is that common patterning techniques struggle to achieve high-resolution batch processing over larger surface areas. To marry the batch processing capabilities of metallic thin films with the conductivity of liquid metals, Hirsch et al.[432,433] devised a biphasic Au–Ga thin film conductor utilizing gold thin films and liquid gallium, with a resulting low sheet resistance of 0.5 Ω/□. Chen et al.[434] reported on a soft sensory skin supporting distributed and bimodal mechanical

© 2024 The Author(s). Advanced Materials Technologies published by Wiley-VCH GmbH

2365709x, 0, Downloaded from https://onlinelibrary.wiley.com/doi/10.1002/admt.202400797 by University Of Oxford, Wiley Online Library on [19/11/2024]. See the Terms and Conditions (https://onlinelibrary.wiley.com/terms-and-conditions) on Wiley Online Library for rules of use; OA articles are governed by the applicable Creative Commons License

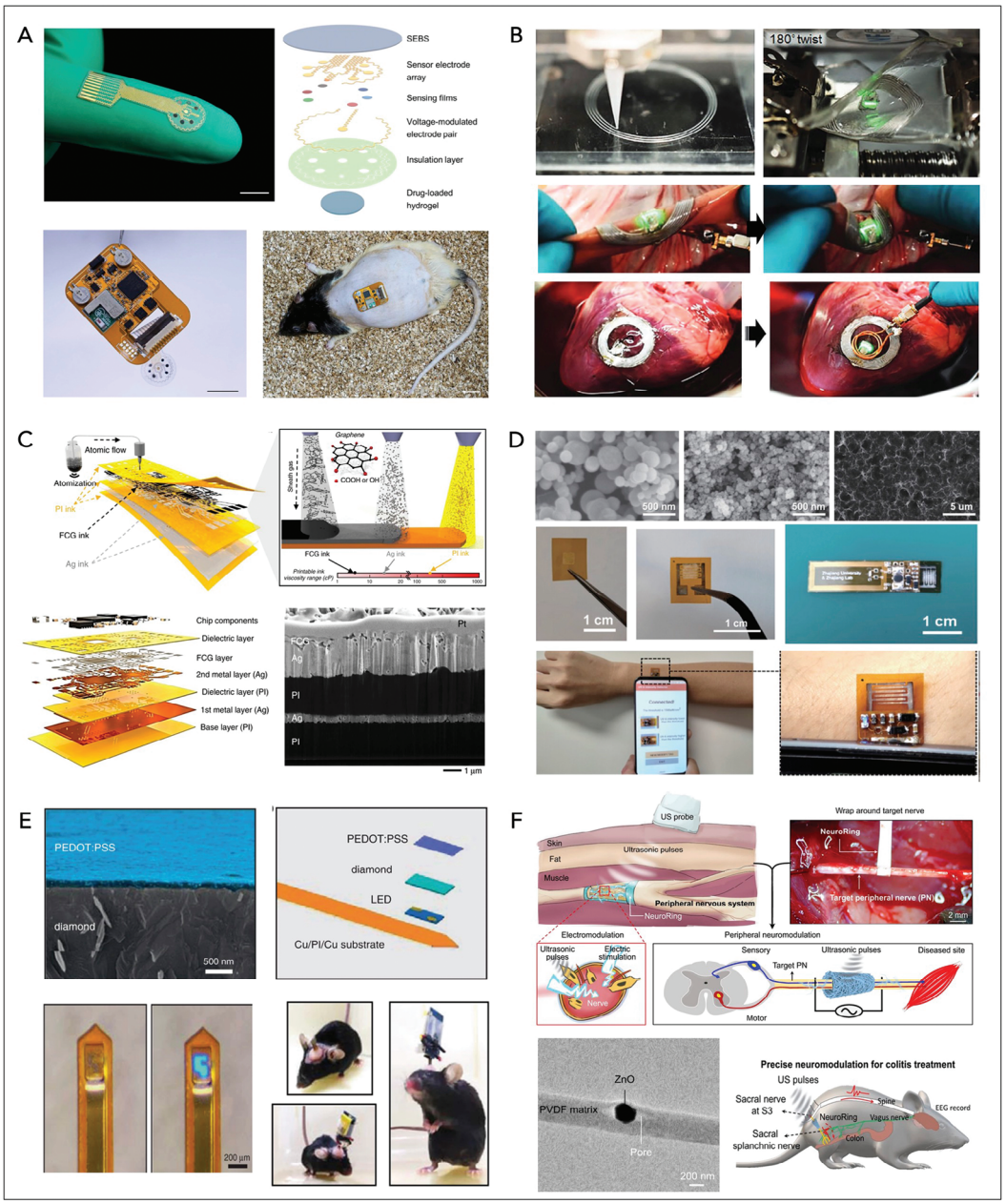


Figure 7. Biocompatible materials for wireless technologies in flexible wearable/implantable bioelectronics. A) Stretchable wireless wearable bioelectronic system for multiplexed monitoring and combination treatment of infected chronic wounds. The thin-film voltage-modulated Au/Cu electrodes are used for controlled drug delivery and electrical stimulation. The fully integrated miniaturized wireless wearable patch was tested on a diabetic rat with an open wound. Reproduced from.[417] Copyright 2023 AAAS (Creative Commons CC BY). B) Ultra-deformable and tissue-adhesive liquid metal antennas fabricated by direct ink writing. The coil-shape antennas were used to light up LEDs by a standard NFC system and tested on ex vivo porcine small intestine surface or heart surface. Reproduced with permission.[437] Copyright 2021 Wiley-VCH GmbH. C) All-printed nanomembrane wireless bioelectronics based on biocompatible solderable graphene. The printing process of aerosol particles from PI, Ag and graphene inks produces a multilayer structure that was used to assemble flexible PCBs for multimodal human-machine interfaces. Reproduced from.[460] Copyright 2020, Springer Nature (Creative Commons CC BY). D) Wireless NFC wearable UV sensor based on a ZnO nanofilm printed on a flexible substrate and utilizing NFC protocol. Reproduced from.[475] Copyright 2023 Wiley-VCH GmbH. E) Wirelessly operated microprobe system for optical interrogation and neurochemical sensing in the deep brain. The device, based on PEDOT:PSS and micro-LEDs, was tested in the ventral tegmental area of freely behaving mice. Reproduced from.[496] Copyright 2020, Springer Nature (Creative Commons CC BY). F) Soft wireless, leadless, battery-free ultrasound receiver (NeuroRing) based on a soft composite made of PVDF fibrous matrix and ZnO particles. The implant was wrapped around the sacral splanchnic nerve in mice: EEG signals were recorded while ultrasound-induced electrical stimulation was performed. Reproduced from.[514] Copyright 2023, Springer Nature (Creative commons CC BY).

© 2024 The Author(s). Advanced Materials Technologies published by Wiley-VCH GmbH

2365709x, 0, Downloaded from https://onlinelibrary.wiley.com/doi/10.1002/admt.202400797 by University Of Oxford, Wiley Online Library on [19/11/2024]. See the Terms and Conditions (https://onlinelibrary.wiley.com/terms-and-conditions) on Wiley Online Library for rules of use; OA articles are governed by the applicable Creative Commons License

sensing over large surface area and suitable for robotic hand manipulation. Resistive pressure and strain sensors were prepared with spray-coated 20 µm-thick liquid metal films (eutectic gallium indium, EGaIn) with sheet resistance of 0.15 Ω/□ and embedded in an Ecoflex matrix. Lin et al.[435] demonstrated electronic textile systems with functionalities in near-field powering and communication created by digital embroidery of liquid metal fibers prepared by infiltrated Galinstan (Ga68.5/In21.5/Sn10) into perfluoroalkoxy alkane (PFA) tubing. Guo et al.[436] reported on a flexible liquid metal (Galinstan) coil for electromagnetic collection from the transmission line for self-powered sensor and electromagnetic generation for wireless charging of cellular telephone. The liquid metal was perfused to elastic silicone tube terminated with Ga-plated copper wire: the resulting device could sustain stretching, twisting and bending with large deformations, and the proposed magnetic energy harvester could scavenge 260 mW power with the wire carrying current of 10 A. Yamagishi et al.[437] fabricated microchannels by direct ink writing on a 7 µm-thick elastomeric substrate to obtain liquid metal microfluidic antennas (Figure 7B). The resulting wireless light-emitting device is powered by a standard NFC system (13.56 MHz, 1 W) and retained a consistent operation under deformations including stretching (>200% uniaxial strain), twisting (180 ° twist), and bending (3.0 mm radius of curvature) while maintaining a high Q factor (>20). Liquid metals have recently been used as hermetic seals for stretchable bioelectronics:[438,439] since they are electric conductors, they can block electromagnetic communication into and out of seal. Adopting specific and customized design can enable the utilization of liquid-metal seals also for WDC, as demonstrated by Shen et al.[440]

6.1.3. Carbon-Based Materials

Carbon-based materials (CBMs) have emerged as compelling alternatives to metals for electrodes and conductive interconnects in bioelectronic systems due to their unique properties and biocompatibility. Graphene, carbon nanotubes (CNTs), and conductive polymers such as polyaniline and poly(3,4-ethylenedioxythiophene) (PEDOT) offer excellent electrical conductivity, mechanical flexibility, and chemical stability, making them ideal candidates for interfacing with biological tissues.[441–443] These materials can be tailored to match the mechanical properties of soft tissues, minimizing tissue damage and inflammation upon implantation. Moreover, CBM-electrodes exhibit enhanced charge injection capabilities, facilitating efficient signal transduction in neural recording and stimulation applications. Additionally, their large surface area-to-volume ratio enables high electrochemical activity, enhancing sensitivity and selectivity for biosensing applications. Furthermore, CBMs can be fabricated using scalable and cost-effective manufacturing techniques.[444–447] Gou et al.[448] presented a novel solid-state pH sensor utilizing oxidized single-walled CNTs functionalized with the conductive polymer poly(1-aminoanthracene) (PAA). Notably, the sensor was integrated with a passively-powered RFID tag, enabling wireless transmission of pH data through simulated skin. Okada et al.[449] recently introduced a flexible and stretchable capacitive sensor featuring conductive polymeric ultrathin films composed of polystyrene-block-polybutadiene (SB) elastomers and single-walled CNTs on a dielectric layer of Ecoflex. The fabricated sensor could wirelessly detect finger bending, blood vessel dilation, and throat swallowing movements. Other examples of the use of CNTs in neural interfaces can be found in literature:[450–455] incorporating them into a fully wireless platform or fabricating wireless antennas/coils entirely with CNTs still remains a challenge because of lower conductivity than metals. However, they can be used to create ultra-thin lightweight antennas with high surface area, leading to improved impedance matching and potentially higher gain at specific frequencies. They also exhibit tunable electronic properties, which can be beneficial in multifunctional devices.

Wireless flexible bioelectronics leveraging graphene-based materials offer promising avenues for advanced biomedical applications. Graphene's exceptional electrical, mechanical, and biocompatible properties make it an ideal candidate for developing flexible wearable and implantable bioelectronic devices.[456–459] By integrating graphene into sensors and electrodes, these devices can wirelessly monitor physiological signals, detect biomarkers, and deliver therapeutic agents with high sensitivity and precision. Additionally, the flexibility of graphene allows for conformal contact with biological tissues, enabling comfortable and unobtrusive wearables for continuous health monitoring. Moreover, it is nearly transparent and flexible, enabling its integration into a wide range of materials and substrates. For instance, Kwon et al.[460] reported on a new class of additive manufacturing to fabricate wireless, multilayered, all-printed, nanomembrane hybrid electronics incorporating machine learning for human-machine interfaces (Figure 7C). The materials were based on high-aspect ratio functionalized conductive graphene that offered gel-free, high-fidelity recording of muscle activities. A synchronized set of EMG devices were capable of real-time classification of individual digit movement for wireless control of a robotic hand, through deep-learning algorithms.

Graphene-based antennas are also explored for high-frequency applications like terahertz (THz) communications or for future 6G networks, due to their high conductivity and flexibility, which are crucial for ultra-high data rates.[461]

6.1.4. Ceramics

Ceramic materials offer a diverse range of properties essential for various biomedical applications. Among the plethora of ceramic materials, several types stand out for their unique characteristics and suitability for wireless bioelectronics. A key category of ceramic materials is bioinert ceramics, such as alumina (Al_2O_3) and zirconia (ZrO_2). They are biocompatible and exhibit minimal interaction with biological tissues, making them ideal for implantable devices. These ceramics provide stable mechanical support and electrical insulation, ensuring long-term functionality and compatibility within the body. Bioinert ceramics find applications in neural interfaces, cochlear implants, and various other implantable medical devices where biocompatibility and durability are paramount.

Conductive ceramics also play a crucial role in flexible bionics and bioelectronics for their ability to facilitate electrical conductivity while maintaining biocompatibility. Materials like titanium nitride (TiN) and iridium oxide (IrO_x) are widely utilized as

© 2024 The Author(s). Advanced Materials Technologies published by Wiley-VCH GmbH

2365709x, 0, Downloaded from https://onlinelibrary.wiley.com/doi/10.1002/admt.202400797 by University Of Oxford, Wiley Online Library on [19/11/2024]. See the Terms and Conditions (https://onlinelibrary.wiley.com/terms-and-conditions) on Wiley Online Library for rules of use; OA articles are governed by the applicable Creative Commons License

electrode materials in neural stimulation and recording devices. These conductive ceramics offer low impedance interfaces with biological tissues, enabling efficient signal transduction while minimizing tissue damage. Additionally, their compatibility with microfabrication techniques allows for the integration of intricate electrode arrays and wireless communication components, further advancing the capabilities of bioelectronic systems.

In the realm of wireless communication and energy harvesting, ferroelectric ceramics emerge as key players. Ferroelectric materials like barium titanate ($BaTiO_3$) and lead magnesium niobate-lead titanate (PMN-PT) possess unique dielectric properties that enable efficient energy storage and conversion. These ceramics are employed in wireless bioelectronic systems for energy harvesting from ambient sources such as body movements, temperature differentials, or ambient electromagnetic fields. Moreover, ferroelectric ceramics can serve as components in RF filters and antennas, facilitating wireless communication between implantable devices and external systems. As subset of ferroelectric materials, piezoelectric ceramics have attracted increasing attention due to their wide range of applications in various implants such as energy harvesters, tissue stimulation, and mechanical sensors.[462,463] Traditional piezoelectric materials like lead zirconium titanate (PZT) are ceramics containing lead, which poses concerns related to brittleness and toxicity, making them unsuitable for use as biomaterials for wearable or implantable bioelectronics.[464] As a result, there has been a focus on developing biocompatible piezoelectric materials for healthcare applications. The most promising lead-free alternatives are zinc oxide (ZnO),[465,466] barium titanate ($BaTiO_3$),[467–469] aluminium nitride (AlN),[470–472] lithium niobate (LiNbO3).[473,474] For instance, Dong et al.[475] proposed a wearable UV sensor based on a ZnO nanofilm on a flexible substrate and utilizing NFC communication protocol (Figure 7D). Comprehensive reviews on biocompatible piezoelectric materials, in particular ceramics, can be found in literature.[161–163,175,476] In overall, ceramics can be used as functional materials in a wireless circuitry or as insulators/encapsulations. In the first case, ceramics like barium titanate or zirconia have high dielectric constants and are often used in capacitive components, substrates, and dielectric resonators. Ceramics are used to enhance impedance matching in antennas and improve the efficiency of dielectric resonator antennas, which are efficient at microwave frequencies and are used in satellite communications.[477] These ceramics can confine electromagnetic fields tightly, improving antenna efficiency and potentially increasing data transfer rates.[478] Low-loss ceramics reduce signal attenuation, which is important for maintaining high data rates over long distances or in high-frequency applications.[479,480] If used as insulators/encapsulations, ceramics can hinder wireless transmission but their usual thickness (nm-μm) does not affect the propagation of EM waves.

6.1.5. Polymers

Polymers are paramount for the fabrication and development of flexible bionics and bioelectronics, thus of flexible wireless devices. Their versatility in terms of properties tunability allows them to serve as both biocompatible substrate materials, external encapsulations and conductive sensing/stimulating materials,[481,482] including thermoplastics, thermosetting polymers and hydrogels. This category of materials encompasses the widest range of preparation and synthesis methods, due the large set of achievable properties and available polymeric materials. For instance, polymers have been developed in recent years with the aim of obtaining tissue-like mechanical properties and guaranteeing a conformal adherence to skin or internal organs.[483–487] Zhang et al.[483] devised a biocompatible DNA-inspired hydrogel mechanoreceptor, based on adenosine monophosphate and quaternized chitosan incorporated into covalently cross-linked polyacrylamide networks, with skin-like mechanical properties and superb biocompatibility. Zhang et al.[484] developed an ionic supramolecular nanofibrillar double-network hydrogel designed to emulate the mechanical and sensing properties of human dermis, based on cross-linked supramolecular sodium alginate nanofibrils and cross-linked polyacrylamide.

In the context of biocompatible polymers, organic semiconductors have attracted much attention, because they can be processed into thin films or flexible substrates for various bioelectronic applications. Additionally, conjugated polymers like poly(3,4-ethylenedioxythiophene) polystyrene sulfonate (PEDOT:PSS) exhibit excellent electrical properties, making them suitable for biocompatible electrodes in neural interfaces and biosensors. PEDOT:PSS has emerged as a key component in wireless bioelectronic systems due to its unique combination of properties. This material exhibits excellent electrical conductivity, flexibility, and biocompatibility, making it well-suited for various applications within bioelectronics. In wireless systems, PEDOT:PSS is often utilized as an electrode material for neural interfaces, biosensors, and other implantable devices. Its ability to conform to irregular surfaces and its compatibility with microfabrication techniques enable seamless integration into miniaturized and flexible electronic systems. Moreover, PEDOT:PSS's biocompatibility ensures minimal tissue reaction upon implantation, promoting long-term stability and functionality of the devices. Additionally, its high charge storage capacity makes it suitable for energy storage applications within wireless implants.[488–493] Wang et al.[494] developed a fully printed flexible temperature sensor based on PEDOT:PSS. By introducing the crosslinker of (3-glycidyloxypropyl)trimethoxysilane (GOPS) and the fluorinated polymer passivation (CYTOP), significant enhancements in humidity stability and temperature sensitivity of PEDOT:PSS based film were achieved (−0.77% $°C^{-}$). A wireless temperature sensing platform was obtained by integrating the printed sensor to a printed flexible hybrid circuit, which performed a stable real-time healthcare monitoring. Singh et al.[495] proposed inkjet-printed amorphous metal oxide/PEDOT:PSS-based diodes on glass, and flexible polyimide substrates, demonstrating a rectification ratio $>10^4$ and operation frequency up to 25 and 15 MHz. Using the diodes, wireless power transfer was demonstrated where the input AC signal is wirelessly transmitted from a distance of 3 cm, at 125 kHz. Liu et al.[496] introduced a wirelessly operated, miniaturized microprobe system for optical interrogation and neurochemical sensing in the deep brain (Figure 7E). Via epitaxial liftoff and transfer printing, microscale light-emitting diodes (micro-LEDs) as light sources and poly(3,4-ethylenedioxythiophene) polystyrene sulfonate (PEDOT:PSS)-coated diamond films as electrochemical sensors are vertically assembled to form implantable

© 2024 The Author(s). Advanced Materials Technologies published by Wiley-VCH GmbH

2365709x, 0, Downloaded from https://onlinelibrary.wiley.com/doi/10.1002/admt.202400797 by University Of Oxford, Wiley Online Library on [19/11/2024]. See the Terms and Conditions (https://onlinelibrary.wiley.com/terms-and-conditions) on Wiley Online Library for rules of use; OA articles are governed by the applicable Creative Commons License

optoelectrochemical probes for real-time optogenetic stimulation and dopamine detection capabilities. A customized, lightweight circuit module was employed for untethered, remote signal control, and data acquisition in vivo, in freely behaving mice. Other functional polymers comprise piezoelectric polymers, such as PVDF, its derivatives and co-polymers,[497–500] or others like PLLA.[501,502]

Additionally, polymers like polyimide, PDMS, and PEEK (polyether ether ketone) are flexible, lightweight, and can be engineered to have specific dielectric properties. They are used as substrates or encapsulating materials that influence the overall dielectric environment of an antenna, affecting impedance matching and potentially reducing antenna gain. In fact, polymers generally have higher dielectric losses than metals or ceramics,[503,504] which can degrade signal quality and reduce data transfer rates, especially at higher frequencies. While polymers enable flexible and lightweight designs, they often require careful engineering to balance flexibility with maintaining sufficient data transfer rates.

6.1.6. Composite Materials

Composite materials are frequently employed to amalgamate the advantages of various materials.[23,303,324,404] Composites can be engineered to provide specific impedance matching characteristics and can be used to fabricate antennas with tailored radiation patterns or tunable gain. By combining materials, composites can achieve a balance between high data rates and other requirements like durability or flexibility. Metals and carbons serve as common fillers to enhance conductivity and augment sensing capabilities. Biocompatible polymers often serve as substrates to confer stretchability and stability to sensing materials or to encapsulate non-biocompatible materials, rendering the resultant device biocompatible. In the realm of wireless devices, these materials are less exploited as conductive elements and more used as substrates or functional materials. Pei et al.[505] used zwitterionic nanocomposite hydrogels as strain sensors in organ motion sensors. These hydrogels were synthesized via a simple one-pot free radical polymerization process combining sulfobetaine methacrylate (SMBA) monomers with dopamine-modified clay and *N,N′*-methylene bis(acrylamide) (MBAA) cross-linking agent. Zwitterionic monomers within the hydrogel provide dipole–dipole interactions, while free catechol dopamine groups permit physical and chemical bonding at the hydrogel–tissue interface, imparting robust hydrogel–tissue adhesion. Consequently, the conductive hydrogels exhibit over 1000% strain and adhesion strength of 19.4 kPa on biotissues, with a gauge factor of 4.3 for a strain range of 0–670%. Choi et al.[506] devised an Ag–Au core–sheath nanowire composite with a poly(styrene–butadiene–styrene) (SBS) elastomer matrix (with a stretchability of 266% and a conductivity of 4.19×10^4 S/cm), for continuous recording of myocardial electrophysiology and cardiac tissue stimulation using an implantable cardiac mesh.

Composite materials also include techniques of scaffolding, where polymers are used as supports for functional fillers or inclusions. Cai et al.[507] developed a novel on-skin graphene strain sensor by encasing graphene foam in a hydrogel. While microscale patterning of graphene poses challenges, utilizing a 3D foam enables bulk synthesis while retaining graphene's conductivity and mechanical properties. The graphene foam, synthesized via chemical vapor deposition upon a template followed by template removal with an etching solution, was infiltrated with a double-network PAM/CA hydrogel, enhancing stretchability and stability. Chitosan was incorporated to confer adhesive properties to the composite, facilitating strong adhesion to the implantation site. This hydrogel enables measurement of a broad range of strains up to 500% with a gauge factor of approximately 1800 and adhesion energy of approximately 200 J/m^2. Park et al.[508] utilized a hydrogel-encased functional fiber hybrid probe interfacing with brain tissue for extended periods. This neural interface comprised bundled functional fibers in a PAAm-Alg hydrogel matrix, featuring polymer optical and microfluidic fibers and a composite of tin and polymer for microelectrode arrays. Utilizing a bundled-fiber approach, substantially lower bending stiffness was achieved compared to conventional probes, with the surrounding hydrogel mechanically isolating each fiber, reducing bending stiffness. The bending stiffness of the hydrogel hybrid probes depends on their hydration state, enabling mechanical adaptation and decreased bending stiffness post-implantation, with fully swollen hybrid probes exhibiting bending stiffnesses measuring 7 N/m.

Other composite materials can possess specific functionalities. An example is piezoelectric composites that have been developed to combine the advantages of piezoelectric polymers (flexibility, compliance, softness) with the high piezoelectric coefficients of inorganic piezoelectric materials,[161,509–511] overcoming the inherent brittleness common to many piezo-ceramics.[463,512,513] For instance, Li et al.[462] devised a piezoelectric composite nanofiber (NF), creating an all-fiber soft sensor capable of detecting weak physiological mechanical stimulation such as blood pulsation. To create this nanofiber sensor, dopamine was introduced to a PVDF solution to enhance its weak piezoelectric effect and low ferroelectric stability, promoting nucleation of β-phase PVDF and maintaining the stability of β-phase PVDF once oriented. These resulting piezoelectric motion sensors demonstrated great sensitivity and accuracy in measuring diaphragmatic and arterial movements when tested in vivo in mice. Li et al.[514] reported on a wireless, leadless and battery-free implant, termed NeuroRing, based on a soft ferroelectret composite made of a PVDF fibrous matrix and ZnO particles (Figure 7F). The device demonstrated functionality as an ultrasound receiver to convert ultrasounds into electrostimulation pulses on the targeted peripheral nerves, such as the sacral splanchnic nerve in mice for colitis treatment.

6.2. Bioresorbable Materials

While most bionic systems necessitate the biostability of the device over time,[398] there are scenarios where a limited device's lifespan could be advantageous. Bioresorbable implants offer the advantage of avoiding additional surgical interventions for removal at the end of their functional lifespan. This feature has been particularly attractive for wireless bioelectronics. Nevertheless, bioresorbable materials entail additional constraints. In particular, all bioresorbable (or biodegradable) materials and their degradation products must demonstrate biocompatibility,[515]

© 2024 The Author(s). Advanced Materials Technologies published by Wiley-VCH GmbH

2365709x, 0, Downloaded from https://onlinelibrary.wiley.com/doi/10.1002/admt.202400797 by University Of Oxford, Wiley Online Library on [19/11/2024]. See the Terms and Conditions (https://onlinelibrary.wiley.com/terms-and-conditions) on Wiley Online Library for rules of use; OA articles are governed by the applicable Creative Commons License

and their biodegradation time should be ideally longer than the expected lifespan. Bioresorbable materials can also be classified based on their chemical nature, i.e. metals, polymers, semiconductors and composites.

6.2.1. Bioresorbable Metals (BrMs)

Most metals are not bioresorbable, and when in contact with aqueous environments and biofluids, they undergo corrosion and oxidation, often generating toxic byproducts.[516,517] Bioresorbable metals (BrMs) are appealing for transient wireless (WPT) bioelectronics because of their attractive properties of high conductivity, ease of synthesis/fabrication and biocompatibility.[518] The most utilized BrMs are Magnesium (Mg), zinc (Zn), and molybdenum (Mo).[519] Owing to their distinct degradation pathways and dissolution kinetics, different metals may be chosen based on factors such as expected functional lifespan, necessary encapsulation, and processing requirements. BrM thin films have been employed to fabricate fully resorbable implantable electronics; for instance, Koo et al.[520] utilized magnesium (Mg) and molybdenum (Mo) in a resorbable neurogenerative therapy device. Choi et al.[29] employed magnesium and tungsten (W) in resorbable cardiac pacemakers. Lu et al.[521] used Mo and W to create LEDs for photodynamic therapies. Lee et al.[522] proposed an on-demand bioresorbable neurostimulator based on an ultrasound-mediated transient mechanism (**Figure 8A**). They made an acoustically triggerable transient TNG and a Mg bioresorbable cuff electrode which enabled electrical stimulation through transcutaneous ultrasound-driven triboelectricity and rapid device elimination via high-intensity ultrasound. The rate of bioresorption differs for each BrM: magnesium displays the fastest resorption rate of 7×10^{-2} μm/h at room temperature in representative biofluids, tungsten degrades at a rate of $(1.7–0.3) \times 10^{-3}$ μm/h, and molybdenum has the slowest resorption rate at 3×10^{-4} μm/h.[523]

In contrast to traditional forms of metals and monometallic thin films, bioresorbable metallic alloys can be adopted as well, such as iron and manganese (FeMn)[524] or metallic glass made with magnesium (Mg), zinc (Zn), and calcium (Ca).[525] In wireless biomedical devices, BrMs and alloys provide a conductive path for antennas or interconnects that dissolve after a certain period, reducing long-term tissue exposure. They can be designed to maintain adequate impedance and gain during their functional period. They can also provide sufficient conductivity and low resistance for short-term high data rate applications. As these metals degrade, their conductive properties diminish, which could reduce data rates over time. For instance, Mg-based antennas in temporary implants can support high data rates initially, enabling robust WDC with external monitors before gradually degrading.[526]

6.2.2. Bioresorbable Inorganics (BrIs)

With an extensive track record of application in the electronics industry owing to its superior semiconducting characteristics, silicon continues to hold significance in the realm of biomedicine. Silicon-based BrIs can be used to influence the dielectric properties of wireless components in bioresorbable devices. In fact, they can affect the impedance and operation of antennas, especially in implantable devices. In temporary sensors they can support data rates sufficient for transmitting critical health data before they degrade: as these materials dissolve, their ability to support high data rates diminishes, limiting the lifespan of the wireless communication system.[527] While bulk silicon (Si) remains inflexible and non-resorbable, nanoscale silicon, in the shape of nanomembranes (Si NMs) can be flexible, adaptable, optical transparent and readily absorbable in biofluids with a sufficiently low in vivo toxicity,[40,303,515,528] thus it is a suitable candidate for WPT/WDC devices. The main dissolution product, silicic acid, is biocompatible and environmentally benign at the low levels of concentration created by silicon in micro/nanomembrane form.[134,529] Unlike Si NMs, silicon oxides are frequently employed as dielectric layers or biofluid barriers, increasingly in wireless bioelectronics. While Si NMs are typically preferred for their rapid resorption times, encapsulation is essential to safeguard devices throughout their expected functional lifespan. Silicon dioxide (SiO_2, SiO_x) and silicon nitride (Si_3N_4, SiN_x) offer several advantages over polymers for encapsulation.[344,519,530,531] Hydrophilic polymers tend to swell in water, leading to polymer fracturing, water permeation, and loss of function before the encapsulating layer is fully resorbed. Shin et al.[532] utilize thermally grown SiO_2 as a biofluid barrier due to its defect-free nature over large areas, allowing for even resorption at slow rates of several hundredths of a nanometer per day, thus shielding devices from water permeation for extended periods. Hu et al.[332] described a class of inorganic material (silicon oxynitride, SiO_xN_y) that can be formed in thin films by plasma-enhanced chemical vapor deposition as stable biofluid barriers for bioresorbable implantable electronics. Demonstrations in wireless light-emitting diodes both in vitro and in vivo illustrated the practical use of these materials strategies (Figure 8B).

6.2.3. Bioresorbable Polymers (BrPs)

The adaptability inherent in polymeric materials has rendered them a compelling choice for resorbable electronics over time. By fine-tuning properties like molecular weight, crystallinity, or hydrophilicity during synthesis, the dissolution rate of polymers can be easily adjusted.[43,519,533,534] Consequently, bioresorbable polymers (BrPs) find extensive application as substrates, encapsulation materials, and biofluid barriers for resorbable bionic/bioelectronic devices.[324,338,515,535,536] Their integration into fully wireless platforms is still challenging due to the higher variability of their properties compared to standard metals. While they generally have higher dielectric losses compared to inorganic materials, they enable temporary operation in biomedical applications where the device eventually degrades. However, the higher dielectric losses can reduce data rates, especially in high-frequency applications. Hence, these materials are designed for short-term use, where moderate data rates are sufficient for the device's operational period; they are not suited, instead, for long-term high data rate applications.

Among the various types, polylactic acid (PLA) stands out as a widely utilized option due to its biocompatibility and biodegradability, making it suitable for applications where gradual

© 2024 The Author(s). Advanced Materials Technologies published by Wiley-VCH GmbH

2365709x, 0, Downloaded from https://onlinelibrary.wiley.com/doi/10.1002/admt.202400797 by University Of Oxford, Wiley Online Library on [19/11/2024]. See the Terms and Conditions (https://onlinelibrary.wiley.com/terms-and-conditions) on Wiley Online Library for rules of use; OA articles are governed by the applicable Creative Commons License

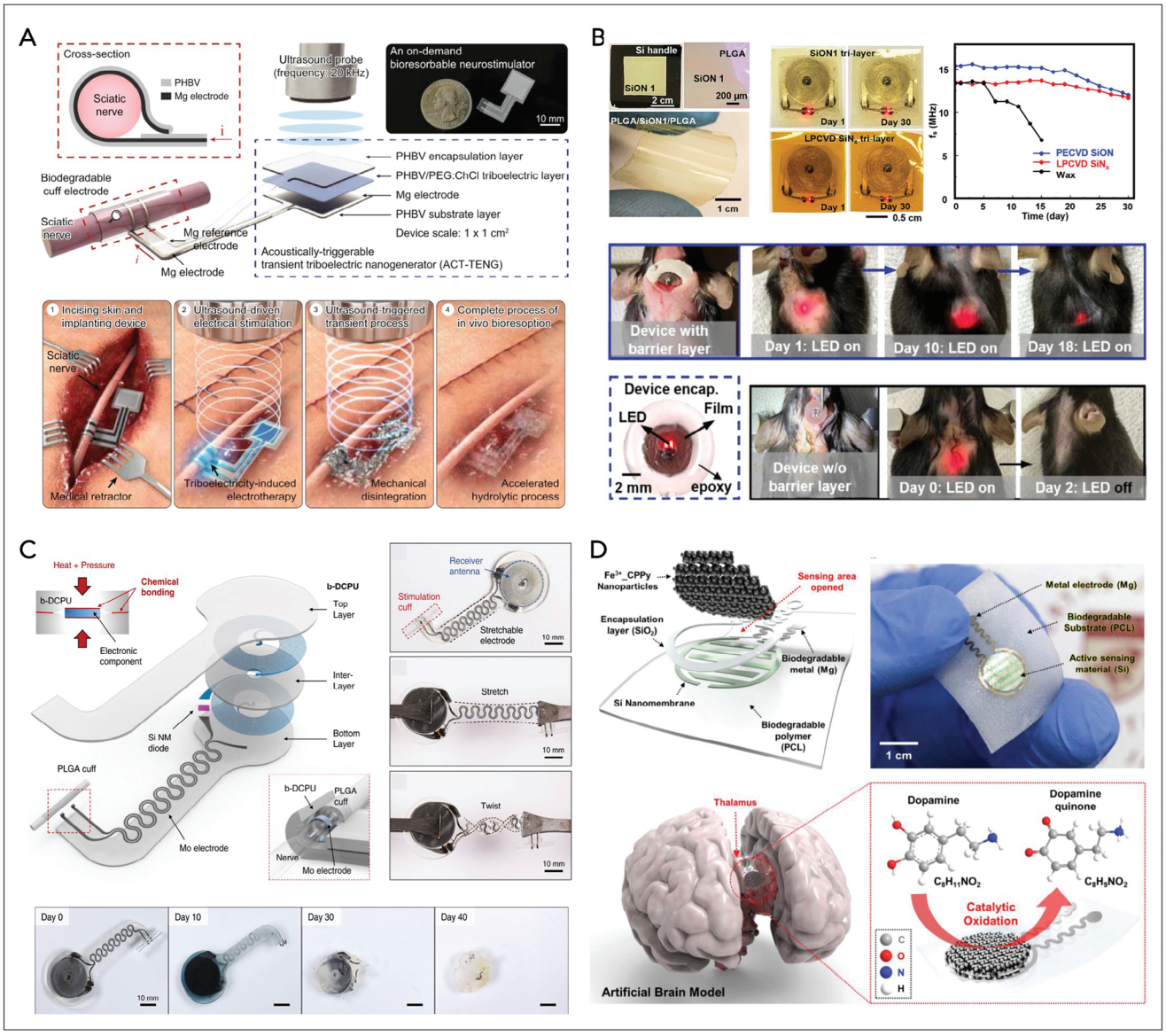


Figure 8. Bioresorbable materials for wireless technologies in flexible wearable/implantable bioelectronics. A) On-demand bioresorbable neurostimulator comprising an acoustically triggerable TNG for transcutaneous electrical stimulation and a Mg biodegradable cuff electrode for application on peripheral nerves. Reproduced from.[522] Copyright 2023, Springer Nature (Creative Commons CC BY). B) Silicon oxynitrides, formed by plasma-enhanced chemical vapour deposition, used as bioresorbable encapsulations for wireless LED, demonstrated in vivo. Reproduced from.[332] Copyright 2024, Wiley-VCH GmbH. C) Stretchable bioresorbable electronic stimulator for neuromuscular regeneration, based on Si NMs, Mo and a dynamic covalent polyurethane (b-DCPU). The bioresorbable harvester comprised a loop antenna in a bilayer, dual-coil configuration with the b-DCPU dielectric interlayer and an RF diode based on Si NM; the electrical interface consisted of exposed Mo electrodes that encircle the nerve tissue. Reproduced from.[539] Copyright 2020, Springer Nature (Creative Commons CC BY). D) Bioresorbable Si NMs with bioresorbable iron-based catalyst nanoparticles for transient electrochemical dopamine monitors in a variety of neurotransmitters. Reproduced with permission.[540] Copyright 2018, Wiley-VCH GmbH.

absorption is desired. Polyglycolic acid (PGA) shares similar properties and is often used in conjunction with PLA to tailor degradation rates. Another prominent BrP is polycaprolactone (PCL), valued for its longer degradation timeline and mechanical strength, suitable for scaffolds and structural components in bioelectronic implants. Additionally, poly(lactic-co-glycolic acid) (PLGA) copolymers offer tunable degradation rates by adjusting the ratio of lactic acid to glycolic acid units, providing versatility in implant design.

Xu et al.[537] present a pioneering PLLA/PCL composite designed as a resorbable substrate and encapsulation material for a bioresorbable ECoG electrode array and intracranial pressure (ICP) sensor. The PLLA/PCL (80:20) composite was selected for its extended degradation period and favorable malleability. Encapsulated electrodes within 10 μm PLLA/PCL exhibited stable performance over 5 days, with complete dissolution of PLLA/PCL occurring approximately 100 days in PBS. With an elastic modulus of ≈10 MPa and an elongation rate of 30%, PLLA/PCL

© 2024 The Author(s). Advanced Materials Technologies published by Wiley-VCH GmbH

2365709x, 0, Downloaded from https://onlinelibrary.wiley.com/doi/10.1002/admt.202400797 by University Of Oxford, Wiley Online Library on [19/11/2024]. See the Terms and Conditions (https://onlinelibrary.wiley.com/terms-and-conditions) on Wiley Online Library for rules of use; OA articles are governed by the applicable Creative Commons License

demonstrated excellent conformity with biotissues. Choi et al.[538] introduced a novel polyanhydride-based polymer (PBTPA) with a hydrophobic nature, for which degradation occurs via surface erosion with minimal swelling, allowing PBTA to serve as a potent and temporary encapsulation layer. By adjusting the precursor ratios, the cross-linking ratio of PBTPA can be altered, thereby modifying its properties. When used as an encapsulation material at 50 µm thickness, PBTPA encapsulating a non-resorbable LED remained stable in PBS for 50 days before eventual failure after 70 days, underscoring PBTPA's efficacy as a fluid barrier. Choi et al.[539] proposed a novel bioresorbable dynamic covalent polyurethane (b-DCPU) for soft, durable bioresorbable electronic stimulators (Figure 8C). This BrP incorporates dynamic covalent bonds, allowing for reversible bond rearrangement; thermally activated dynamic bond exchange reactions confer robust self-adhering properties, while oxygen plasma treatment facilitates bonding between b-DCPU and other inorganic sensor materials, ensuring prolonged electrical stability. With a modifiable cross-linking density, b-DCPU functions effectively as a biofluid barrier, taking over a year to fully degrade in PBS with a thickness of 200 µm.

6.2.4. Bioresorbable Composites (BrCs)

Bioresorbable composites (BrCs) encompasses properties of matrices and fillers under the conditions that both of them have to be bioresorbable. Kim et al.[540] engineered flexible, transient electrochemical dopamine monitors encapsulating Si NMs with catalytic Fe nanoparticles, as alternative to the commonly utilized yet non-transient Pt nanoparticles (Figure 8D). While minimal changes in current were observed when a solution of neurotransmitters devoid of dopamine passed over the dopamine sensor, a noticeable alteration in current was discerned with a solution containing 1×10^{-6} M of dopamine. Furthermore, the sensor was capable of complete dissolution in PBS solution at physiological temperatures, with most components dissolving entirely within 15 hours. Zhang et al.[541] who devised a conductive silk hydrogel (CSFH) composite for use as an implantable intracranial pressure sensor. The gentle conditions requisite for silk processing made it facile to modify silk and incorporate functional dopants tailored to the intended application; in this composite's instance, CNTs were employed to dope the silk hydrogel, enhancing its conductivity while preserving the desired mechanical properties. The CSFH exhibited commendable mechanical attributes, boasting an elastic modulus ranging between 0.001 and 0.15 MPa and sustaining 100% strain without significant compromise to its sensing capabilities or enduring deformation. Won et al.[542] pursued a similar route to develop bioresorbable materials for interconnects and encapsulants, employing natural waxes for their hydrophobic and biodegradable characteristics. Through the integration of W nanoparticles into candelilla wax, a conductive wax was formulated, exhibiting conductivity of up to 4 kS/m. However, the mechanical properties of waxes may prove inadequate for certain applications; while waxes in layers thinner than 200 µm can bend to a radius of 20 mm, cracks start to emerge at thicknesses of 300 µm under the same bending radius. The use of BrCs in fully wireless wearable/implantable bioelectronic systems is still not clearly explored and will need future advancements to achieve tailored device properties. They can be engineered to optimize the dielectric and conductive properties of temporary wireless devices, ensuring good impedance matching and adequate antenna performance during the device's functional lifespan. However, like other bioresorbable materials, BrCs are designed for temporary applications where moderate data rates suffice.

7. Applications: Devices and Systems

Wireless systems for flexible bionics and wearable/implantable bioelectronics have gained remarkable attention in academic and commercial research. This section described several examples of bio-integrated devices and systems for WPT and WDC, classified according to the final application. **Table 3** summarizes research and commercial devices from previous works. Other comprehensive compilations can be found in.[94,265,543,544]

7.1. Neurological Monitoring

Previous studies on bioelectronics for neurological monitoring have proposed several distinctive advancements and developments, for recording the brain's electrical signals or for monitoring intracranial pressure (ICP).[541] Park et al.[508] engineered hybrid probes embedded in a soft PAAm-Alg hydrogel matrix, for recording electrophysiological signals associated with optical stimulation. Yu et al.[545] introduced bioresorbable silicon electrodes to measure reliably in vivo electrophysiological signals in adult rat animal models. The devices detected normal physiologic and epileptiform activity, both in acute and chronic recordings. Xu et al.[537] proposed an ECoG system and intracranial pressure sensor integrated onto a single fully biodegradable sensing platform, demonstrating potential applications in implantable devices enabled by a biodegradable composite material of poly(l-lactide) and polycaprolactone (PLLA/PCL). Xie et al.[546] presented a portable wireless ECoG system using a high-resolution 32-channel flexible electrodes array to collect electrical signals of brain activities and to stimulate the lesions (**Figure 9A**). Signal acquisition, processing and transmission are performed with Bluetooth Low Energy 4 (LTE4) for wireless communication with cell phone. In-vivo experiments on a rat show that the flexible ECoG system can accurately record electrical signals of brain activities and transmit them to cell phone with a maximal sampling rate of 30k sampling/s per channel. It demonstrates that the epilepsy lesions can be detected, located and treated through the ECoG system. Keramatzadeh et al.[547] designed and validated in vivo on anesthetized rats another example of multi-channel wireless micro-ECoG system consisting of a semi-implantable, ultra-compact recording unit and an external unit, interfaced through a 2.4 GHz RF data telemetry link with 2 Mbps data transfer rate (Figure 9B).

Kang et al.[134] introduced a silicon nanomembrane-based ICP strain sensor capable of complete resorption within days in aqueous solutions. This sensor featured a diaphragm with serpentine Si NM serving as the piezoresistive element. The sensor was linked to an external wireless communicator via Mo percutaneous wires, potentially posing a risk of secondary infection.

© 2024 The Author(s). Advanced Materials Technologies published by Wiley-VCH GmbH

2365709x, 0, Downloaded from https://onlinelibrary.wiley.com/doi/10.1002/admt.202400797 by University Of Oxford, Wiley Online Library on [19/11/2024]. See the Terms and Conditions (https://onlinelibrary.wiley.com/terms-and-conditions) on Wiley Online Library for rules of use; OA articles are governed by the applicable Creative Commons License

Table 3. Representative wireless devices and systems in flexible bionics and bioelectronics proposed in previous works, and grouped based on the target application. For each device, its development stage, its type (applicability) and the wireless technique adopted are indicated.

Category / Device description	Application (target disease, organs, etc.)	Stage/ Supplier	Type of device	WPT or WDC	Wireless technique	Refs.
Neurological monitoring						
Wireless platform for EEG recordings	Neurodevelopmental monitoring	Pre-clinical/clinical	Wearable	WPT & WDC	NFMRC & Bluetooth	[603]
Point-of-care EEG (AI-powered wireless EEG platform)	Neurological diagnosis for seizures	Clinical, commercial/Ceribell	Wearable	n.d.	n.d.	[604]
Epilog (Wireless EEG device)	Real-time monitoring (sleep, epilepsy, etc.)	Commercial/Epitel	Wearable	WDC	Bluetooth	[605]
REMI (Remote EEG monitoring system)	Seizure monitoring	Commercial/Epitel	Wearable	WDC	Bluetooth	[606,607]
Wireless optoelectronic probe to monitor oxygenation	Monitoring of oxygen partial pressure in deep brain	Pre-clinical	Implantable	WDC	Bluetooth	[608]
BrainStatue™ EEG Amplifier	Brain's real-time electrical activity monitoring	Commercial/Bittium	Wearable	WDC	Bluetooth	[609]
Wireless neurosensing system	Monitoring of brain signals	Pre-clinical	Wearable	WDC	WDI (RF interrogator)	[610]
1024-channel-scalable wireless rodent headset	Neuromonitoring and Neurostimulation	Pre-clinical	Wearable	WDC	ZigBee	[611]
Ultrasonic neural dust	Recording in peripheral nerves	Pre-clinical	Implantable	WPT & WDC	UPT & WDT (Ultrasound)	[58]
Electro-stimulation						
Wireless neural stimulation patch	Neurostimulation	Pre-clinical	Implantable	WPT	ICPT	[612]
Wireless, battery-free neurostimulator in rodents	Neurostimulation	Pre-clinical	Implantable	WPT	NFMRC	[613]
Wearable neurostimulator	Neurostimulation	Pre-clinical	Wearable	WDC	WDT (RF)	[614]
Wireless neurostimulator	Neurostimulation for stroke recovery	Pre-clinical	Wearable	WDC	ZigBee	[274]
Wireless brain-spine interface	Neurostimulation for spinal cord injury	Pre-clinical, Clinical	Implantable	WPT & WDC	ICPT & WDT (LC)	[615,616]
Functional electrical stimulation	Chronic spinal and muscular stimulation	Pre-clinical	Implantable	WPT & WDC	ICPT & WDT (IR)	[562]
mm-scale neural stimulator	Neurostimulation	Pre-clinical	Implantable	WPT & WDC	UPT & WDT (Ultrasound)	[170]
Stimulator for spinal cord	Epidural spinal cord stimulation	Pre-clinical	Implantable	WPT & WDC	ICPT & NFC	[617]
Light-delivery therapies						
AI-enabled multichannel telemetry for PDT	PDT	Pre-clinical	Implantable	WPT & WDC	NFMRC & NFC	[570]
Wireless photonic PDT	PDT, cancer therapy	Pre-clinical	Implantable	WPT	NFMRC	[568]
Self-powered therapeutic pellet	PDT, cancer therapy	Pre-clinical	Implantable	WPT	UPT	[618]
Implantable ionic therapeutic platform	PDT	Pre-clinical	Implantable	WPT	CCPT	[619]
Flexible upconversion implant	PDT, neural	Pre-clinical	Implantable	WPT	OPT (NIR light)	[620]
Helios®	Optogenetics	Commercial/Plexon	Implantable	WPT	NFMRC	[621]
Wireless closed-loop stretchable device	Optogenetics, spinal cord injury	Pre-clinical	Implantable	WDC	BLE	[622]
Wireless multilateral devices	Optogenetics, social behaviors	Pre-clinical	Implantable	WDC	NFC	[623]
Optofluidic cuff system	Optogenetics	Pre-clinical	Implantable	WPT & WDC	NFMRC & NFC	[67]

(*Continued*)

© 2024 The Author(s). Advanced Materials Technologies published by Wiley-VCH GmbH

2365709x, 0, Downloaded from https://onlinelibrary.wiley.com/doi/10.1002/admt.202400797 by University Of Oxford, Wiley Online Library on [19/11/2024]. See the Terms and Conditions (https://onlinelibrary.wiley.com/terms-and-conditions) on Wiley Online Library for rules of use; OA articles are governed by the applicable Creative Commons License

Table 3. (Continued)

Category / Device description	Application (target disease, organs, etc.)	Stage/ Supplier	Type of device	WPT or WDC	Wireless technique	Refs.
Wireless solar-powered optoelectronic system	Optogenetics, neuromodulation	Pre-clinical	Implantable	WPT & WDC	PE-WIPT & Bluetooth	[624]
Wireless subdermal platform	Optogenetics	Pre-clinical	Implantable	WPT	NFMRC	[625]
Smart NIR light emitting contact lens	Diabetic retinopathy	Pre-clinical	Wearable	WPT	NFMRC	[626]
Drug delivery						
MiniMed™	Diabetes	Commercial/Medtronic	Wearable	WDC	Bluetooth	[627]
InPen™ smart insulin pen system	Diabetes	Commercial/Medtronic	Wearable	WDC	Bluetooth	[628]
IntelliCap®	GI tract treatment	Commercial/Medimetrics	Ingestible	WDC	WDI (RF transceiver)	[629]
Cellnovo Diabetes Management System	Diabetes	Commercial/Cellnovo	Wearable	WDC	Bluetooth	[630]
Wireless smart contact lens	Diabetic retinopathy	Pre-clinical	Wearable	WPT	NFMRC/ICPT	[631]
Battery-free wireless wound dressing	Wound healing	Pre-clinical	Wearable	WDC	NFC	[632]
Wireless optofluidic neural probe	Behavioral disorders	Pre-clinical	Implantable	WPT & WDC	NFMRC & NFC	[51,68]
Self-powered, light-controlled, bioresorbable platform	Pain relief	Pre-clinical	Implantable	WPT	OPT	[633]
Wireless, bioresorbable corrosion-triggered device	Insulin delivery, cancer treatment	Pre-clinical	Implantable	WPT	NFMRC	[338]
Ultrasonically powered implantable potentiostat	Multi-purpose delivery	Pre-clinical	Implantable	WPT	Ultrasound	[634]
Ultrasound-based microneedle system	Diabetes	Pre-clinical	Wearable	WDC	Bluetooth	[635]
System based on mesoporous microneedles-iontophoresis	Diabetes	Pre-clinical	Wearable	WDC	Bluetooth	[636]
Wireless smart contact lens	Diabetic diagnosis and therapy	Pre-clinical	Wearable	WPT & WDC	ICPT & RF	[631]
Ultrasonic treatments						
Wireless brain stimulation system	Bilateral neuromodulation	Pre-clinical	Implantable	WPT	ICPT	[586]
Mobile stimulation system	Transcranial ultrasound stimulation	Pre-clinical	Implantable	WDC	Bluetooth	[637]
Ultrasound energy harvester	Retinal stimulation	Pre-clinical	Wearable	WPT	UPT	[590]
Wearable ultrasound system	Transcranial ultrasound stimulation	Pre-clinical	Wearable	WPT	UPT	[638]
Wearable ultrasound patch	Functional hemodynamic monitoring	Pre-clinical/Clinical	Wearable	WDC	Bluetooth	[639]
Cardiovascular monitoring						
Multi-sensor wireless platform (SeisMote)	Monitoring cardiovascular function	Pre-clinical	Wearable	WPT & WDC	NFMRC & BLE	[640]
Self-powered platform with implantable TNG	Heart monitoring	Pre-clinical	Implantable	WPT & WDC	KE-WIPT & NFC	[641]
Mobile Cardiac Telemetry (MCOT)	Diagnosis and treatment of arrhythmias	Commercial/Philips	Wearable	WDC	Bluetooth	[642]
Cardiac monitoring system	Heart sound segmentation	Pre-clinical	Wearable	WDC	WDT (MQTT, Wi-fi)	[643]
SmartCardia wireless patch	ECG ambulatory monitoring for cardiac arrhythmias detection	Clinical/Commercial	Wearable	WDC	Bluetooth	[644]

(*Continued*)

© 2024 The Author(s). Advanced Materials Technologies published by Wiley-VCH GmbH

2365709x, 0, Downloaded from https://onlinelibrary.wiley.com/doi/10.1002/admt.202400797 by University Of Oxford, Wiley Online Library on [19/11/2024]. See the Terms and Conditions (https://onlinelibrary.wiley.com/terms-and-conditions) on Wiley Online Library for rules of use; OA articles are governed by the applicable Creative Commons License

Table 3. (Continued)

Category / Device description	Application (target disease, organs, etc.)	Stage/ Supplier	Type of device	WPT or WDC	Wireless technique	Refs.
Intraocular pressure monitoring						
Wireless theranostic smart contact lens	IOP monitoring in glaucoma	Pre-clinical	Wearable	WDC	BLE	[599]
Wireless theranostic contact lens	Electrical sensing and regulation of IOP	Pre-clinical	Wearable	WPT	ICPT	[354]
Hydrogel contact lens	IOP monitoring	Pre-clinical	Wearable	WPT	ICPT	[645]
Soft contact lens	IOP monitoring in glaucoma	Pre-clinical	Wearable	WDC	NFC	[597]
Strain sensor in doughnut-shaped contact lens	IOP monitoring	Pre-clinical	Wearable	WDC	NFC	[646]
Smart contact lens with high environmental stability	IOP monitoring for ocular hypertension	Pre-clinical	Wearable	WDC	NFC	[647]

Nomenclature: n.d.: not disclosed; WPT: wireless power transfer; WDC: wireless data communication; MQTT: Message Queuing Telemetry Transport; EEG: electroencephalogram; ECG: electrocardiogram.

Nonetheless, they demonstrated the use of the sensor with a partially resorbable implanted wireless communicator utilizing NFC technology, suggesting the feasibility of a fully wireless sensor. Shin et al.[532,548] developed bioresorbable ICP platforms comprising four Si NM sensors (two strain sensors built upon an air-filled flexible diaphragm and two temperature sensors), encapsulated using thermally grown SiO_2 thin films. In these systems, a millimeter-scale bioresorbable Fabry-Perot interferometers and two-dimensional photonic crystal structures enabled precise, continuous wireless measurements of pressure and temperature, although with some limitations such as noise susceptibility due to reflection spectrum dependence on light incidence angle and biofluid-induced light absorption.

7.2. Electro-Stimulation

Wireless systems for electrical stimulations harness WPT to deliver precise electrical impulses to targeted tissues or organs within the body. From neuromuscular electrical activation[549–551] to neural modulation, they have demonstrated remarkable efficacy in various biomedical applications. Applications of neurostimulation comprise modulating nerve systems,[552] restoring sensory pathways[553] and fostering neural regeneration.[554,555] Particularly, they become necessary when molecular therapies are inefficient due to obstacles such as the blood brain barrier. In the recent years, deep brain stimulation (DBS) technologies[556] have evolved remarkably, providing useful strategies for treating disorders including but not limited to Parkinson's, epilepsy, dystonia, essential tremor, obsessive compulsive disorder and Alzheimer's disease.[63,92,557,558] Neural stimulation commonly employs a series of rectangular pulses, regulated in either current or voltage, administered at precise frequencies and temporal patterns. Recent research has explored the potential advantages of using pulse waveforms that deviate from the standard rectangular shape.[559,560] For wireless neurostimulators, there are two main options for where to place the control electronics responsible for generating stimulus patterns and selecting channels: either on the electrode assembly itself or on an external controller. If placed on the electrode assembly, intricate digital and analog circuits must be integrated into the limited space available on the implanted device to store stimulus parameters and deliver stimuli according to a specified pattern. Conversely, positioning the control electronics on an external controller offers the possibility of completely eliminating active electronics on the implant, as energy transfer to the device can be achieved on a per-pulse basis.[558] Sahin and Pikov[558] discuss different approaches for wireless microstimulators (including RF, pulsed ultrasound, near-infrared), with particular emphasis for intraspinal neuroprosthetics which need fewer electrodes/channels and experience larger translational and rotational displacements than cortical devices. Yun et al.[561] presented a fully implantable neural stimulator that can be remotely controlled, enabling precise electrical stimulation in freely moving small animals. The system consisted of modular units of a surface-type cortical array, a depth-type array for providing rewards, a liquid crystal polymer (LCP)-based package, a battery and ZigBee telemetry. The device was successfully implanted in rodents, allowing for stimulation of specific neural circuits wirelessly. Quantitative results

© 2024 The Author(s). Advanced Materials Technologies published by Wiley-VCH GmbH

2365709x, 0, Downloaded from https://onlinelibrary.wiley.com/doi/10.1002/admt.202400797 by University Of Oxford, Wiley Online Library on [19/11/2024]. See the Terms and Conditions (https://onlinelibrary.wiley.com/terms-and-conditions) on Wiley Online Library for rules of use; OA articles are governed by the applicable Creative Commons License

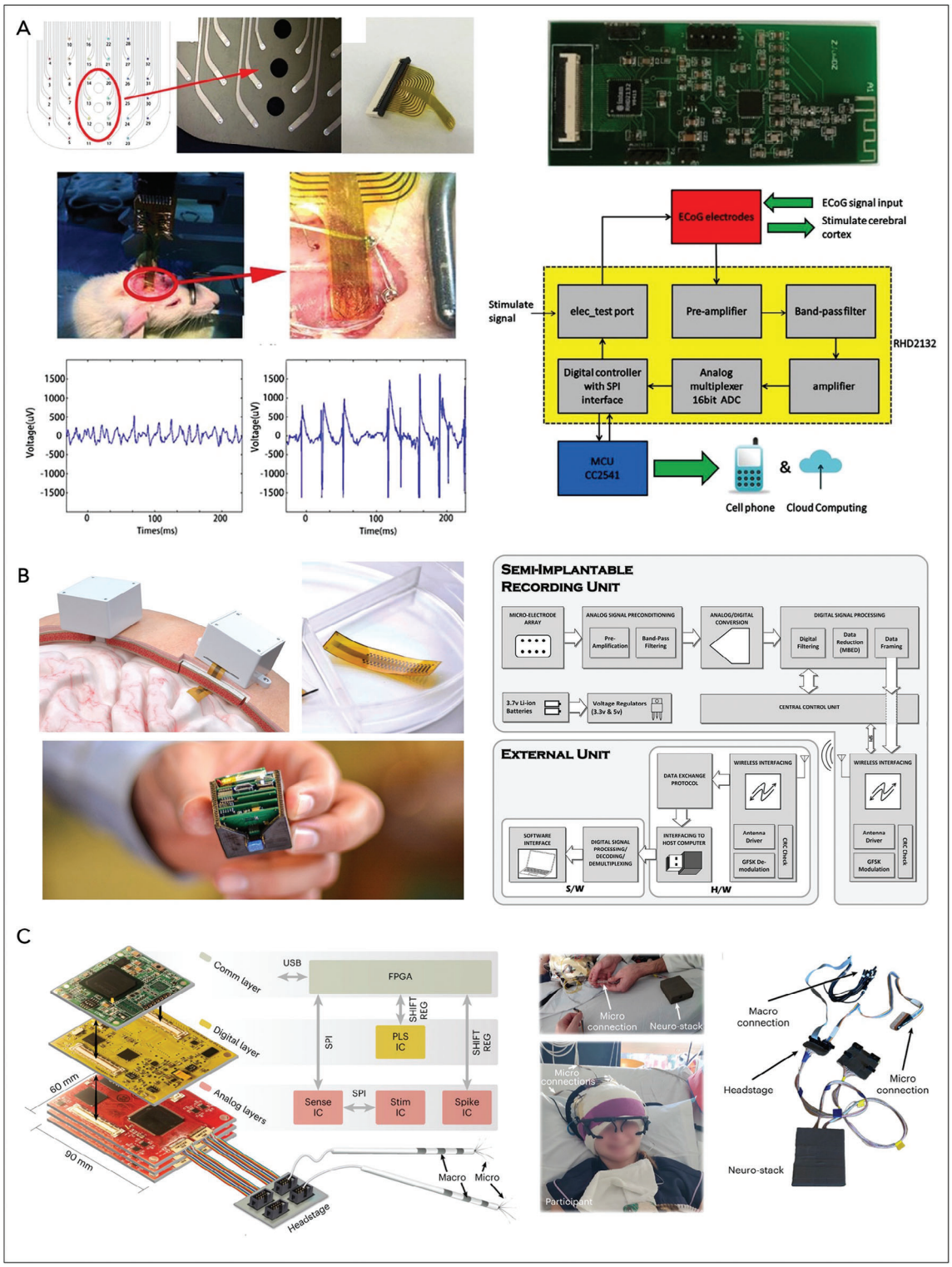


Figure 9. Examples of wireless technologies used in flexible wearable and implantable bioelectronics for neurological monitoring and electro-stimulation. A) Portable wireless ECoG flexible system with 32 channels and based on BLE wireless communication with cell phone. The device was tested to collect electrical signals of brain activities in rats and to stimulate the lesions. Reproduced from.[546] Copyright 2017, Springer Nature (Creative Commons CC BY). B) Wireless, miniaturized, semi-implantable ECoG system based on a compact 12 × 6 microelectrode-array recording unit and an external unit, interfaced by a 2.4 GHz RF data telemetry link. Reproduced from.[547] Copyright 2020, Springer Nature (Creative Commons CC BY). C) Wearable bidirectional closed-loop neuromodulation system (Neuro-stack) for recording single-neuron and local field potential activity during stationary and ambulatory behavior in humans. Reproduced from.[565] Copyright 2023, Springer Nature (Creative Commons CC BY).

© 2024 The Author(s). Advanced Materials Technologies published by Wiley-VCH GmbH

2365709x, 0, Downloaded from https://onlinelibrary.wiley.com/doi/10.1002/admt.202400797 by University Of Oxford, Wiley Online Library on [19/11/2024]. See the Terms and Conditions (https://onlinelibrary.wiley.com/terms-and-conditions) on Wiley Online Library for rules of use; OA articles are governed by the applicable Creative Commons License

indicate that the stimulator achieved precise control over stimulation parameters, including frequency, duration, and amplitude, with high accuracy and reliability. Burton et al.[65] demonstrated a fully implantable, wireless, battery-free platform that allows for chronic DBS in rodents with the capability to control stimulation parameters digitally in real time, to provide stimulation over several frequencies with biphasic pulses and constant voltage control. Efficacy of the system is demonstrated with a readout of stimulation-evoked neural activity in vivo and chronic stimulation of the medial forebrain bundle in freely moving rats to evoke characteristic head motion for over 36 days. The same authors[562] introduced a passive resonator optimized power transfer design that enables voltage compliances of ± 20 V and power over 300 mW at device volumes of 0.2 cm^2. The system enabled multichannel, biphasic, current-controlled operation at clinically relevant voltage and current ranges with digital control and telemetry in freely behaving animals. Preliminary chronic results indicate that implanted devices remain operational over 6 weeks in both intact and spinal cord injured rats and are capable of producing fine control of spinal and muscle stimulation. Alpaugh et al.[563] developed a similar small wireless implantable micro-stimulator that can deliver chronic stimulation in freely moving mice over several weeks and which allows for behavioral analysis.[564] Topalovic et al.[565] introduced a wearable bidirectional closed-loop neuromodulation system (Neuro-stack) to record single-neuron and local field potential (LFP) activity during stationary and ambulatory behavior in humans (Figure 9C). The device could support recording from up to 256 contacts for a total of 128 monopolar or bipolar recordings with a sampling rate of up to 6,250 Hz. Furthermore, it allowed delivery of bipolar/monopolar stimulation to any 32 out of 256 contacts simultaneously. In the context of electro-stimulation for wound healing and tissue regeneration, Jiang et al.[566] developed a flexible bioelectronic system consisting of wirelessly powered, closed-loop sensing and stimulation circuits with skin-interfacing hydrogel electrodes capable of on-demand adhesion and detachment. They demonstrated continuous monitoring of skin impedance and temperature in mice, as well as delivery of electrical stimulation in response to the wound environment. Across preclinical wound models, the treatment group healed ≈25% more rapidly and with ≈50% enhancement in dermal remodeling compared with control. Activation of pro-regenerative genes in monocyte and macrophage cell populations was also observed, which may enhance tissue regeneration, neovascularization and dermal recovery.

7.3. Light-Delivery Therapies

Light-delivery therapies, such as photodynamic therapy (PDT) and optogenetics, have emerged as promising modalities for treating various medical conditions, including cancer, neurological disorders, and chronic pain. The development of wireless wearable and implantable flexible systems has revolutionized the delivery of light-based therapies, offering targeted and minimally invasive approaches that enhance patient comfort and treatment efficacy.

Lee et al.[59] presented a subdermally implantable device powered by magnetic resonant coupling for optogenetic stimulation of regions of the deep brain, with reliable operation and good chronic stability. The device was shaped as an ultrathin injectable probe with a micro-LED at its tip, an overall footprint of ≈9.8 mm (diameter) and total thickness lower than 1.3 mm. A double-loop primary coil was used to support simultaneous operation of a large collection of devices in all regions of a standard home cage (30 × 30 cm) with good spatial uniformity (variation of light intensity on the same height was less than 30%).

PDT is a noninvasive method for cancer therapy involving the generation of reactive oxygen species via the photochemical excitation of photosensitizers to induce death into cancer cells. Yokoi et al.[567] developed a wireless PDT system that uses cyclometalated iridium (III) (Ir(III)) complexes that can be excited with blue light (470 nm), against the common near-infrared light used for PDT devices. In particular, they developed a light-emitting diode device equipped with a receiver coil powered wirelessly through NFMRC: upon irradiation, triplet oxygen is excited to singlet oxygen which induced cell death in HeLa S3 human cervical carcinoma cells. Bansal et al.[568] demonstrated a wireless implantable photonic device that achieved therapeutic light delivery for PDT. The device consisted of a 3D helical coil extracting energy from the incident RF field and a PCB integrating the RF rectifier and two LEDs. It was shown to wirelessly activate photosensitizers in situ in a porcine model of tissue and suppress tumor activity in vivo in a murine cancer model by delivering light doses for PDT. Kim et al.[569] introduced a flexible and fully implantable wireless optoelectronic system for continuous PDT for cancer therapy and simultaneous tumor size monitoring in real-time. The device consisted of micro-LED (624 nm) to delivery light with a fully programmable intensity, and of Si phototransistor to monitor the tumor size. The device operation by wireless power and data transmissions with a cell phone was confirmed through in vitro experiments, ray-tracing simulation results, and a tumor xenograft mouse model in vivo. Kim et al.[570] proposed DeepLabCut (DLC)-informed low-power WDC with an integrated Monte Carlo thermal/light simulation platform. The WDC used the parameters from the stimulator to enable adequate illumination of tumors and it was validated with in vivo Hypericin and Foscan mediated PDT, using cancer xenograft models.

7.4. Drug Delivery

Wireless bioelectronic devices have emerged as promising tools for precise and targeted drug delivery, enabling real-time monitoring and controlled release of therapeutics in response to physiological cues (**Figure 10A**). Wireless implantable devices aim to deliver drugs to specific brain regions in response to neural activity patterns detected by embedded sensors. Such systems allow for on-demand drug release, optimizing treatment efficacy while minimizing side effects. Several mechanisms of drug release may be exploited, e.g. electrophoresis, electroosmosis, piezoelectric micropumps, dissolvable gates, etc.[571] The wireless connectivity of these devices not only facilitates remote programming but also enables continuous adjustment of drug delivery parameters in real-time, enhancing treatment flexibility and patient outcomes. Furthermore, researchers have explored the integration of wireless bioelectronic devices with feedback control algorithms to enable closed-loop drug delivery systems,

© 2024 The Author(s). Advanced Materials Technologies published by Wiley-VCH GmbH

2365709x, 0, Downloaded from https://onlinelibrary.wiley.com/doi/10.1002/admt.202400797 by University Of Oxford, Wiley Online Library on [19/11/2024]. See the Terms and Conditions (https://onlinelibrary.wiley.com/terms-and-conditions) on Wiley Online Library for rules of use; OA articles are governed by the applicable Creative Commons License

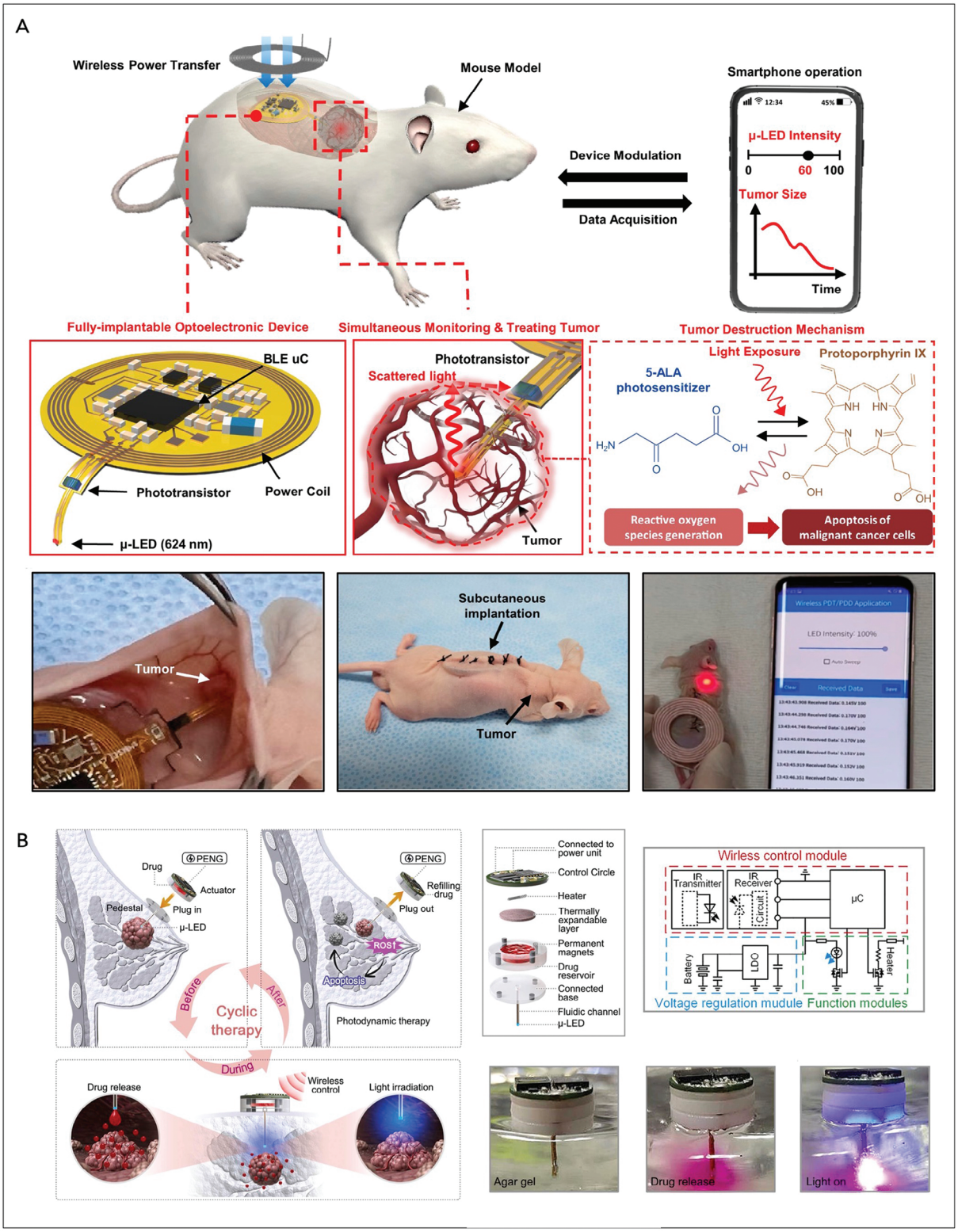


Figure 10. Examples of wireless technologies used in flexible wearable and implantable bioelectronics for light-delivery therapies and drug delivery. A) Flexible and fully implantable wireless optoelectronic system for continuous PDT for cancer therapy trough a micro-LED and simultaneous tumor size monitoring in real-time through a Si phototransistor. Reproduced from.[569] Copyright 2023, Springer Nature (Creative Commons CC BY). B) Self-powered, wireless and detachable drug/light injector for cancer treatment, based on a semi-invasive pedestal with a micro-LED and a syringe needle, an actuator containing a drug reservoir, a thermally-driven pump and a wireless control circuit based on NFMRC. Reproduced with permission.[579] Copyright 2023, Elsevier.

© 2024 The Author(s). Advanced Materials Technologies published by Wiley-VCH GmbH

2365709x, 0, Downloaded from https://onlinelibrary.wiley.com/doi/10.1002/admt.202400797 by University Of Oxford, Wiley Online Library on [19/11/2024]. See the Terms and Conditions (https://onlinelibrary.wiley.com/terms-and-conditions) on Wiley Online Library for rules of use; OA articles are governed by the applicable Creative Commons License

combining, for example, continuous glucose monitoring with insulin infusion,[572,573] or triggering anti-epileptic drugs into the brain based on the electrophysiological brain activity detected and monitored by wireless EEG sensors.[574,575]

Moreover, advances in wireless bioelectronics have led to the development of wearable drug delivery devices that offer portability and ease of use for patients. These wearable patches may be equipped with wireless communication capabilities for remote programming and monitoring of drug delivery parameters, and delivering controlled doses of medication.[571,576] These technologies can be also applied to wireless-controlled ingestible capsules for targeted drug delivery to the gastrointestinal tract, enabling precise drug release at specific locations along the digestive tract based on wireless commands from external devices.[577,578]

In summary, wireless bioelectronic devices hold great promise for revolutionizing drug delivery by enabling remote control, feedback-based optimization, and wearable/portable solutions. From implantable systems for targeted drug delivery to closed-loop systems for adaptive therapy and wearable devices for convenient administration, the integration of wireless communication technology into drug delivery platforms offers unprecedented opportunities for personalized and precise healthcare interventions. As research in this field continues to advance, we can expect further innovations in wireless bioelectronics to transform the landscape of drug delivery and improve patient outcomes.

Lin et al.[579] presented a self-powered, wireless and detachable drug/light injector that conforms to the properties of metronomic PDT for cancer treatment (Figure 10B). The device consisted a semi-invasive pedestal with a micro-LED and a syringe needle, with an actuator containing a drug reservoir, a thermally-driven pump and a wireless control circuit based on magnetic resonance. They demonstrated to deliver on-demand dosages of drugs and light into the tumor cells under the skin: self-powering was achieved using body motion energy through PNG.

7.5. Ultrasonic Treatments

Ultrasonic therapies delivered via wireless bioelectronic devices represent a cutting-edge approach in modern medicine, offering non-invasive and targeted treatments for a wide range of medical conditions.[259,580,581] These therapies harness the power of ultrasonic waves to penetrate deep into tissues, promoting tissue regeneration, pain relief, and therapeutic effects without the need for surgery or invasive procedures. One notable example is the development of wireless ultrasound devices for the treatment of musculoskeletal disorders such as arthritis and tendonitis. These devices utilize focused ultrasound waves to generate localized heating and promote tissue healing, providing effective pain relief and improving mobility for patients. Moreover, wireless ultrasound therapy devices offer the advantage of portability and ease of use, allowing patients to receive treatment in the comfort of their own homes or during daily activities. Another application of ultrasonic therapies through wireless bioelectronic devices is in the field of cancer treatment. High-intensity focused ultrasound (HIFU) therapy, delivered via wireless ultrasound devices, has emerged as a promising approach for non-invasive tumor ablation.[582,583] HIFU technology enables precise targeting of tumors while sparing surrounding healthy tissue, minimizing side effects and improving patient outcomes. Furthermore, ultrasonic therapies delivered via wireless bioelectronic devices hold potential for neurological applications, such as neuromodulation and brain stimulation. Transcranial focused ultrasound (tFUS) therapy, administered through wireless ultrasound devices, has shown promise in the treatment of neurological disorders such as Parkinson's disease, depression, and essential tremor.[581,584,585] By precisely targeting specific brain regions with focused ultrasound waves, tFUS therapy can modulate neuronal activity and alleviate symptoms associated with these conditions. Moreover, the wireless nature of these devices allows for non-invasive and convenient delivery of therapy, minimizing patient discomfort and enabling outpatient treatment options. Kim et al.[586] developed a wireless ultrasonic brain stimulation system for concurrent bilateral neuromodulation in freely moving rodents (**Figure 11A**). The ultrasound transducers were based on PZT ceramics with a resonance frequency of 380 kHz and a diameter of 7 mm. The driving system was based on a system on chip that generated a pulse width modulated signal, and a pair of RF amplifier circuits. Additionally, wireless ultrasound devices have the potential to revolutionize wound healing and tissue regeneration. Low-intensity pulsed ultrasound (LIPUS) therapy, delivered wirelessly through portable ultrasound devices, has been shown to accelerate the healing of fractures, soft tissue injuries, and chronic wounds.[587–589] By promoting cellular proliferation and collagen synthesis, LIPUS therapy enhances tissue repair processes, leading to faster recovery times and improved functional outcomes.

Ultrasounds may also be adopted indirectly for supplying power to bioelectronics for other treatments (e.g. electrostimulation). For instance, Jiang et al.[590] used ultrasounds as energy harvesting mechanism to power wirelessly a bioelectronic device for potential retinal electrical stimulation. The flexible device employed an environmentally friendly lead-free piezocomposite as the core element, plus wavy-shaped electrodes for external contact and a silicone encapsulation. Furthermore, wireless ultrasound devices equipped with advanced real-time imaging modalities, such as ultrasound elastography and contrast-enhanced ultrasound, enable clinicians to monitor treatment progress, assess tissue quality and perfusion in real-time, guiding treatment decisions, adjusting parameters as needed and optimizing patient care. For instance, Hu et al.[591] reported a wearable ultrasonic device for continuous, real-time and direct cardiac function assessment (Figure 11B). The device was built on styrene-butylene-styrene (SEBS), embodying piezoelectric transducer arrays and liquid metal composite electrodes. A centre frequency of 3 MHz was chosen for deep tissue imaging, whereas a deep learning neural network was applied to extract key information from the continuous stream of ultrasound images.

7.6. Cardiovascular Monitoring

The prior incorporation of bioelectronic systems into cardiovascular contexts has yielded notable breakthroughs along with accompanying challenges. Boutry et al.[592] introduced a biodegradable, wireless, and battery-free arterial blood flow sensor developed for continuous post-discharge monitoring. This sensor features a poly(glycerol sebacate) (PGS) dielectric layer with pyrami-

© 2024 The Author(s). Advanced Materials Technologies published by Wiley-VCH GmbH

2365709x, 0, Downloaded from https://onlinelibrary.wiley.com/doi/10.1002/admt.202400797 by University Of Oxford, Wiley Online Library on [19/11/2024]. See the Terms and Conditions (https://onlinelibrary.wiley.com/terms-and-conditions) on Wiley Online Library for rules of use; OA articles are governed by the applicable Creative Commons License

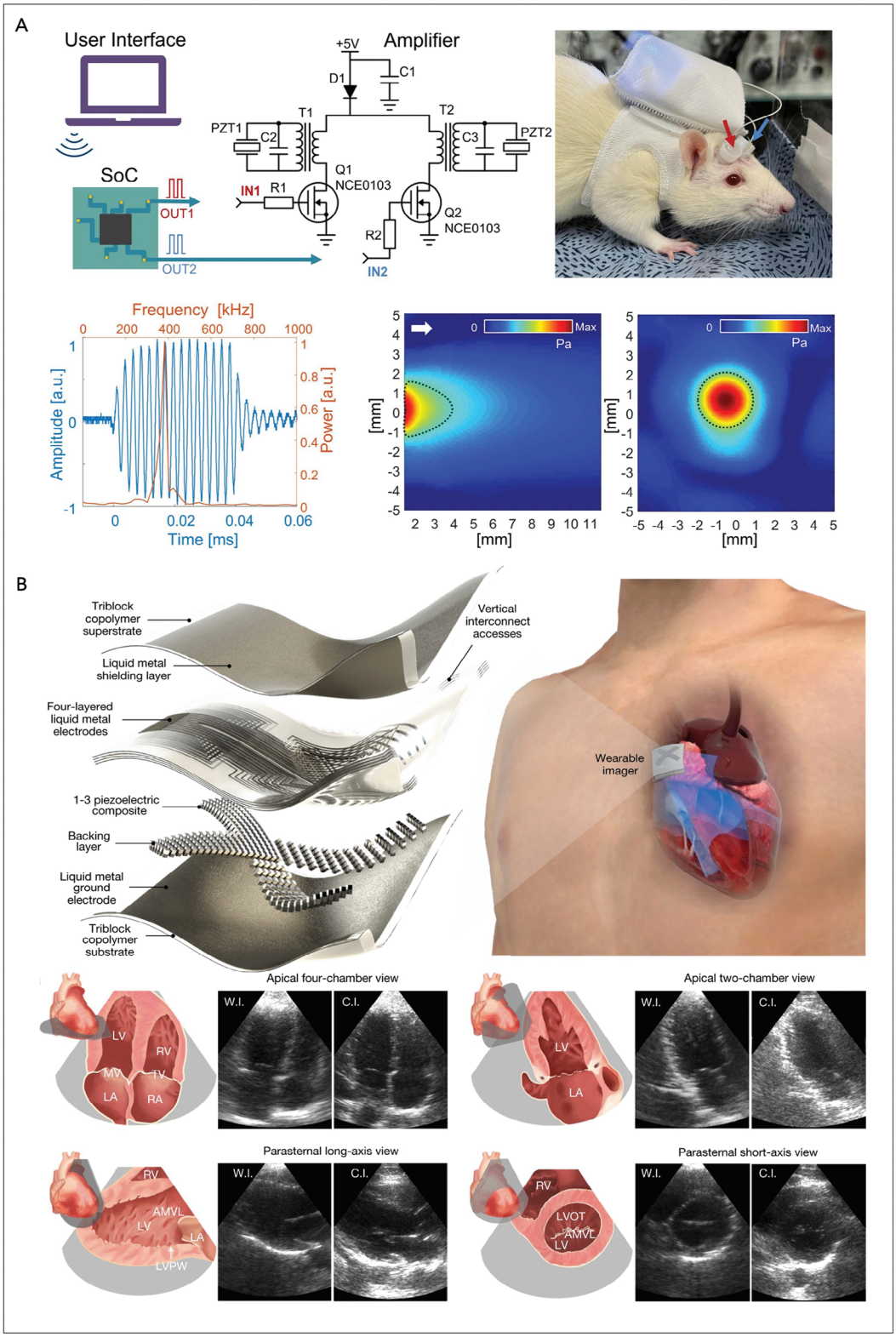


Figure 11. Examples of wireless technologies used in flexible wearable and implantable bioelectronics for ultrasonic treatments. A) Wireless ultrasonic brain stimulation system for concurrent bilateral neuromodulation in freely moving rodents. Reproduced from.[586] Copyright 2022, Frontiers. B) Wearable ultrasonic device for continuous, real-time and direct cardiac function assessment. The device is ultra-stretchable thanks to the liquid metal composite electrodes and the soft triblock copolymer substrate/encapsulation. Reproduced from.[591] Copyright 2023, Springer Nature (Creative Commons CC BY).

© 2024 The Author(s). Advanced Materials Technologies published by Wiley-VCH GmbH

2365709x, 0, Downloaded from https://onlinelibrary.wiley.com/doi/10.1002/admt.202400797 by University Of Oxford, Wiley Online Library on [19/11/2024]. See the Terms and Conditions (https://onlinelibrary.wiley.com/terms-and-conditions) on Wiley Online Library for rules of use; OA articles are governed by the applicable Creative Commons License

dal microstructures for enhanced sensitivity in pressure-sensitive regions. Poly(octamethylene maleate (anhydride) citrate) (POMaC) and polyhydroxybutyrate/polyhydroxyvalerate (PHB/PHV) serve as packaging layers, with PHB/PHV providing stiffness in muscle contact areas and POMaC offering softness in artery contact areas, thus ensuring greater sensitivity to arterial deformation than respiratory movements. Rigo et al.[593] reported on an implantable vascular bioelectronic device endowed with a miniaturized strain sensor via a high-resolution capillary-based microneedle printing method (**Figure 12A**). The sensor was integrated into a wireless vascular stent, resulting in a biocompatible, battery-free, wireless monitoring system. Choi et al.[506] proposed an Ag–Au nanocomposite for electrode development aimed at measuring cardiac electrophysiological signals in large animal models like swine. They designed a cardiac mesh resembling a simplified version of the swine heart, comprising seven repetitive segments of six electrodes each, welded together to form a 2D fan shape. This design enables complete coverage of the swine heart's ventricles when folded, facilitating specific sensing and stimulation of multiple locations. Yang et al.[594] presented a novel adhesive to encapsulate and adhere an interconnected array of 64 electrodes to rabbit hearts for electrical spatiotemporal mapping. The adhesive consists of a mechanically compliant, electrically conductive and optically transparent encapsulating coating, based on a combination of photocurable covalent networks (polyethylene glycol-lactide acid diacrylate, PEG-LA-DA) with ionic networks (sodium alginate, SA). In a constant-pressure system, the adhered electrode system demonstrated the ability to record high-quality normalized electrograms, comparable in amplitude to previously developed devices. Moreover, adhesion remained stable even after eight hours with minimal delamination.

7.7. Intraocular Pressure Monitoring

Intraocular pressure (IOP) is often measured a few times per year, posing challenges in obtaining an accurate IOP history for patients. Moreover, the IOP assessment is crucial in glaucoma treatment. Standard IOP measurement methods (e.g. tonometry[595]), indirectly gauge IOP and are impeded by intricate operational requirements and individual variances in corneal biomechanics. Accurate IOP monitoring requires small form factors, wireless operation and soft materials. Lee et al.[596] devised a microscale IOP sensor comprising a pressure-sensitive optical resonant cavity fabricated with a SiN membrane and Si mirror. The sensor's membrane deforms inward under a given IOP, reducing the cavity gap and generating a distinctive resonance spectral signature for each IOP level. To optimize the reflectivity of the SiN membrane, a gold nanodot array was incorporated, matching it with the reflective bottom Si mirror to maximize the optical resonance amplitude. Zhang et al.[597] introduced a new category of intelligent soft contact lenses, allowing for continuous monitoring of intraocular pressure (IOP) round the clock, including during sleep (Figure 12B). Remarkably, these smart soft contact lenses were developed using various commercially available brands of soft contact lenses, preserving their inherent characteristics such as lens power, biocompatibility, softness, transparency, wettability, oxygen transmissibility, and suitability for overnight wear. The study demonstrated that these smart soft contact lenses can seamlessly adapt to different corneal shapes and thicknesses in human eyes, thereby accurately measuring absolute intraocular pressure in everyday conditions. In vivo testing conducted on rabbit, dog, and human eyes, ranging from normal to hypertensive conditions, validated the superior accuracy in measurement, consistency within subjects, and comfort experienced by users compared to existing wearable ocular tonometers. Araci et al.[598] proposed another approach for IOP measurement, i.e. a microfluidic device integrated into an intraocular lens used in cataract surgery. This sensor, featuring an airtight microfluidic channel open to intraocular aqueous liquid on one end and a gas reservoir on the other, allowed visual assessment of the interface between the gas and aqueous intraocular liquid via a camera. Benchtop and in vivo testing demonstrated excellent sensitivity to pressure changes and reproducibility, offering a promising alternative for glaucoma monitoring post-hospital discharge. Yang et al.[354] introduced an intelligent wireless theranostic contact lens tailored for real-time monitoring and regulation of IOP. Through extensive testing, it was found that the contact lens demonstrated exceptional accuracy in measuring IOP levels, with a reported precision of up to 95%. Additionally, the regulatory function of the lens exhibited precise control over IOP, with the ability to adjust pressure levels within a range of ±2 mmHg. Moreover, the wireless RF communication technology enabled seamless data transmission, with a transmission efficiency of over 90%. A similar device was presented by Kim et al.[599] consisting of a smart contact lens with a sensitive gold hollow nanowire based IOP sensor, a flexible drug delivery system, wireless power and communication systems and an application specific integrated circuit chip for both monitoring and control of IOP in glaucoma.

7.8. Other Applications

Other applications of wireless wearable/implantable bioelectronics regard biomolecule sensing, strain sensing and monitoring of other physiological parameters. Biomolecule sensors are frequently utilized for dopamine detection, employing non-bioresorbable Pt nanoparticles as catalysts or bioresorbable alternatives, such as Fe-based nanoparticles.[540] Another application that holds significance, especially in diabetes management, regards continuous glucose monitoring.[600,601] Wang et al.[445] introduced an injectable device for real-time and in vivo detection of disease biomarkers, based on helical CNF fiber bundles mimicking the hierarchical muscle structure, enhancing sensor flexibility and averting mechanical mismatch post-implantation. Integration of various sensing components into single-ply sensing fibers facilitated specific biomolecule detection, while twisting multiple fibers together yielded a multi-ply sensing fiber capable of detecting multiple biomarkers like H_2O_2 in tumors and glucose and Ca^{2+} ions in blood.

Other applications of flexible bionics and bioelectronics include wearable and implantable sensors of organ motion or their change in shape and/or volume. Pei et al.[505] introduced an innovative hydrogel strain sensor inspired by the adhesive properties of mussels, incorporating characteristics such as wet adhesion, ion conductivity, self-healing, and flexibility. This

© 2024 The Author(s). Advanced Materials Technologies published by Wiley-VCH GmbH

2365709x, 0, Downloaded from https://onlinelibrary.wiley.com/doi/10.1002/admt.202400797 by University Of Oxford, Wiley Online Library on [19/11/2024]. See the Terms and Conditions (https://onlinelibrary.wiley.com/terms-and-conditions) on Wiley Online Library for rules of use; OA articles are governed by the applicable Creative Commons License

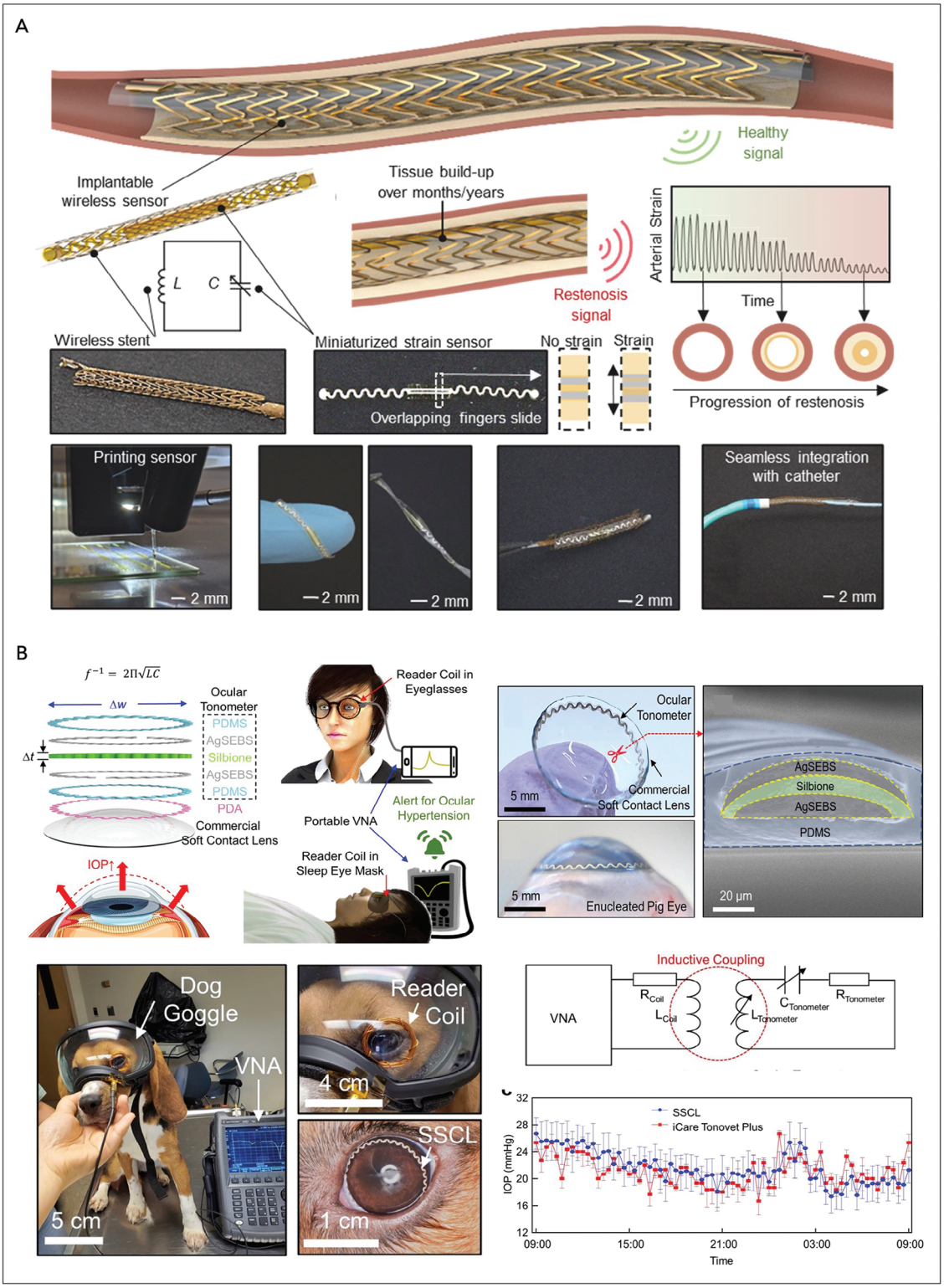


Figure 12. Examples of wireless technologies used in flexible wearable and implantable bioelectronics for cardiovascular monitoring and intraocular pressure monitoring. A) Implantable vascular bioelectronic device endowed with a miniaturized strain sensor via a high-resolution capillary-based microneedle printing method. The implantable device consisted of a wireless stent and capacitive strain sensor with correlating LC circuit. The detected wireless signals can be correlated with the progression of restenosis. Reproduced with permission.[593] Copyright 2023, Elsevier. B) Smart soft contact lenses for continuous 24-hour monitoring of intraocular pressure, validated in vivo in rabbits, dogs and human eyes. Reproduced from.[597] Copyright 2022, Springer Nature (Creative Commons CC BY) (C) (D).

© 2024 The Author(s). Advanced Materials Technologies published by Wiley-VCH GmbH

2365709x, 0, Downloaded from https://onlinelibrary.wiley.com/doi/10.1002/admt.202400797 by University Of Oxford, Wiley Online Library on [19/11/2024]. See the Terms and Conditions (https://onlinelibrary.wiley.com/terms-and-conditions) on Wiley Online Library for rules of use; OA articles are governed by the applicable Creative Commons License

sensor, constructed from PDA–clay–PSBMA hydrogel material, demonstrated real-time wireless sensing capabilities. Its strong adhesion allowed the hydrogel to seal and aid in the repair of injuries, facilitating postoperative monitoring. Furthermore, it exhibited high sensitivity with a gauge factor of 2 at strains up to 200%, attributed to its close conformal contact and high ionic conductivity. Stauffer et al.[3] addressed the challenge of passive wireless resonant sensors' suitability for high deformations exceeding 20% without impeding bladder filling. They devised a soft, implantable bladder volume sensor with a continuous wireless readout system devoid of active components (**Figure 13A**). This stretchable sensor, consisting of an implantable RLC circuit with a stretchable capacitor adhered to the bladder, employed a gold-coated titanium dioxide nanowire (Au–TiO_2 NW) embedded in an ultrasoft silicone elastomer matrix. Operating at a resonance frequency between 1 and 20 MHz, the sensor could communicate through greater tissue depths compared to devices using higher resonance frequencies.

As a further application, Kalidasan et al.[602] showed that multifilament surgical sutures functionalized with a conductive polymer and incorporating pledgets with capacitive sensors operated via RFID can be used to monitor physicochemical states of deep surgical sites in live pigs. The wireless sensing system comprised three key components: (1) a medical-grade non-resorbable suture rendered responsive to RF fields by a conductive polymer coating; (2) a battery-free electronic pledget containing a nonlinear circuit and capacitive sensor to convert physiological signals into shifts in the circuit's resonant frequency; and (3) a custom RD system for transmission of 1–2 GHz wireless signals and reception of backscattered 2–4 GHz second harmonic signals. Owing to the RF conductivity, the entire surgical stitch functioned as a dipole antenna and responded to the incident wireless signal through wireless backscattering.

In the context of neonatal intensive care (NIC), wireless technologies have also been introduced recently to facilitate physiological monitoring. For instance, Chung et al.[126] reported the fabrication of a NIC unit consisting of a pair of devices that could reconstruct full vital signs information with clinical-grade precision (Figure 13B). The devices consisted of a collection of thin, narrow serpentine metal traces (Cu, 50 to 100 μm in width, 5 μm in thickness) that interconnect multiple, chip-scale integrated circuit components. One device, based on electrodes made of filamentary metal mesh microstructures in a fractal geometry, was mounted on the chest to record ECGs. The other device was applied on the base of the foot to simultaneously record photoplethysmograms (PPGs). A microfluidic chamber filled with a nontoxic ionic liquid (1-ethyl-3-methylimidazolium ethyl sulfate) was used to provide mechanical isolation between the interconnected components and the skin. Each device was shown to record as well skin temperature data to get measurements of heart rate, respiration rate, blood oxygenation. Tests were conducted on neonates with gestational ages ranging from 28 weeks to full term.

8. Future Outlook and Challenges

With the increasing demand of personalized medicine and bionic applications, untethered and battery-free, soft and flexible wireless micro-systems have increasingly sparked interest among research groups and industrial companies. In this Review article, we described the fundamental mechanisms of wireless powering and data transfer that are currently available with the corresponding requirements in terms of design, power, footprint. We highlighted the materials commonly used to fabricate and assemble these platforms. The paper is a timely report on these emerging technologies whose technical maturity is increasing and consolidating rapidly in the recent years, leading to their preclinical/clinical implementation and commercial development.

To provide a guideline for future research, in **Table 4** we report a list of representative design/system requirements for WPT and WDC in flexible bionics and bioelectronics, accounting for the main applications. There is much scope to improve and expand capabilities for wireless systems by leveraging multidisciplinary parallel developments in related fields, involving micro and nanoengineering, artificial intelligence, material science, advanced electronics, biomedical engineering, healthcare. While recent breakthroughs have propelled the development of contactless and wireless technologies, numerous challenges have to be addressed for the full deployment of wireless technologies: they are outlined in brief below.

8.1. Developing Materials

The needs of personalized medicine increasingly require novel tailored materials with biocompatible or biodegradable properties, to avoid major immunological or inflammatory responses during the application and operation of the wireless devices. Additionally, the constituent materials need to offer physical and biomechanical properties (flexibility, conformability and tissue-like mechanics) that match with those of the surrounding tissue. These properties often represent non-negligible challenges for a high-performing continuous wireless operation; thus, research needs to be oriented towards the development of new solutions for reliable, ultra-flexible wireless devices.

8.2. Strengthening the Energy Supply

Many research efforts should be made for improving existing energy harvesting techniques, increasing the power budget, advancing energy storage devices. Achieving reliable and efficient power supply is essential to allow the wireless operation of devices outside specialized environments or standard conditions. On the other hand, if wider power budgets are needed for the sources, lower-power consumption is crucial for the future development of wireless technologies, especially if they will reach higher degrees of miniaturization.

8.3. Enhancing Mechanical Integrity and Device Reliability

The need for long-time wearability or chronic implantation for bionic and bioelectronic systems poses the challenge of developing materials and devices that can endure mechanical stresses and deformation without losing their functionality. Therefore, the materials should be ideally with high fatigue resistance and durability after a high number (≈millions) of stretching or bending cycles. Mechanical integrity of the active materials and the

© 2024 The Author(s). Advanced Materials Technologies published by Wiley-VCH GmbH

2365709x, 0, Downloaded from https://onlinelibrary.wiley.com/doi/10.1002/admt.202400797 by University Of Oxford, Wiley Online Library on [19/11/2024]. See the Terms and Conditions (https://onlinelibrary.wiley.com/terms-and-conditions) on Wiley Online Library for rules of use; OA articles are governed by the applicable Creative Commons License

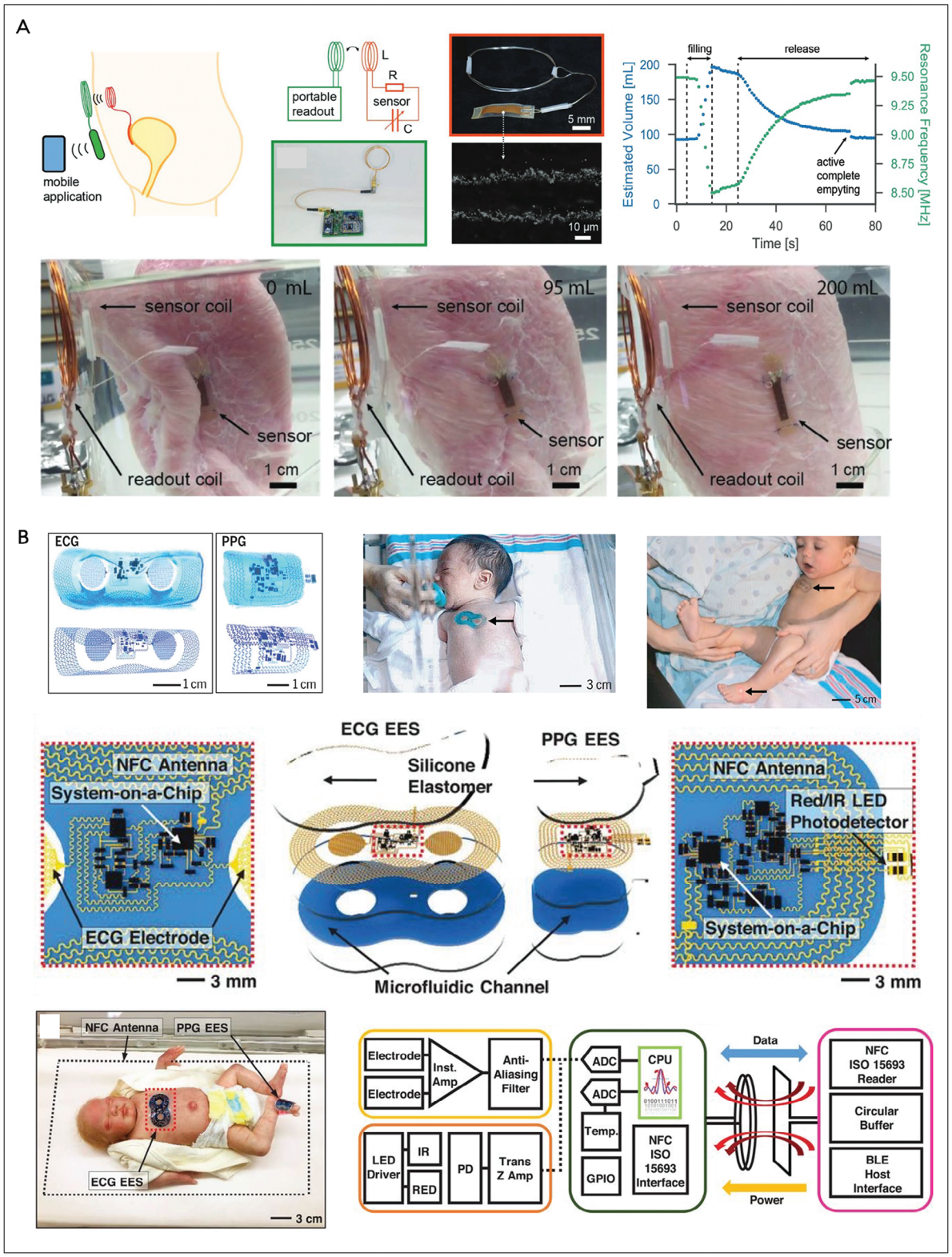


Figure 13. Examples of wireless technologies used in flexible wearable and implantable bioelectronics for other applications. A) Soft electronic strain sensor for real-time monitoring of bladder volume. The system consisted of an implantable RLC circuit with a stretchable capacitor adhered to the bladder, employed a gold-coated titanium dioxide nanowire embedded in an ultrasoft silicone elastomer. Reproduced with permission.[3] Copyright 2018, Wiley-VCH GbmH. B) Neonatal intensive care unit consisting of a pair of devices that could reconstruct full vital signs information with clinical-grade precision. Reproduced from.[126] Copyright 2019, AAAS (Creative Commons CC BY).

© 2024 The Author(s). Advanced Materials Technologies published by Wiley-VCH GmbH

2365709x, 0, Downloaded from https://onlinelibrary.wiley.com/doi/10.1002/admt.202400797 by University Of Oxford, Wiley Online Library on [19/11/2024]. See the Terms and Conditions (https://onlinelibrary.wiley.com/terms-and-conditions) on Wiley Online Library for rules of use; OA articles are governed by the applicable Creative Commons License

Table 4. Representative design/system requirements for WPT and WDC for the main applications in flexible bionics and bioelectronics.

Application	WPT	WDC
Implantable medical devices	• Frequency: 10–100 kHz, 10–100 MHz, 925 MHz, 1–5 GHz, to penetrate biological tissues effectively • Power efficiency: high to maximize power delivery while minimizing heat generation • Safety: minimized EM exposure to avoid tissue heating or damage • Size: compact and lightweight to fit within the implantable device constraints • Biocompatibility: use of biocompatible/bioresorbable materials to prevent adverse reactions Refs. [92–94,648,649]	• Frequency: 400–600 MHz or 2.4 GHz to balance penetration and data rate • Data rate: 10–100 kbps, 0.5-1 Mbps, 2–20 Mbps to sufficiently transmit patient data • Range: short-range (cm-m) to a receiver outside the body • Security: strong encryption to protect sensitive medical data • Latency: low latency to ensure real-time monitoring and response Refs. [94,650–653]
Wearable health monitors	• Frequency: typically 6.78 MHz or 13.56 MHz for short-range ICPT • Power efficiency: moderate to high efficiency to extend battery life • Safety: low EMI to prevent interference with other devices • Size and flexibility: compact and flexible materials to conform to the body's shape • User comfort: lightweight and ergonomic design for all-day wearability Refs. [654–658]	• Frequency: typically 2.4 GHz (Bluetooth, ZigBee) for compatibility with consumer devices • Data rate: 250 kbps – 2 Mbps for continuous health monitoring • Range: short to medium range (up to 10 m) for smartphones or home hubs • Security: encrypted communication to protect personal health information • Interoperability: compatibility with various smartphones and health apps • Power consumption: low power to support long-term use without frequent charging Refs. [659–663]
Smart contact lenses and eye implants	• Frequency: 13.56 MHz, UHF or 30–300 GHz for efficiency power transfer over short distances • Power efficiency: high efficiency due to limited space for energy storage • Miniaturization: extremely small and lightweight components to fit within the contact lens • Biocompatibility: safe materials to not irritate the eye or obstruct vision Refs. [664–668]	• Frequency: UHF for high data rates and short-range communication • Data rate: high data rates (up to several Mbps) for transmitting visual data or health metrics • Range: very short range (cm) to a wearable receiver • Security: secure data transmission to protect sensitive health and vision data • Latency: low latency for real-time applications like vision correction or augmented reality Refs. [664,665,669,670]
Smart patches and epidermal electronics	• Frequency: typically 6.78 MHz or 13.56 MHz for short-range ICPT • Power efficiency: high efficiency to power sensors and electronics embedded in the patch • Flexibility: use of flexible materials to conform to the skin • Biocompatibility: safe materials that do not cause skin irritation or allergic reactions Refs. [671–674]	• Frequency: typically 2.4 GHz (BLE, ZigBee) for consumer device compatibility • Data range: 250 kbps – 1 Mbps, 1–20 Mpbs, >1 Gbps for transmitting sensor data • Range: short to medium range (up to 10 m) to a smartphone or other receiver • Security: secure communication protocols to protect personal health data Refs. [126,675–680]
Ingestible capsules and sensors	• Frequency: 1–10 MHz, 13.56 MHz, 400–600 MHz to ensure power transfer through the body • Power efficiency: high efficiency to maximize battery life and reduce replacements • Size: miniaturized components to fit within ingestible capsules • Biocompatibility: safe materials for ingestion and passage through the gastrointestinal tract Refs. [681–683]	• Frequency: 400–900 MHz for effective transmission through the body • Data rate: 10–250 kbps to transmit sensor readings • Range: short range (m) to an external receiver or wearable hub • Security: secure data transmission to protect sensitive health data • Latency: low latency for real-time health monitoring • Power consumption: low power to ensure the capsule functions throughout its transit in the body Refs. [684–688]

N.B. The most common or typical ranges of frequencies and data transfer rates are reported for each category; however, they should be considered as representative values and not as inclusive of any possible work present in literature or of any instantiation of a wireless device.

© 2024 The Author(s). Advanced Materials Technologies published by Wiley-VCH GmbH

2365709x, 0, Downloaded from https://onlinelibrary.wiley.com/doi/10.1002/admt.202400797 by University Of Oxford, Wiley Online Library on [19/11/2024]. See the Terms and Conditions (https://onlinelibrary.wiley.com/terms-and-conditions) on Wiley Online Library for rules of use; OA articles are governed by the applicable Creative Commons License

device architecture is a key element for guaranteeing a proper device operation. Especially for a stable wireless operation, it is crucial to retain the mechanical properties of tracks and interconnects within coils or antennas. Besides the properties of the substrates and active layers, encapsulations play an important role for the whole device integrity: high crack onset strains (COS, >2-3%) and ultra-high hermeticity (i.e. impermeability to water and ions) are needed.[344]

8.4. Improving Accuracy of Sensing/Stimulation Capabilities

Wireless detection systems for transmitting the retrieved data will benefit from an increase in the quality and volume of the data acquired in order to provide a more accurate and efficient diagnostics. The data transfer rate is essential to improve precision and develop more dynamic and quickly responding architectures. Machine learning and artificial intelligence can offer multiple strategies and techniques to handle bigger amounts of data, enhancing the effectiveness of physiological monitoring, feedback control algorithms and simultaneous actuation of several operations per unit time.

8.5. Widening Wireless Bandwidth

Different frequency bands are used for wireless medical devices, i.e. 9–315 kHz for all implantable medical devices, 30–37.5 MHz for membrane implants, 401–406 MHz for ultra-low power active medical implants, 2.4-2.5 GHz for low power active medical implants. It is thus important that these frequencies, together with regulations and standards are globally harmonized and unified for medical device wireless communications due to the cross-border mobility of patients wearing or bearing wireless systems. Widening these bandwidths would also allow to enhance the timing resolution of the devices and to accelerate the pre-processing of information on-device.

8.6. Increasing Efficiency of Closed-Loop Operations

Future wireless bionics and bioelectronics should ideally be semi or fully autonomous, thus based on closed-loop operations where biosensors will be used to provide feedback to a control system to trigger the actual device. Therefore, there is a need of leveraging recent advances in biosensors and feedback-control algorithms to enable more efficient and personalized systems.

8.7. Expanding Applicability

In order to design and develop more complex and sophisticated biomedical devices, new and more functionalities should be combined. Wireless operation should be ideally coupled with enhanced capabilities, especially in the fields of drug delivery and release of therapeutic agents, or of multimodal stimulation based on optical, electrical and electromechanical triggers. Multifunctionality and versatility will be key features for any future wireless bionic and bioelectronic system. Expanding the applicability of these devices will enable their clinical translation, where invasiveness, side effects, physiological heterogeneity and long-term stability play an important role.

In summary, while tethered implantable systems have facilitated significant advancements in medical research, to overcome their limitations wireless and batteryless bionics will perform an important role in the future of healthcare, personalized medicine, biorobotics and biomedical research, contributing to synergetic multi-disciplinary achievements, enhancing experimental validity and broadening the scope of scientific inquiry.

Acknowledgements

MM thanks heartfeltly Gabriele, Andrea, Rossana, Francesco, Franco and Pina. MM also acknowledges three institutions (Italian Institute of Technology, école Polytechnique Fédérale de Lausanne and University of Oxford) for their contribution to building his scientific and cultural expertise. The authors acknowledge funding (salaries) from the Biotechnology and Biological Sciences Research Council David Phillips Fellowship (BB/T009314/1).

Conflict of Interest

The authors declare no conflict of interest.

Keywords

bionics, data transfer, energy harvesting, flexible, power transfer, wearable and implantable bioelectronics, wireless

Received: July 7, 2024
Revised: August 12, 2024
Published online:

[1] A. P. F. Turner, *Chem. Soc. Rev.* **2013**, *42*, 3184.
[2] Y. Jang, S. M. Kim, K. J. Kim, H. J. Sim, B.-J. Kim, J. W. Park, R. H. Baughman, A. Ruhparwar, Kim, *ACS Sens.* **2019**, *4*, 2893.
[3] F. Stauffer, Q. Zhang, K. Tybrandt, B. Llerena Zambrano, J. Hengsteler, A. Stoll, C. Trüeb, M. Hagander, J.-M. Sujata, F. Hoffmann, J. Schuurmans Stekhoven, J. Quack, H. Zilly, J. Goedejohann, M. P. Schneider, T. M. Kessler, W. R. Taylor, R. Küng, J. Vörös, *Adv. Mater. Technol.* **2018**, *3*, 1800031.
[4] K. Scholten, E. Meng, *Int. J. Pharm.* **2018**, *544*, 319.
[5] S.-J. Kim, D.-S. Lee, I.-G. Kim, D.-W. Sohn, J.-Y. Park, B.-K. Choi, S.-W. Kim, *Kaohsiung J. Med. Sci.* **2012**, *28*, 123.
[6] Y. Ma, Q. Zheng, Y. Liu, B. Shi, X. Xue, W. Ji, Z. Liu, Y. Jin, Y. Zou, Z. An, W. Zhang, X. Wang, W. Jiang, Z. Xu, Z. L. Wang, Z. Li, H. Zhang, *Nano Lett.* **2016**, *16*, 6042.
[7] M. Mariello, K. Wu, M. v. Allmen, M. V. Gompel, S. P. Lacour, Y. Leterrier, in *2022 IEEE International Conference on Flexible and Printable Sensors and Systems (FLEPS)* **2022**, 1–4, https://doi.org/10.1109/FLEPS53764.2022.9781582.
[8] J. Kim, A. S. Campbell, B. E.-F. de Ávila, J. Wang, *Nat. Biotechnol.* **2019**, *37*, 389.
[9] F. Fallegger, A. Trouillet, F.-V. Coen, G. Schiavone, S. P. Lacour, *APL Bioeng.* **2023**, *7*, 036109.
[10] F. Wu, E. Stark, P-.C. Ku, K. D. Wise, G. Buzsaki, *Neuron* **2015**, *88*, 1136.
[11] K. K. Ghosh, L. D. Burns, E. D. Cocker, A. Nimmerjahn, Y. Ziv, A. E. Gamal, M. J. Schnitzer, *Nat. Methods* **2011**, *8*, 871.

© 2024 The Author(s). Advanced Materials Technologies published by Wiley-VCH GmbH

2365709x, 0, Downloaded from https://onlinelibrary.wiley.com/doi/10.1002/admt.202400797 by University Of Oxford, Wiley Online Library on [19/11/2024]. See the Terms and Conditions (https://onlinelibrary.wiley.com/terms-and-conditions) on Wiley Online Library for rules of use; OA articles are governed by the applicable Creative Commons License

[12] S. L. Resendez, J. H. Jennings, R. L. Ung, V. M. K. Namboodiri, Z. C. Zhou, J. M. Otis, H. Nomura, J. A. McHenry, O. Kosyk, G. D. Stuber, *Nat. Protoc.* **2016**, *11*, 566.
[13] E. S. Boyden, F. Zhang, E. Bamberg, G. Nagel, K. Deisseroth, *Nat. Neurosci.* **2005**, *8*, 1263.
[14] K. O. Deisseroth, *Nat. Methods* **2011**, *8*, 26.
[15] K. D. Piatkevich, E. E. Jung, C. Straub, C. Linghu, D. Park, H.-J. Suk, D. R. Hochbaum, D. Goodwin, E. Pnevmatikakis, N. Pak, T. Kawashima, C.-T. Yang, J. L. Rhoades, O. Shemesh, S. Asano, Y.-G. Yoon, L. Freifeld, J. L. Saulnier, C. Riegler, F. Engert, T. Hughes, M. Drobizhev, B. Szabo, M. B. Ahrens, S. W. Flavell, B. L. Sabatini, E. S. Boyden, *Nat. Chem. Biol.* **2018**, *14*, 352.
[16] L. A. Gunaydin, L. Grosenick, J. C. Finkelstein, I. V. Kauvar, L. E. Fenno, A. Adhikari, S. Lammel, J. J. Mirzabekov, R. D. Airan, K. A. Zalocusky, K. M. Tye, P. Anikeeva, R. C. Malenka, K. Deisseroth, *Cell* **2014**, *157*, 1535.
[17] A. Canales, X. Jia, U. P. Froriep, R. A. Koppes, C. M. Tringides, J. Selvidge, C. Lu, C. Hou, L. Wei, Y. Fink, P. Anikeeva, *Nat. Biotechnol.* **2015**, *33*, 277.
[18] F. Pisanello, G. Mandelbaum, M. Pisanello, I. A. Oldenburg, L. Sileo, J. E. Markowitz, R. E. Peterson, A. Della Patria, T. M. Haynes, M. S. Emara, B. Spagnolo, S. R. Datta, M. De Vittorio, B. L. Sabatini, *Nat. Neurosci.* **2017**, *20*, 1180.
[19] D. G. Barone, A. Carnicer-Lombarte, P. Tourlomousis, R. S. Hamilton, M. Prater, A. L. Rutz, I. B. Dimov, G. G. Malliaras, S. P. Lacour, A. A. B. Robertson, K. Franze, J. W. Fawcett, C. E. Bryant, *Proc. Natl. Acad. Sci* **2022**, *119*, e2115857119.
[20] M. A. Lee, X. Jin, S. Muthupalani, N. A. Bakh, X. Gong, M. S. Strano, *J. Nanobiotechnology* **2023**, *21*, 133.
[21] R. Caldwell, M. G. Street, R. Sharma, P. Takmakov, B. Baker, L. Rieth, *Biomaterials* **2020**, *232*, 119731.
[22] R. G. Hauser, S. A. Casey, C. B. Gitter, C. Y. Tang, R. H. Abdelhadi, C. C. Gornick, L. Stanberry, J. D. Sengupta, *J. Interv. Card. Electrophysiol. Int. J. Arrhythm. Pacing* **2021**, *62*, 507.
[23] S. P. Lacour, G. Courtine, J. Guck, *Nat. Rev. Mater.* **2016**, *1*, 1.
[24] G. Schiavone, F. Fallegger, X. Kang, B. Barra, N. Vachicouras, E. Roussinova, I. Furfaro, S. Jiguet, I. Seáñez, S. Borgognon, A. Rowald, Q. Li, C. Qin, E. Bézard, J. Bloch, G. Courtine, M. Capogrosso, S. P. Lacour, *Adv. Mater.* **2020**, *32*, 1906512.
[25] F. Fallegger, G. Schiavone, S. P. Lacour, *Adv. Mater.* **2020**, *32*, 1903904.
[26] J. W. Phillips, A. Prominski, B. Tian, *VIEW* **2022**, *3*, 20200157.
[27] M. L. Bernard, *Ochsner J* **2016**, *16*, 238.
[28] M. A. Miller, P. Neuzil, S. R. Dukkipati, V. Y. Reddy, *J. Am. Coll. Cardiol.* **2015**, *66*, 1179.
[29] Y. S. Choi, R. T. Yin, A. Pfenniger, J. Koo, R. Avila, K. Benjamin Lee, S. W. Chen, G. Lee, G. Li, Y. Qiao, A. Murillo-Berlioz, A. Kiss, S. Han, S. M. Lee, C. Li, Z. Xie, Y.-Y. Chen, A. Burrell, B. Geist, H. Jeong, J. Kim, H.-J. Yoon, A. Banks, S.-K. Kang, Z. J. Zhang, C. R. Haney, A. V. Sahakian, D. Johnson, T. Efimova, Y. Huang, et al., *Nat. Biotechnol.* **2021**, *39*, 1228.
[30] P. Gutruf, R. T. Yin, K. B. Lee, J. Ausra, J. A. Brennan, Y. Qiao, Z. Xie, R. Peralta, O. Talarico, A. Murillo, S. W. Chen, J. P. Leshock, C. R. Haney, E. A. Waters, C. Zhang, H. Luan, Y. Huang, G. Trachiotis, I. R. Efimov, J. A. Rogers, *Nat. Commun.* **2019**, *10*, 5742.
[31] E. Cingolani, J. I. Goldhaber, E. Marbán, *Nat. Rev. Cardiol.* **2018**, *15*, 139.
[32] A. Gilletti, J. Muthuswamy, *J. Neural Eng.* **2006**, *3*, 189.
[33] A. Sridharan, S. D. Rajan, J. Muthuswamy, *J. Neural Eng.* **2013**, *10*, 066001.
[34] D. Fan, D. Rich, T. Holtzman, P. Ruther, J. W. Dalley, A. Lopez, M. A. Rossi, J. W. Barter, D. Salas-Meza, S. Herwik, T. Holzhammer, J. Morizio, H. H. Yin, *PLoS One* **2011**, *6*, e22033.
[35] P. Blomstedt, M. I. Hariz, *Acta Neurochir. (Wien)* **2005**, *147*, 1061.
[36] I. R. Minev, P. Musienko, A. Hirsch, Q. Barraud, N. Wenger, E. M. Moraud, J. Gandar, M. Capogrosso, T. Milekovic, L. Asboth, R. F. Torres, N. Vachicouras, Q. Liu, N. Pavlova, S. Duis, A. Larmagnac, J. Vörös, S. Micera, Z. Suo, G. Courtine, S. P. Lacour, *Science* **2015**, *347*, 159.
[37] J. K. Nguyen, D. J. Park, J. L. Skousen, A. E. Hess-Dunning, D. J. Tyler, S. J. Rowan, C. Weder, J. R. Capadona, *J. Neural Eng.* **2014**, *11*, 056014.
[38] A. Carnicer-Lombarte, S.-T. Chen, G. G. Malliaras, D. G. Barone, *Front. Bioeng. Biotechnol.* **2021**, *9*, 622524.
[39] S. Kwon, Y.-T. Kwon, Y.-S. Kim, H.-R. Lim, M. Mahmood, W.-H. Yeo, *Biosens. Bioelectron.* **2020**, *151*, 111981.
[40] S.-K. Kang, J. Koo, Y. K. Lee, J. A. Rogers, *Acc. Chem. Res.* **2018**, *51*, 988 .
[41] S. Saska, L. Pilatti, A. Blay, J. A. Shibli, *Polymers* **2021**, *13*, 563.
[42] Q. Yang, Z. Hu, M.-H. Seo, Y. Xu, Y. Yan, Y.-H. Hsu, J. Berkovich, K. Lee, T.-L. Liu, S. McDonald, H. Nie, H. Oh, M. Wu, J.-T. Kim, S. A. Miller, Y. Jia, S. Butun, W. Bai, H. Guo, J. Choi, A. Banks, W. Z. Ray, Y. Kozorovitskiy, M. L. Becker, M. A. Pet, M. R. MacEwan, J.-K. Chang, H. Wang, Y. Huang, J. A. Rogers, *Nat. Commun.* **2022**, *13*, 6518.
[43] X. Yu, W. Shou, B. K. Mahajan, X. Huang, H. Pan, *Adv. Mater.* **2018**, *30*, 1707624 .
[44] L. Lu, P. Gutruf, L. Xia, D. L. Bhatti, X. Wang, A. Vazquez-Guardado, X. Ning, X. Shen, T. Sang, R. Ma, G. Pakeltis, G. Sobczak, H. Zhang, D.-O. Seo, M. Xue, L. Yin, D. Chanda, X. Sheng, M. R. Bruchas, J. A. Rogers, *Proc. Natl. Acad. Sci. USA* **2018**, *115*, E1374.
[45] C. J. Stoodley, A. M. D'Mello, J. Ellegood, V. Jakkamsetti, P. Liu, M. B. Nebel, J. M. Gibson, E. Kelly, F. Meng, C. A. Cano, J. M. Pascual, S. H. Mostofsky, J. P. Lerch, P. T. Tsai, *Nat. Neurosci.* **2017**, *20*, 1744.
[46] U. Jürgens, S. R. Hage, *Methods San Diego Calif* **2006**, *38*, 195.
[47] L. Kingsbury, S. Huang, J. Wang, K. Gu, P. Golshani, Y. E. Wu, W. Hong, *Cell* **2019**, *178*, 429.
[48] W. Zhang, M. M. Yartsev, *Cell* **2019**, *178*, 413.
[49] Y. Zhang, D. C. Castro, Y. Han, Y. Wu, H. Guo, Z. Weng, Y. Xue, J. Ausra, X. Wang, R. Li, G. Wu, A. Vázquez-Guardado, Y. Xie, Z. Xie, D. Ostojich, D. Peng, R. Sun, B. Wang, Y. Yu, J. P. Leshock, S. Qu, C.-J. Su, W. Shen, T. Hang, A. Banks, Y. Huang, J. Radulovic, P. Gutruf, M. R. Bruchas, J. A. Rogers, *Proc. Natl. Acad. Sci* **2019**, *116*, 21427.
[50] A. Zhou, S. R. Santacruz, B. C. Johnson, G. Alexandrov, A. Moin, F. L. Burghardt, J. M. Rabaey, J. M. Carmena, R. Muller, *Nat. Biomed. Eng.* **2019**, *3*, 15.
[51] Y. Wu, M. Wu, A. Vázquez-Guardado, J. Kim, X. Zhang, R. Avila, J.-T. Kim, Y. Deng, Y. Yu, S. Melzer, Y. Bai, H. Yoon, L. Meng, Y. Zhang, H. Guo, L. Hong, E. E. Kanatzidis, C. R. Haney, E. A. Waters, A. R. Banks, Z. Hu, F. Lie, L. P. Chamorro, B. L. Sabatini, Y. Huang, Y. Kozorovitskiy, J. A. Rogers, *Nat. Commun.* **2022**, *13*, 5571.
[52] G. Gagnon-Turcotte, Y. LeChasseur, C. Bories, Y. Messaddeq, Y. De Koninck, B. Gosselin, *IEEE Trans. Biomed. Circuits Syst.* **2017**, *11*, 1.
[53] H. Mei, P. P. Irazoqui, *Nat. Biotechnol.* **2014**, *32*, 1008.
[54] G. Shin, A. M. Gomez, R. Al-Hasani, Y. R. Jeong, J. Kim, Z. Xie, A. Banks, S. M. Lee, S. Y. Han, C. J. Yoo, J.-L. Lee, S. H. Lee, J. Kurniawan, J. Tureb, Z. Guo, J. Yoon, S.-I. Park, S. Y. Bang, Y. Nam, M. C. Walicki, V. K. Samineni, A. D. Mickle, K. Lee, S. Y. Heo, J. G. McCall, T. Pan, L. Wang, X. Feng, T.-I. Kim, J. K. Kim, et al., *Neuron* **2017**, *93*, 509.
[55] S. I. Park, G. Shin, J. G. McCall, R. Al-Hasani, A. Norris, L. Xia, D. S. Brenner, K. N. Noh, S. Y. Bang, D. L. Bhatti, K.-I. Jang, S.-K. Kang, A. D. Mickle, G. Dussor, T. J. Price, R. W. Gereau, M. R. Bruchas, J. A. Rogers, *Proc. Natl. Acad. Sci* **2016**, *113*, E8169.
[56] K. L. Montgomery, A. J. Yeh, J. S. Ho, V. Tsao, S. Mohan Iyer, L. Grosenick, E. A. Ferenczi, Y. Tanabe, K. Deisseroth, S. L. Delp, A. S. Y. Poon, *Nat. Methods* **2015**, *12*, 969.
[57] J. Charthad, M. J. Weber, T. C. Chang, A. Arbabian, *IEEE J. Solid-State Circuits* **2015**, *50*, 1741.

© 2024 The Author(s). Advanced Materials Technologies published by Wiley-VCH GmbH

2365709x, 0, Downloaded from https://onlinelibrary.wiley.com/doi/10.1002/admt.202400797 by University Of Oxford, Wiley Online Library on [19/11/2024]. See the Terms and Conditions (https://onlinelibrary.wiley.com/terms-and-conditions) on Wiley Online Library for rules of use; OA articles are governed by the applicable Creative Commons License

[58] D. Seo, R. M. Neely, K. Shen, U. Singhal, E. Alon, J. M. Rabaey, J. M. Carmena, M. M. Maharbiz, *Neuron* **2016**, *91*, 529.
[59] S. Lee, A. J. Cortese, A. P. Gandhi, E. R. Agger, P. L. McEuen, A. C. Molnar, *IEEE Trans. Biomed. Circuits Syst.* **2018**, *12*, 1256.
[60] H. Ding, L. Lu, Z. Shi, D. Wang, L. Li, X. Li, Y. Ren, C. Liu, D. Cheng, H. Kim, N. C. Giebink, X. Wang, L. Yin, L. Zhao, M. Luo, X. Sheng, *Proc. Natl. Acad. Sci* **2018**, *115*, 6632.
[61] M. Rezaei, E. Maghsoudloo, C. Bories, Y. De Koninck, B. Gosselin, *IEEE Trans. Biomed. Circuits Syst.* **2018**, *12*, 271.
[62] D. A. Schwarz, M. A. Lebedev, T. L. Hanson, D. F. Dimitrov, G. Lehew, J. Meloy, S. Rajangam, V. Subramanian, P. J. Ifft, Z. Li, A. Ramakrishnan, A. Tate, K. Z. Zhuang, M. A. L. Nicolelis, *Nat. Methods* **2014**, *11*, 670.
[63] S. M. Won, L. Cai, P. Gutruf, J. A. Rogers, *Nat. Biomed. Eng.* **2023**, *7*, 405.
[64] V. Sivaji, D. W. Grasse, S. A. Hays, J. E. Bucksot, R. Saini, M. P. Kilgard, R. L. Rennaker, *J. Neurosci. Methods* **2019**, *320*, 26.
[65] A. Burton, S. N. Obaid, A. Vázquez-Guardado, M. B. Schmit, T. Stuart, L. Cai, Z. Chen, I. Kandela, C. R. Haney, E. A. Waters, H. Cai, J. A. Rogers, L. Lu, P. Gutruf, *Proc. Natl. Acad. Sci* **2020**, *117*, 2835.
[66] H. Zhang, P. Gutruf, K. Meacham, M. C. Montana, X. Zhao, A. M. Chiarelli, A. Vázquez-Guardado, A. Norris, L. Lu, Q. Guo, C. Xu, Y. Wu, H. Zhao, X. Ning, W. Bai, I. Kandela, C. R. Haney, D. Chanda, R. W. Gereau, J. A. Rogers, *Sci. Adv.* **2019**, *5*, eaaw0873.
[67] Y. Zhang, A. D. Mickle, P. Gutruf, L. A. McIlvried, H. Guo, Y. Wu, J. P. Golden, Y. Xue, J. G. Grajales-Reyes, X. Wang, S. Krishnan, Y. Xie, D. Peng, C.-J. Su, F. Zhang, J. T. Reeder, S. K. Vogt, Y. Huang, J. A. Rogers, R. W. Gereau, *Sci. Adv.* **2019**, *5*, eaaw5296.
[68] J.-W. Jeong, J. G. McCall, G. Shin, Y. Zhang, R. Al-Hasani, M. Kim, S. Li, J. Y. Sim, K.-I. Jang, Y. Shi, D. Y. Hong, Y. Liu, G. P. Schmitz, L. Xia, Z. He, P. Gamble, W. Z. Ray, Y. Huang, M. R. Bruchas, J. A. Rogers, *Cell* **2015**, *162*, 662.
[69] C. Kathe, F. Michoud, P. Schönle, A. Rowald, N. Brun, J. Ravier, I. Furfaro, V. Paggi, K. Kim, S. Soloukey, L. Asboth, T. H. Hutson, I. Jelescu, A. Philippides, N. Alwahab, J. Gandar, D. Huber, C. I. De Zeeuw, Q. Barraud, Q. Huang, S. P. Lacour, G. Courtine, *Nat. Biotechnol.* **2021**, 198.
[70] Y. S. Choi, H. Jeong, R. T. Yin, R. Avila, A. Pfenniger, J. Yoo, J. Y. Lee, A. Tzavelis, Y. J. Lee, S. W. Chen, H. S. Knight, S. Kim, H.-Y. Ahn, G. Wickerson, A. Vázquez-Guardado, E. Higbee-Dempsey, B. A. Russo, M. A. Napolitano, T. J. Holleran, L. A. Razzak, A. N. Miniovich, G. Lee, B. Geist, B. Kim, S. Han, J. A. Brennan, K. Aras, S. S. Kwak, J. Kim, E. A. Waters, et al., *Science* **2022**, *376*, 1006.
[71] A. D. Mickle, S. M. Won, K. N. Noh, J. Yoon, K. W. Meacham, Y. Xue, L. A. McIlvried, B. A. Copits, V. K. Samineni, K. E. Crawford, D. H. Kim, P. Srivastava, B. H. Kim, S. Min, Y. Shiuan, Y. Yun, M. A. Payne, J. Zhang, H. Jang, Y. Li, H. H. Lai, Y. Huang, S.-I. Park, R. W. Gereau, J. A. Rogers, *Nature* **2019**, *565*, 361.
[72] W. Ouyang, W. Lu, Y. Zhang, Y. Liu, J. U. Kim, H. Shen, Y. Wu, H. Luan, K. Kilner, S. P. Lee, Y. Lu, Y. Yang, J. Wang, Y. Yu, A. J. Wegener, J. A. Moreno, Z. Xie, Y. Wu, S. M. Won, K. Kwon, C. Wu, W. Bai, H. Guo, T.-L. Liu, H. Bai, G. Monti, J. Zhu, S. R. Madhvapathy, J. Trueb, M. Stanslaski, et al., *Nat. Biomed. Eng.* **2023**, *7*, 1252.
[73] M. Mariello, *Nanoenergy Adv* **2022**, *2*, 344.
[74] M. H. Ansari, M. A. Karami, *J. Phys. Conf. Ser.* **2015**, *660*, 012121.
[75] H. Ouyang, Z. Liu, N. Li, B. Shi, Y. Zou, F. Xie, Y. Ma, Z. Li, H. Li, Q. Zheng, X. Qu, Y. Fan, Z. L. Wang, H. Zhang, Z. Li, *Nat. Commun.* **2019**, *10*, 1821.
[76] C. Dagdeviren, P. Joe, O. L. Tuzman, K.-I. Park, K. J. Lee, Y. Shi, Y. Huang, J. A. Rogers, *Extreme Mech. Lett.* **2016**, *9*, 269.
[77] C. Dagdeviren, Y. Shi, P. Joe, R. Ghaffari, G. Balooch, K. Usgaonkar, O. Gur, P. L. Tran, J. R. Crosby, M. Meyer, Y. Su, R. Chad Webb, A. S. Tedesco, M. J. Slepian, Y. Huang, J. A. Rogers, *Nat. Mater.* **2015**, *14*, 728.
[78] C. Dagdeviren, B. D. Yang, Y. Su, P. L. Tran, P. Joe, E. Anderson, J. Xia, V. Doraiswamy, B. Dehdashti, X. Feng, B. Lu, R. Poston, Z. Khalpey, R. Ghaffari, Y. Huang, M. J. Slepian, J. A. Rogers, *Proc. Natl. Acad. Sci* **2014**, *111*, 1927.
[79] G. Yao, L. Kang, J. Li, Y. Long, H. Wei, C. A. Ferreira, J. J. Jeffery, Y. Lin, W. Cai, X. Wang, *Nat. Commun.* **2018**, *9*, 5349.
[80] R. A. Bullen, T. C. Arnot, J. B. Lakeman, F. C. Walsh, *Biosens. Bioelectron.* **2006**, *21*, 2015.
[81] P. Cinquin, C. Gondran, F. Giroud, S. Mazabrard, A. Pellissier, F. Boucher, J.-P. Alcaraz, K. Gorgy, F. Lenouvel, S. Mathé, P. Porcu, S. Cosnier, *PLoS One* **2010**, *5*, e10476.
[82] J. A. Castorena-Gonzalez, et al., *Electroanalysis* **2013**, *25*, 1579.
[83] M. Falk, C. W. Narváez Villarrubia, S. Babanova, P. Atanassov, S. Shleev, *ChemPhysChem* **2013**, *14*, 2045.
[84] M. Hyland, H. Hunter, J. Liu, E. Veety, D. Vashaee, *Appl. Energy* **2016**, *182*, 518.
[85] K. Nan, S. D. Kang, K. Li, K. J. Yu, F. Zhu, J. Wang, A. C. Dunn, C. Zhou, Z. Xie, M. T. Agne, H. Wang, H. Luan, Y. Zhang, Y. Huang, G. J. Snyder, J. A. Rogers, *Sci. Adv.* **2018**, *4*, eaau5849.
[86] A. Kim, M. Ochoa, R. Rahimi, B. Ziaie, *IEEE Access* **2015**, *3*, 89.
[87] Y. Huang, J. Zhou, P. Ke, X. Guo, C. K. Yiu, K. Yao, S. Cai, D. Li, Y. Zhou, J. Li, T. H. Wong, Y. Liu, L. Li, Y. Gao, X. Huang, H. Li, J. Li, B. Zhang, Z. Chen, H. Zheng, X. Yang, H. Gao, Z. Zhao, X. Guo, E. Song, H. Wu, Z. Wang, Z. Xie, K. Zhu, X. Yu, *Nat. Electron.* **2023**, *6*, 1041.
[88] S. I. Park, D. S. Brenner, G. Shin, C. D. Morgan, B. A. Copits, H. U. Chung, M. Y. Pullen, K. N. Noh, S. Davidson, S. J. Oh, J. Yoon, K.-I. Jang, V. K. Samineni, M. Norman, J. G. Grajales-Reyes, S. K. Vogt, S. S. Sundaram, K. M. Wilson, J. S. Ha, R. Xu, T. Pan, T.-I. Kim, Y. Huang, M. C. Montana, J. P. Golden, M. R. Bruchas, R. W. Gereau, J. A. Rogers, *Nat. Biotechnol.* **2015**, *33*, 1280.
[89] A. Khalifa, Y. Karimi, Q. Wang, W. Montlouis, S. Garikapati, M. Stanacevic, N. Thakor, R. Etienne-Cummings, *IEEE Trans. Biomed. Circuits Syst.* **2018**, *12*, 521.
[90] P. Gutruf, V. Krishnamurthi, A. Vázquez-Guardado, Z. Xie, A. Banks, C.-J. Su, Y. Xu, C. R. Haney, E. A. Waters, I. Kandela, S. R. Krishnan, T. Ray, J. P. Leshock, Y. Huang, D. Chanda, J. A. Rogers, *Nat. Electron.* **2018**, *1*, 652.
[91] Y. Jia, Z. Wang, S. A. Mirbozorgi, M. Ghovanloo, in *2015 IEEE Biomedical Circuits and Systems Conference (BioCAS)* **2015**, pp. 1–4, https://doi.org/10.1109/BioCAS.2015.7348392.
[92] A. Singer, J. T. Robinson, *Adv. Healthcare Mater.* **2021**, *10*, 2100664.
[93] S. R. Khan, S. K. Pavuluri, G. Cummins, M. P. Y. Desmulliez, *Sensors* **2020**, *20*, 3487.
[94] S. Yoo, J. Lee, H. Joo, S.-H. Sunwoo, S. Kim, D.-H. Kim, *Adv. Healthcare Mater.* **2021**, *n/a*, 2100614.
[95] J.-C. Chiao, C. Li, J. Lin, R. H. Caverly, J. C. M. Hwang, H. Rosen, A. Rosen, *IEEE J. Microw.* **2023**, *3*, 134.
[96] F. Merli, L. Bolomey, J-.F. Zurcher, G. Corradini, E. Meurville, A. K. Skrivervik, *IEEE Trans. Antennas Propag.* **2011**, *59*, 3544.
[97] K. T. Selvan, R. F. Janaswamy, F. Distances, *IEEE Antennas Propag. Mag.* **2017**, *59*, 12.
[98] J. Zhu, H. Cheng, *Sensors* **2018**, *18*, 4364.
[99] S. I. Park, G. Shin, A. Banks, J. G. McCall, E. R. Siuda, M. J. Schmidt, H. U. Chung, K. N. Noh, J. G.-H. Mun, J. Rhodes, M. R. Bruchas, J. A. Rogers, *J. Neural Eng.* **2015**, *12*, 056002.
[100] Z. Xie, R. Avila, Y. Huang, J. A. Rogers, *Adv. Mater.* **2020**, *32*, 1902767.
[101] D. M. Dobkin, *The RF in RFID: UHF RFID in Practice*, Newnes, Amsterdam **2012**.
[102] J. S. Ho, Y. Tanabe, S. M. Iyer, A. J. Christensen, L. Grosenick, K. Deisseroth, S. L. Delp, A. S. Y. Poon, *Phys. Rev. Appl.* **2015**, *4*, 024001.
[103] S. M. Michaelson, *Health Phys.* **1991**, *61*, 3.
[104] B. Pophof, B. Henschenmacher, D. R. Kattnig, J. Kuhne, A. Vian, G. Ziegelberger, *Health Phys.* **2023**, *124*, 31.

© 2024 The Author(s). Advanced Materials Technologies published by Wiley-VCH GmbH

2365709x, 0, Downloaded from https://onlinelibrary.wiley.com/doi/10.1002/admt.202400797 by University Of Oxford, Wiley Online Library on [19/11/2024]. See the Terms and Conditions (https://onlinelibrary.wiley.com/terms-and-conditions) on Wiley Online Library for rules of use; OA articles are governed by the applicable Creative Commons License

[105] P. Wust, B. Kortüm, U. Strauss, J. Nadobny, S. Zschaeck, M. Beck, U. Stein, P. Ghadjar, *Sci. Rep.* **2020**, *10*, 13488.
[106] K. Niotaki, N. B. Carvalho, A. Georgiadis, X. Gu, S. Hemour, K. Wu, D. Matos, D. Belo, R. Pereira, R. Figueiredo, H. Chaves, B. Mendes, R. Correia, A. Oliveira, V. Palazzi, F. Alimenti, P. Mezzanotte, L. Roselli, F. Benassi, A. Costanzo, D. Masotti, G. Paolini, A. Eid, J. Hester, M. M. Tentzeris, N. Shinohara, *IEEE J. Microw.* **2023**, *3*, 763.
[107] H. Sun, *Far-Field Wireless Power Transmission and Ambient RF Energy Harvesting: Concepts, Designs, Applications*, Scholars' Press, **2015**.
[108] T. Khan, Nasimuddin, Y. M. M. Antar, *Elements of Radio Frequency Energy Harvesting and Wireless Power Transfer Systems*, CRC Press, **2023**.
[109] H. J. Visser, R. Vullers, in *Micro Energy Harvesting*, John Wiley & Sons, Ltd, **2015**, pp. 321–346.
[110] A. S. Marincic, *IEEE Trans. Power Appar. Syst.* **1982**, *PAS-101*, 4064.
[111] N. Tesla, *Apparatus for transmitting electrical energy* **1914**.
[112] S. D. Barman, A. W. Reza, N. Kumar, M. d. E. Karim, A. B. Munir, *Renew. Sustain. Energy Rev.* **2015**, *51*, 1525.
[113] F. Xu, S. Wei, D. Yuan, J. Li, *Electronics* **2023**, *12*, 1506.
[114] E. M. Ali, M. Alibakhshikenari, B. S. Virdee, M. Soruri, E. Limiti, *Electronics* **2021**, *10*, 2779.
[115] W. L. Stutzman, G. A. Thiele, *Antenna Theory and Design*, John Wiley & Sons, Hoboken, NJ **2012**.
[116] J. Sallan, J. L. Villa, A. Llombart, J. F. Sanz, *IEEE Trans. Ind. Electron.* **2009**, *56*, 2140.
[117] C. Degen, *EURASIP J. Wirel. Commun. Netw.* **2021**, 121.
[118] M. Fareq, M. Fitra, M. Irwanto, S. Hasan, M. Arinal, *J. Phys. Conf. Ser.* **2014**, *495*, 012019.
[119] A. Kurs, A. Karalis, R. Moffatt, J. D. Joannopoulos, P. Fisher, M. Soljačić´, *Science* **2007**, *317*, 83.
[120] S. L. Ho, J. Wang, W. N. Fu, M. Sun, *IEEE Trans. Magn.* **2011**, *47*, 1522.
[121] J. Zhang, C. Cheng, in *Proceedings of 2014 3rd Asia-Pacific Conference on Antennas and Propagation* **2014**, pp. 720–723, https://doi.org/10.1109/APCAP.2014.6992598.
[122] Z. N. Low, R. A. Chinga, R. Tseng, J. Lin, *IEEE Trans. Ind. Electron.* **2009**, *56*, 1801.
[123] S. Cecil, G. Schmid, K. Lamedschwandner, A. Oberleitner, M. Bammer, J. Morak, *2010 Second International Workshop on Near Field Communication* **2010**, pp. 65–70, https://doi.org/10.1109/NFC.2010.14.
[124] A. Christ, T. Samaras, A. Klingenböck, N. Kuster, *Phys. Med. Biol.* **2006**, *51*, 4951.
[125] J. Kim, A. Banks, H. Cheng, Z. Xie, S. Xu, K.-I. Jang, J. W. Lee, Z. Liu, P. Gutruf, X. Huang, P. Wei, F. Liu, K. Li, M. Dalal, R. Ghaffari, X. Feng, Y. Huang, S. Gupta, U. Paik, J. A. Rogers, *Small* **2015**, *11*, 906.
[126] H. U. Chung, B. H. Kim, J. Y. Lee, J. Lee, Z. Xie, E. M. Ibler, K. Lee, A. Banks, J. Y. Jeong, J. Kim, C. Ogle, D. Grande, Y. Yu, H. Jang, P. Assem, D. Ryu, J. W. Kwak, M. Namkoong, J. B. Park, Y. Lee, D. H. Kim, A. Ryu, J. Jeong, K. You, B. Ji, Z. Liu, Q. Huo, X. Feng, Y. Deng, Y. Xu, et al., *Science* **2019**, *363*, eaau0780.
[127] J. Kim, A. Banks, Z. Xie, S. Y. Heo, P. Gutruf, J. W. Lee, S. Xu, K.-I. Jang, F. Liu, G. Brown, J. Choi, J. H. Kim, X. Feng, Y. Huang, U. Paik, J. A. Rogers, *Adv. Funct. Mater.* **2015**, *25*, 4761.
[128] T. R. Ray, J. Choi, A. J. Bandodkar, S. Krishnan, P. Gutruf, L. Tian, R. Ghaffari, J. A. Rogers, *Chem. Rev.* **2019**, *119*, 5461.
[129] A. Lazaro, R. Villarino, D. A. S. Girbau, *Sensors* **2018**, *18*, 3746.
[130] S. Y. R. Hui, W. Zhong, C. K. Lee, *IEEE Trans. Power Electron.* **2014**, *29*, 4500.
[131] C. Rong, C. Lu, Y. Zeng, X. Tao, X. Liu, R. Liu, X. He, M. Liu, *IET Power Electron* **2021**, *14*, 1541.
[132] A. S. Y. Poon, S. O'Driscoll, T. H. Meng, *IEEE Trans. Antennas Propag.* **2010**, *58*, 1739.
[133] A. M. Jawad, R. Nordin, S. K. Gharghan, H. M. Jawad, M. Ismail, *Energies* **2017**, *10*, 1022.
[134] S.-K. Kang, R. K. J. Murphy, S.-W. Hwang, S. M. Lee, D. V. Harburg, N. A. Krueger, J. Shin, P. Gamble, H. Cheng, S. Yu, Z. Liu, J. G. McCall, M. Stephen, H. Ying, J. Kim, G. Park, R. C. Webb, C. H. Lee, S. Chung, D. S. Wie, A. D. Gujar, B. Vemulapalli, A. H. Kim, K.-M. Lee, J. Cheng, Y. Huang, S. H. Lee, P. V. Braun, W. Z. Ray, J. A. Rogers, *Nature* **2016**, *530*, 71.
[135] Y. Leng, D. Luo, Z. Li, F. Yu, *Heliyon* **2023**, *9*, e21121.
[136] V. Tyurnev, *J. Commun. Technol. Electron.* **2002**, *47*, 848.
[137] K. Schuylenbergh, R. Puers, *Inductive Powering: Basic Theory and Application to Biomedical Systems*, Springer, Dordrecht **2009**.
[138] A. Denisov, E. Yeatman, in *2010 International Conference on Body Sensor Networks* **2010**, pp. 84–89, https://doi.org/10.1109/BSN.2010.27.
[139] Q. Hua, L. A. Rytoft, B. K. Kroyer, O. Rahbek, S. V. Kold, M. Shen, in *2022 IEEE Nordic Circuits and Systems Conference (NorCAS)* **2022**, pp. 1–6, https://doi.org/10.1109/NorCAS57515.2022.9934626.
[140] J. Wang, M. P. Leach, E. G. Lim, Z. Wang, Z. Jiang, R. Pei, Y. Huang, *A Conformal Split-Ring Loop as a Self-Resonator for Wireless Power Transfer*, Vol. *8*, IEEE Access, **2020**, pp. 911–919.
[141] B. John, C. Spink, M. Braunschweig, R. Ranjan, D. Schroeder, A. Koops, G. Woldt, G. Adam, W. H. Krautschneider, *Electron. Lett.* **2018**, *54*, 1315.
[142] M. Alghrairi, N. Sulaiman, W. Z. W. Hasan, H. Jaafar, S. Mutashar, *Indones. J. Electr. Eng. Comput. Sci.* **2022**, *25*, 771.
[143] H. Bhamra, J.-W. Tsai, Y.-W. Huang, Q. Yuan, J. V. Shah, P. Irazoqui, *IEEE Trans. Biomed. Circuits Syst.* **2017**, *11*, 1204.
[144] J. Bao, S. S. Hu, Z. M. Xie, *Int. J. Antennas Propag.* **2022**, *2022*, e8619514.
[145] A. Basir, I. A. Shah, H. Yoo, *IEEE Trans. Antennas Propag.* **2022**, *70*, 8368.
[146] L. Huang, A. Hu, *Electron. Lett.* **2015**, *51*, 1806.
[147] R. Jegadeesan, K. Agarwal, Y.-X. Guo, S.-C. Yen, N. V. Thakor, *IEEE Trans. Microw. Theory Tech.* **2017**, *65*, 280.
[148] R. Erfani, F. Marefat, A. M. Sodagar, P. Mohseni, in *2017 IEEE International Symposium on Circuits and Systems (ISCAS)* **2017**, pp. 1–4, https://doi.org/10.1109/ISCAS.2017.8050940.
[149] A. Koruprolu, S. Nag, R. Erfani, P. Mohseni, in *2018 IEEE Biomedical Circuits and Systems Conference (BioCAS)* **2018**, pp. 1–4, https://doi.org/10.1109/BIOCAS.2018.8584824.
[150] S. Nag, A. Koruprolu, S. M. Saikh, R. Erfani, P. Mohseni, *IEEE Trans. Circuits Syst. II Express Briefs* **2020**, *67*, 1804.
[151] A. I. Al-Kalbani, M. R. Yuce, J.-M. Redouté, *IEEE Antennas Wirel. Propag. Lett.* **2014**, *13*, 1168.
[152] Y. Zhaksylyk, E. Halvorsen, U. Hanke, M. Azadmehr, *Electronics* **2020**, *9*, 476.
[153] S. Miziev, W. A. Pawlak, N. Howard, *Front. Neurosci.* **2024**, *17*, 1320441.
[154] C. Lecluyse, B. Minnaert, M. Kleemann, *Energies* **2021**, *14*, 5862.
[155] M. Z. Erel, K. C. Bayindir, M. T. Aydemir, S. K. Chaudhary, J. M. Guerrero, *IEEE Access* **2022**, *10*, 3116.
[156] S. Obaid, L. Lu, *IEEE Photonics J* **2019**, *11*, 1.
[157] G. V. B. Cochran, M. W. Johnson, M. P. Kadaba, F. Vosburgh, M. W. Ferguson-Pell, V. R. Palmeiri, *J. Orthop. Res.* **1985**, *3*, 508.
[158] B. L. Turner, S. Senevirathne, K. Kilgour, D. McArt, M. Biggs, S. Menegatti, M. A. Daniele, *Adv. Healthcare Mater.* **2021**, *10*, 2100986.
[159] H. Basaeri, D. B. Christensen, S. Roundy, *Smart Mater. Struct.* **2016**, *25*, 123001.
[160] R. Krimholtz, D. A. Leedom, G. L. Matthaei, *Electron. Lett.* **1970**, *6*, 398.
[161] M. Mariello, in *Handbook of Energy Materials*, (Ed: R. Gupta), Springer Nature, Singapore **2022**, pp. 1–41.
[162] M. Mariello, *Nanoenergy Adv* **2022**, *2*, 64.

© 2024 The Author(s). Advanced Materials Technologies published by Wiley-VCH GmbH

2365709x, 0, Downloaded from https://onlinelibrary.wiley.com/doi/10.1002/admt.202400797 by University Of Oxford, Wiley Online Library on [19/11/2024]. See the Terms and Conditions (https://onlinelibrary.wiley.com/terms-and-conditions) on Wiley Online Library for rules of use; OA articles are governed by the applicable Creative Commons License

[163] H. Wei, H. Wang, Y. Xia, D. Cui, Y. Shi, M. Dong, C. Liu, T. Ding, J. Zhang, Y. Ma, N. Wang, Z. Wang, Y. Sun, R. Wei, Z. Guo, *J. Mater. Chem. C* **2018**, *6*, 12446.
[164] D. Damjanovic, in *Piezoelectric and Acoustic Materials for Transducer Applications* (Eds: A. Safari, E. K. Akdoğan), Springer US, Boston, MA **2008**, pp. 59–79.
[165] T. Zhang, H. Liang, Z. Wang, C. Qiu, Y. B. Peng, X. Zhu, J. Li, X. Ge, J. Xu, X. Huang, J. Tong, J. Ou-Yang, X. Yang, F. Li, B. Zhu, *Sci. Adv.* **2022**, *8*, eabk0159.
[166] S. Islam, A. Kim, in *2018 IEEE International Microwave Biomedical Conference (IMBioC)* **2018**, pp. 70–72, https://doi.org/10.1109/IMBIOC.2018.8428943.
[167] R. Hinchet, H.-J. Yoon, H. Ryu, M.-K. Kim, E.-K. Choi, D.-S. Kim, S.-W. Kim, *Science* **2019**, *365*, 491.
[168] X. Xiao, X. Meng, D. Kim, S. Jeon, B.-J. Park, D. S. Cho, D.-M. Lee, S.-W. Kim, *Small Methods* **2023**, *7*, 2201350.
[169] B. C. Johnson, K. Shen, D. Piech, M. M. Ghanbari, K. Y. Li, R. Neely, J. M. Carmena, M. M. Maharbiz, R. Muller, *2018 IEEE Custom Integrated Circuits Conference (CICC)*, **2018**, pp. 1–4, https://doi.org/10.1109/CICC.2018.8357047.
[170] D. K. Piech, B. C. Johnson, K. Shen, M. M. Ghanbari, K. Y. Li, R. M. Neely, J. E. Kay, J. M. Carmena, M. M. Maharbiz, R. Muller, *Nat. Biomed. Eng.* **2020**, *4*, 207.
[171] W. D. O'Brien, *Prog. Biophys. Mol. Biol.* **2007**, *93*, 212.
[172] D. Seo, H.-Y. Tang, J. M. Carmena, J. M. Rabaey, E. Alon, B. E. Boser, M. M. Maharbiz, *2015 37th Annual International Conference of the IEEE Engineering in Medicine and Biology Society (EMBC)*, IEEE, Milan **2015**, pp. 2673–2676, https://doi.org/10.1109/EMBC.2015.7318942.
[173] J. Wang, T. He, C. Lee, *Nano Energy* **2019**, *65*, 104039.
[174] C. Dagdeviren, F. Javid, P. Joe, T. von Erlach, T. Bensel, Z. Wei, S. Saxton, C. Cleveland, L. Booth, S. McDonnell, J. Collins, A. Hayward, R. Langer, G. Traverso, *Nat. Biomed. Eng.* **2017**, *1*, 807.
[175] M. Mariello, F. Guido, V. M. Mastronardi, M. T. Todaro, D. Desmaële, M. De Vittorio, *Nano Energy* **2019**, *57*, 141.
[176] Q. Zheng, B. Shi, Z. Li, Z. L. Wang, *Adv. Sci.* **2017**, *4*, 1700029.
[177] Y. Zi, S. Niu, J. Wang, Z. Wen, W. Tang, Z. L. Wang, *Nat. Commun.* **2015**, *6*, 8376.
[178] ITU Radio Regulations, *ITU*, https://www.itu.int:443/en/publications/ITU-R/Pages/publications.aspx.
[179] H. Yahya Alkhalaf, M. Yazed Ahmad, H. Ramiah, *Sensors* **2022**, *22*, 6371.
[180] C. A. Balanis, *Antenna Theory: Analysis and Design*, Wiley–Blackwell, Hoboken, NJ **2005**.
[181] G. S. N. Raju, *Antennas and Wave Propagation*, Pearson Education India, **2006**.
[182] Q. Awais, Y. Jin, H. T. Chattha, M. Jamil, H. Qiang, B. A. Khawaja, *IEEE Access* **2018**, *6*, 35857.
[183] A. Zurbuchen, A. Haeberlin, L. Bereuter, A. Pfenniger, S. Bosshard, M. Kernen, P. Philipp Heinisch, J. Fuhrer, R. Vogel, *IEEE Trans. Biomed. Eng.* **2018**, *65*, 424.
[184] J. Briscoe, S. Dunn, *Nano Energy* **2015**, *14*, 15.
[185] P. Li, J. Ryu, S. Hong, *Piezoelectric/Triboelectric Nanogenerators for Biomedical Applications. Nanogenerators*, IntechOpen, **2019**.
[186] H. D. Akaydin, N. Elvin, Y. Andreopoulos, *J. Intell. Mater. Syst. Struct.* **2010**, *21*, 1263.
[187] F. Dell'Anna, T. Dong, P. Li, Y. Wen, Z. Yang, M. R. Casu, M. Azadmehr, Y. Berg, *IEEE Circuits Syst. Mag.* **2018**, *18*, 27.
[188] H. Zhang, X.-S. Zhang, X. Cheng, Y. Liu, M. Han, X. Xu, S. Wang, F. Yang, A. S. Smitha, H. Zhang, *Nano Energy* **2015**, *C*, 296.
[189] Z. Xu, C. Jin, A. Cabe, D. Escobedo, A. Gruslova, S. Jenney, A. B. Closson, L. Dong, Z. Chen, M. D. Feldman, J. X. J. Zhang, *Adv. Healthcare Mater.* **2021**, *10*, 2002100.
[190] C. Fang, T. Tong, T. Bu, Y. Cao, S. Xu, Y. Qi, C. Zhang, *Adv. Intell. Syst.* **2020**, *2*, 1900129.
[191] J. Henniker, *Nature* **1962**, *196*, 474.
[192] U. Khan, S.-W. Kim, *ACS Nano* **2016**, *10*, 6429.
[193] P. Adhikary, M. A. P. Mahmud, T. Solaiman, Z. L. Wang, *Nano Today* **2022**, *45*, 101513.
[194] J. Zhang, Y. He, C. Boyer, K. Kalantar-Zadeh, S. Peng, D. Chu, C. H. Wang, *Nanoscale Adv* **2021**, *3*, 5465.
[195] T. Cheng, Q. Gao, Z. L. Wang, *Adv. Mater. Technol.* **2019**, *4*, 1800588.
[196] J. Li, L. Kang, Y. Long, H. Wei, Y. Yu, Y. Wang, C. A. Ferreira, G. Yao, Z. Zhang, C. Carlos, L. German, X. Lan, W. Cai, X. Wang, *ACS Appl. Mater. Interfaces* **2018**, *10*, 42030.
[197] A. Ben Amar, A. B. Kouki, H. Cao, *Sensors* **2015**, *15*, 28889.
[198] J. Zhu, A. Wang, H. Hu, H. Zhu, *Energies* **2017**, *10*, 2024.
[199] H. Ryu, H.-J. Yoon, S.-W. Kim, *Adv. Mater.* **2019**, *31*, 1802898.
[200] S. M. A. Z. Shawon, A. X. Sun, V. S. Vega, B. D. Chowdhury, P. Tran, Z. D. Carballo, J. A. Tolentino, J. Li, M. S. Rafaqut, S. Danti, M. J. Uddin, *Nano Energy* **2021**, *82*, 105691.
[201] T. Wu, J.-M. Redouté, M. R. Yuce, in *2018 40th Annual International Conference of the IEEE Engineering in Medicine and Biology Society (EMBC)* **2018**, pp. 4657–4660, https://doi.org/10.1109/EMBC.2018.8513146.
[202] J. Kim, J. Seo, D. Jung, T. Lee, H. Ju, J. Han, N. Kim, J. Jeong, S. Cho, J. H. Seol, J. Lee, *Proc. Natl. Acad. Sci* **2020**, *117*, 16856.
[203] E. Moon, D. Blaauw, J. D. Phillips, *IEEE Trans. Electron Devices* **2017**, *64*, 2432.
[204] A. Blakers, N. Zin, K. R. McIntosh, K. Fong, *Energy Procedia* **2013**, *33*, 1.
[205] R. R. King, D. C. Law, K. M. Edmondson, C. M. Fetzer, G. S. Kinsey, H. Yoon, R. A. Sherif, N. H. Karam, *Appl. Phys. Lett.* **2007**, *90*, 183516.
[206] S. Khatoon, S. K. Yadav, V. Chakravorty, J. Singh, R. B. Singh, M. S. Hasnain, S. M. M. Hasnain, *Mater. Sci. Energy Technol.* **2023**, *6*, 437.
[207] J. Y. Kim, J.-W. Lee, H. S. Jung, H. Shin, N.-G. Park, *Chem. Rev.* **2020**, *120*, 7867.
[208] D. H. Nguyen, *Sustainability* **2023**, *15*, 8146.
[209] M. Jakesová, T. A. Sjöström, V. Derek, D. Poxson, M. Berggren, E. D. Glowacki, D. T. Simon, *Npj Flex. Electron.* **2019**, *3*, 14.
[210] N. Jaziri, A. Boughamoura, J. Müller, B. Mezghani, F. Tounsi, M. Ismail, *Energy Rep* **2020**, *6*, 264.
[211] F. Tohidi, S. Ghazanfari Holagh, A. Chitsaz, *Appl. Therm. Eng.* **2022**, *201*, 117793.
[212] B. Safaei, S. Erdem, M. Karimzadeh Kolamroudi, S. Arman, *Mech. Adv. Mater. Struct.* **2023**, *0*, 1.
[213] Y. Yang, X.-J. Wei, J. Liu, *J. Phys. Appl. Phys.* **2007**, *40*, 5790.
[214] A. Álvarez-Carulla, A. Saiz-Vela, M. Puig-Vidal, J. López-Sánchez, J. Colomer-Farrarons, P. L.. Miribel-Català, *Sci. Rep.* **2023**, *13*, 1637.
[215] S. Yang, Y. Li, L. Deng, S. Tian, Y. Yao, F. Yang, C. Feng, J. Dai, P. Wang, M. Gao, *Microsyst. Nanoeng.* **2023**, *9*, 1.
[216] Y. Yang, S. Wang, Y. Zhang, Z. L. Wang, *Nano Lett.* **2012**, *12*, 6408.
[217] H. Xue, Q. Yang, D. Wang, W. Luo, W. Wang, M. Lin, D. Liang, Q. Luo, *Nano Energy* **2017**, *38*, 147.
[218] M. Baba, K. Nemoto, C. Onuki, T. Yamazawa, S. Wakakuwa, H. Tanaka, T. Sekino, T. Nakayama, N. Yamada, M. Takeda, *Sens. Actuators Phys.* **2023**, *352*, 114199.
[219] H. Ryu, S.-W. Kim, *Small* **2021**, *17*, 1903469.
[220] A. Thakre, A. Kumar, H.-C. Song, D.-Y. Jeong, J. Ryu, *Sensors* **2019**, *19*, 2170.
[221] C. Barton, J. Gallaway, P. Atanassov, *Chem. Rev.* **2004**, *104*, 4867.
[222] W. Gellett, M. Kesmez, J. Schumacher, N. Akers, S. D. Minteer, *Electroanalysis* **2010**, *22*, 727.
[223] S. Cosnier, A. Le Goff, M. Holzinger, *Electrochem. Commun.* **2014**, *38*, 19.
[224] M. Rasmussen, R. E. Ritzmann, I. Lee, A. J. Pollack, D. Scherson, *J. Am. Chem. Soc.* **2012**, *134*, 1458.

© 2024 The Author(s). Advanced Materials Technologies published by Wiley-VCH GmbH

2365709x, 0, Downloaded from https://onlinelibrary.wiley.com/doi/10.1002/admt.202400797 by University Of Oxford, Wiley Online Library on [19/11/2024]. See the Terms and Conditions (https://onlinelibrary.wiley.com/terms-and-conditions) on Wiley Online Library for rules of use; OA articles are governed by the applicable Creative Commons License

[225] L. Halámková, J. Halámek, V. Bocharova, A. Szczupak, L. Alfonta, E. Katz, *J. Am. Chem. Soc.* **2012**, *134*, 5040.
[226] S. El Ichi-Ribault, J.-P. Alcaraz, F. Boucher, B. Boutaud, R. Dalmolin, J. Boutonnat, P. Cinquin, A. Zebda, D. K. Martin, *Electrochim. Acta* **2018**, *269*, 360.
[227] D. Lee, S. H. Jeong, S. Yun, S. Kim, J. Sung, J. Seo, S. Son, J. T. Kim, L. Susanti, Y. Jeong, S. Park, K. Seo, S. J. Kim, T. D. Chung, *Biosens. Bioelectron.* **2021**, *171*, 112746.
[228] V. Nair, A. N. Dalrymple, Z. Yu, G. Balakrishnan, C. J. Bettinger, D. J. Weber, K. Yang, J. T. Robinson, *Science* **2023**, *382*, eabn4732.
[229] S. Vaddiraju, I. Tomazos, D. J. Burgess, F. C. Jain, F. Papadimitrakopoulos, *Biosens. Bioelectron.* **2010**, *25*, 1553.
[230] H. Jiang, I. Woodhouse, V. Selvamani, J. L. Ma, R. Tang, C. J. Goergen, T. Soleimani, R. Rahimi, *IEEE Trans. Biomed. Eng.* **2021**, *68*, 747.
[231] Z. Dong, Z. Li, F. Yang, C.-W. Qiu, J. S. Ho, *Nat. Electron.* **2019**, *2*, 335.
[232] Z. Zhao, G. D. Spyropoulos, C. Cea, J. N. Gelinas, D. Khodagholy, *Sci. Adv.* **2022**, *8*, eabm7851.
[233] X. Tian, Q. Zeng, S. A. Kurt, R. R. Li, D. T. Nguyen, Z. Xiong, Z. Li, X. Yang, X. Xiao, C. Wu, B. C. K. Tee, D. Nikolayev, C. J. Charles, J. S. Ho, *Nat. Commun.* **2023**, *14*, 4335.
[234] A. Lodh, A. Samrat, *Int. J. Eng. Res. Technol.* **2018**, *2*.
[235] *Ultra-Low-Power Short-Range Radios*, Springer, New York, NY **2015**.
[236] *IEEE J. Transl. Eng. Health Med.* **2019**, *8*, 2500107.
[237] H. Taleb, A. Nasser, G. Andrieux, N. Charara, E. Motta Cruz, *Wirel. Netw.* **2021**, *27*, 5271.
[238] A. Lazaro, M. Boada, R. Villarino, D. Girbau, *IEEE Access* **2020**, *8*, 2200.
[239] C. Gong, D. Liu, Z. Miao, W. Wang, M. Li, *Sensors* **2017**, *17*, 1358.
[240] A. Kiourti, *IEEE Antennas Propag. Mag.* **2018**, *60*, 14.
[241] Y. Zhang, C. Liu, X. Liu, K. Zhang, *Int. J. RF Microw. Comput.-Aided Eng.* **2020**, *30*, e22105.
[242] M. J. Weber, Y. Yoshihara, A. Sawaby, J. Charthad, T. C. Chang, A. Arbabian, *IEEE J. Solid-State Circuits* **2018**, *53*, 1089.
[243] C. C. Collins, *IEEE Trans. Biomed. Eng.* **1967**, *14*, 74.
[244] N. Yusof, B. Bais, J. Yunas, N. Soin, B. Y. Majlis, *Membranes* **2021**, *11*, 996.
[245] Y. Peng, B. M. F. Rahman, T. Wang, G. Wang, X. Liu, X. Wen, *J. Electron. Test.* **2014**, *30*, 665.
[246] C. Fearday, T. A. Ward, N. Soin, U. Hashim, N. M. Karim, *Microsyst. Technol.* **2017**, *23*, 1433.
[247] C.-C. Yeh, S.-H. Lo, M.-X. Xu, Y.-J. Yang, *Microelectron. Eng.* **2019**, *213*, 55.
[248] C. Zhang, L.-F. Wang, Q.-A. Huang, *J. Micromechanics Microengineering* **2014**, *24*, 125021.
[249] L. Dong, L.-F. Wang, Q.-A. Huang, *IEEE Microw. Wirel. Compon. Lett.* **2016**, *26*, 543.
[250] M.-Z. Xie, L.-F. Wang, B.-B. Zhou, Q.-A. Huang, *IEEE Sens. J.* **2020**, *20*, 13833.
[251] B. K. Chung, *Microelectron. J.* **2006**, *37*, 1419.
[252] B. Wang, Z. Cao, *Electronics* **2019**, *8*, 1022.
[253] H. Jiang, N. M. Carter, A. Zareei, S. Nejati, J. F. Waimin, S. Chittiboyina, E. E. Niedert, T. Soleimani, S. A. Lelièvre, C. J. Goergen, R. Rahimi, *ACS Appl. Bio Mater.* **2020**, *3*, 4012.
[254] E. M. Jung, J. Dinkel, N. Verloh, M. Brandenstein, C. Stroszczynski, F. Jung, J. Rennert, *Clin. Hemorheol. Microcirc. 79*, 463.
[255] F. Li, D. Li, F. Yan, *Sensors* **2018**, *18*, 4083.
[256] T. Bos, W. Dehaene, M. Verhelst, in *2019 IEEE Biomedical Circuits and Systems Conference (BioCAS)* **2019**, pp. 1–4, https://doi.org/10.1109/BIOCAS.2019.8918755.
[257] B. Jaafar, J. Luo, D. Firfilionis, A. Soltan, J. Neasham, P. Degenaar, *Sensors* **2020**, *20*, 31.
[258] T. C. Chang, M. L. Wang, J. Charthad, M. J. Weber, A. Arbabian, *2017 IEEE Int. Solid-State Circuits Conf. ISSCC* **2017**, pp. 460–461, https://doi.org/10.1109/ISSCC.2017.7870460.
[259] L. Jiang, J. Wu, *Prog. Mater. Sci.* **2023**, *136*, 101110.
[260] M. Sun, Q. Xu, T. Wang, S. Mao, G. A. Justin, W. Jia, Z-.H. Mao, in *2021 IEEE/ACM International Symposium on Low Power Electronics and Design (ISLPED)* **2021**, p. 1, https://doi.org/10.1109/ISLPED52811.2021.9502502.
[261] J. Lee, E. Mok, J. Huang, L. Cui, A-.H. Lee, V. Leung,P. Mercier, S. Shellhammer, L. Larson, P. Asbeck, R. Rao, Y-.K. Song, A. Nurmikko, F. Laiwalla, in *2019 9th International IEEE/EMBS Conference on Neural Engineering (NER)* **2019**, pp. 871–874, https://doi.org/10.1109/NER.2019.8717023.
[262] P. Feng, M. Maslik, T. G. Constandinou, in *2019 IEEE Biomedical Circuits and Systems Conference (BioCAS)* **2019**, pp. 1–4, https://doi.org/10.1109/BIOCAS.2019.8919152.
[263] T. Wang, Q. Xu, W. Jia, Z.-H. Mao, H. Tang, M. Sun, *IEEE J. Emerg. Sel. Top. Power Electron.* **2021**, *9*, 6259.
[264] S. Hosur, Z. Kashani, S. K. Karan, S. Priya, M. Kiani, *IEEE Trans. Biomed. Circuits Syst.* **2024**, *18*, 383.
[265] S. A. H. Mohsan, H. Qian, H. Amjad, *Front. Inf. Technol. Electron. Eng.* **2023**, *24*, 767.
[266] D. Chen, R. Li, J. Xu, D. Li, C. Fei, Y. Yang, *Nano Energy* **2023**, *117*, 108845.
[267] E. D. Nwalike, K. A. Ibrahim, F. Crawley, Q. Qin, P. Luk, Z. Luo, *Energies* **2023**, *16*, 5711.
[268] P. Zhang, L. Lin, D. Zang, X. Guo, M. Liu, *Small Weinh. Bergstr. Ger.* **2017**, *13*.
[269] L. Dong, C. Jin, A. B. Closson, I. Trase, H. C. Richards, Z. Chen, J. X. J. Zhang, *Nano Energy* **2020**, *76*, 105076.
[270] J. Rosenthal, M. S. Reynolds, in *2020 IEEE International Conference on RFID (RFID)* **2020**, pp. 1–6, https://doi.org/10.1109/RFID49298.2020.9244882.
[271] J. Rosenthal, M. S. Reynolds, *IEEE Trans. Microw. Theory Tech.* **2019**, *67*, 4015.
[272] S. Abdulmalek, A. Nasir, W., *Healthcare* **2022**, *10*, 1993.
[273] C. Lin, C. Han, J. Mao, S. Yu, Z. Zhang, *Annu. Int. Conf. IEEE Eng. Med. Biol. Soc. IEEE Eng. Med. Biol. Soc. Annu. Int. Conf.* **2023**, *2023*, 1.
[274] G. Kim, H. Yun, M. Ryu, Y. Shin, H. Kim, Y. Yang, *Exp. Neurobiol.* **2010**, *19*, 165.
[275] N. Baker, *Comput. Control Eng. J.* **2005**, *16*, 20.
[276] C. Miozzi, G. Saggio, E. Gruppioni, G. Marrocco, *IEEE J. Electromagn. RF Microw. Med. Biol.* **2022**, *6*, 219.
[277] H. Liu, T. Zhao, W. Jiang, R. Jia, D. Niu, G. Qiu, L. Fan, X. Li, W. Liu, B. Chen, Y. Shi, L. Yin, B. Lu, *Adv. Funct. Mater.* **2015**, *25*, 7071.
[278] J. M. Kahn, J. R. Barry, *Proc. IEEE* **1997**, *85*, 265.
[279] R. Feiner, T. Dvir, *Nat. Rev. Mater.* **2017**, *3*, 1.
[280] J. W. Salatino, K. A. Ludwig, T. D. Y. Kozai, E. K. Purcell, *Nat. Biomed. Eng.* **2017**, *1*, 862.
[281] T. D. Y. Kozai, A. S. Jaquins-Gerstl, A. L. Vazquez, A. C. Michael, X. T. Cui, *ACS Chem. Neurosci.* **2014**, *6*, 48.
[282] P. Thevenot, W. Hu, L. Tang, *Curr. Top. Med. Chem.* **2008**, *8*, 270.
[283] S. Kamath, D. Bhattacharyya, C. Padukudru, R. B. Timmons, L. Tang, *J. Biomed. Mater. Res., Part A* **2008**, *86*, 617.
[284] G. Cattaneo, C. Bräuner, G. Siekmeyer, A. Ding, S. Bauer, M. Wohlschlögel, L. Lang, T. Hierlemann, M. Akimov, C. Schlensak, A. Schüßler, H.-P. Wendel, S. Krajewski, *J. Mater. Sci. Mater. Med.* **2019**, *30*, 67.
[285] C. N. Elias, Y. Oshida, J. H. C. Lima, C. A. Muller, *J. Mech. Behav. Biomed. Mater.* **2008**, *1*, 234.
[286] A. F. bin A. Fadzil, A. Pramanik, A. K. Basak, C. Prakash, S. Shankar, *Ann. 3D Print. Med.* **2022**, *8*, 100082.

© 2024 The Author(s). Advanced Materials Technologies published by Wiley-VCH GmbH

2365709x, 0, Downloaded from https://onlinelibrary.wiley.com/doi/10.1002/admt.202400797 by University Of Oxford, Wiley Online Library on [19/11/2024]. See the Terms and Conditions (https://onlinelibrary.wiley.com/terms-and-conditions) on Wiley Online Library for rules of use; OA articles are governed by the applicable Creative Commons License

[287] A. L. Benabid, T. Costecalde, A. Eliseyev, G. Charvet, A. Verney, S. Karakas, M. Foerster, A. Lambert, B. Morinière, N. Abroug, M.-C. Schaeffer, A. Moly, F. Sauter-Starace, D. Ratel, C. Moro, N. Torres-Martinez, L. Langar, M. Oddoux, M. Polosan, S. Pezzani, V. Auboiroux, T. Aksenova, C. Mestais, S. Chabardes, *Lancet Neurol.* **2019**, *18*, 1112.
[288] B. Harland, Z. Aqrawe, M. Vomero, C. Boehler, E. Cheah, B. Raos, M. Asplund, S. J. O'Carroll, D. Svirskis, *Adv. Sci.* **2022**, *9*, 2105913.
[289] O. L. Bockeria, K. G. Potlovsky, M. A. Bazhin, D. I. Minaev, T. G. Le, V. A. Shvartz, A. S. Satyukova, *Biomed. Eng.* **2020**, *53*, 388.
[290] S. Wang, Q. Cui, P. Abiri, M. Roustaei, E. Zhu, Y.-R. Li, K. Wang, S. Duarte, L. Yang, R. Ebrahimi, M. Bersohn, J. Chen, T. K. Hsiai, *Sci. Adv.* **2023**, *9*, eadj0540.
[291] F. Fallegger, G. Schiavone, E. Pirondini, F. B. Wagner, N. Vachicouras, L. Serex, G. Zegarek, A. May, P. Constanthin, M. Palma, M. Khoshnevis, D. Van Roost, B. Yvert, G. Courtine, K. Schaller, J. Bloch, S. P. Lacour, *Adv. Sci.* **2021**, *8*, 2003761.
[292] D. K. Freeman, S. J. Byrnes, *IEEE Trans. Antennas Propag.* **2019**, *67*, 4073.
[293] S. Ma, T. Björninen, L. Sydänheimo, M. H. Voutilainen, L. Ukkonen, *IEEE Trans. Antennas Propag.* **2021**, *69*, 760.
[294] S. S. Mosavinejad, P. Rezaei, A. A. Khazaei, *AEU – Int. J. Electron. Commun.* **2022**, *154*, 154303.
[295] G. Singh, J. Kaur, *Iran. J. Sci. Technol. Trans. Electr. Eng.* **2023**, 1.
[296] M. Gao, J. D. Rosenthal, K. Wu, G. A. Ramírez, Z. Sipus, S. P. Lacour, A. K. Skrivervik, *IEEE Trans. Biomed. Circuits Syst.* **2024**, *18*, 27.
[297] M. Gao, Z. Sipus, A. K. Skrivervik, *IEEE Open J. Antennas Propag.* **2023**, *4*, 537.
[298] A. Skrivervik, M. Bosiljevac, Z. Sipus, *IEEE Trans. Antennas Propag.* **2019**, *PP*, 1.
[299] R. Chen, A. Canales, P. Anikeeva, *Nat. Rev. Mater.* **2017**, *2*, 1.
[300] S. Xu, Y. Zhang, L. Jia, K. E. Mathewson, K.-I. Jang, J. Kim, H. Fu, X. Huang, P. Chava, R. Wang, S. Bhole, L. Wang, Y. J. Na, Y. Guan, M. Flavin, Z. Han, Y. Huang, J. A. Rogers, *Science* **2014**, *344*, 70.
[301] D.-H. Kim, N. Lu, R. Ma, Y.-S. Kim, R.-H. Kim, S. Wang, J. Wu, S. M. Won, H. Tao, A. Islam, K. J. Yu, T. Kim, R. Chowdhury, M. Ying, L. Xu, M. Li, H.-J. Chung, H. Keum, M. McCormick, P. Liu, Y.-W. Zhang, F. G. Omenetto, Y. Huang, T. Coleman, J. A. RoRogers, *Science* **2011**, *333*, 838.
[302] O. Veiseh, J. C. Doloff, M. Ma, A. J. Vegas, H. H. Tam, A. R. Bader, J. Li, E. Langan, J. Wyckoff, W. S. Loo, S. Jhunjhunwala, A. Chiu, S. Siebert, K. Tang, J. Hollister-Lock, S. Aresta-Dasilva, M. Bochenek, J. Mendoza-Elias, Y. Wang, M. Qi, D. M. Lavin, M. Chen, N. Dholakia, R. Thakrar, I. Lacík, G. C. Weir, J. Oberholzer, D. L. Greiner, R. Langer, D. G. Anderson, *Nat. Mater.* **2015**, *14*, 643.
[303] J. A. Rogers, T. Someya, Y. Huang, *Science* **2010**, *327*, 1603.
[304] F. Vitale, D. G. Vercosa, A. V. Rodriguez, S. S. Pamulapati, F. Seibt, E. Lewis, J. S. Yan, K. Badhiwala, M. Adnan, G. Royer-Carfagni, M. Beierlein, C. Kemere, M. Pasquali, J. T. Robinson, *Nano Lett.* **2018**, *18*, 326.
[305] G. Schiavone, S. P. Lacour, *Sci. Transl. Med.* **2019**, *11*, eaaw5858.
[306] J.-W. Jeong, G. Shin, S. I. Park, K. J. Yu, L. Xu, J. A. Rogers, *Neuron* **2015**, *86*, 175.
[307] Z. J. Du, C. L. Kolarcik, T. D. Y. Kozai, S. D. Luebben, S. A. Sapp, X. S. Zheng, J. A. Nabity, X. T. Cui, *Acta Biomater.* **2017**, *53*, 46.
[308] L. Luan, X. Wei, Z. Zhao, J. J. Siegel, O. Potnis, C. A. Tuppen, S. Lin, S. Kazmi, R. A. Fowler, S. Holloway, A. K. Dunn, R. A. Chitwood, C. Xie, *Sci. Adv.* **2017**, *3*, e1601966.
[309] J. H. Lee, H. Kim, J. H. Kim, S.-H. Lee, *Lab Chip* **2016**, *16*, 959.
[310] T. Sekitani, T. S. Someya, *Adv. Mater.* **2010**, *22*, 2228.
[311] D.-H. Kim, J. Xiao, J. Song, Y. Huang, J. A. S. Rogers, *Adv. Mater.* **2010**, *22*, 2108.
[312] S. Wang, J. Xu, W. Wang, G.-J. N. Wang, R. Rastak, F. Molina-Lopez, J. W. Chung, S. Niu, V. R. Feig, J. Lopez, T. Lei, S.-K. Kwon, Y. Kim, A. M. Foudeh, A. Ehrlich, A. Gasperini, Y. Yun, B. Murmann, J. B.-H. Tok, Z. Bao, *Nature* **2018**, *555*, 83.
[313] T.-H. Han, H. Kim, S.-J. Kwon, T.-W. Lee, *Mater. Sci. Eng. R Rep.* **2017**, *118*, 1.
[314] H. Jang, Y. J. Park, X. Chen, T. Das, M.-S. Kim, J.-H. Ahn, *Adv. Mater.* **2016**, *28*, 4184.
[315] Y. Sun, W. M. Choi, H. Jiang, Y. Y. Huang, J. A. Rogers, *Nat. Nanotechnol.* **2006**, *1*, 201.
[316] X. Feng, B. D. Yang, Y. Liu, Y. Wang, C. Dagdeviren, Z. Liu, A. Carlson, J. Li, Y. Huang, J. A. Rogers, *ACS Nano* **2011**, *5*, 3326.
[317] J. Y. Oh, S. Rondeau-Gagné, Y.-C. Chiu, A. Chortos, F. Lissel, G.-J. N. Wang, B. C. Schroeder, T. Kurosawa, J. Lopez, T. Katsumata, J. Xu, C. Zhu, X. Gu, W.-G. Bae, Y. Kim, L. Jin, J. W. Chung, J. B.-H. Tok, Z. Bao, *Nature* **2016**, *539*, 411.
[318] M. Kaltenbrunner, T. Sekitani, J. Reeder, T. Yokota, K. Kuribara, T. Tokuhara, M. Drack, R. Schwödiauer, I. Graz, S. Bauer-Gogonea, S. Bauer, T. Someya, *Nature* **2013**, *499*, 458.
[319] H. Lu, X. Li, Q. Lei, *Front. Chem.* **2021**, *9*,.
[320] S. Gong, W. Cheng, *Adv. Energy Mater.* **2017**, *7*, 1700648.
[321] S. Xu, Y. Zhang, J. Cho, J. Lee, X. Huang, L. Jia, J. A. Fan, Y. Su, J. Su, H. Zhang, H. Cheng, B. Lu, C. Yu, C. Chuang, T.-I. Kim, T. Song, K. Shigeta, S. Kang, C. Dagdeviren, I. Petrov, P. V. Braun, Y. Huang, U. Paik, J. A. Rogers, *Nat. Commun.* **2013**, *4*, 1543.
[322] J. Duan, X. Liang, J. Guo, K. Zhu, L. Zhang, *Adv. Mater.* **2016**, *28*, 8037.
[323] Z. Wang, L. Chen, Y. Chen, P. L., *Research* **2020**, *2020*.
[324] K. Scholten, E. Meng, *Lab Chip* **2015**, *15*, 4256.
[325] H.-J. Kim, Z. Dong, J. S. Ho, in *Handbook of Neuroengineering* (Ed: N. V. Thakor), Springer Nature, Singapore **2023** pp. 851–876.
[326] J. Baker-Jarvis, S. Kim, *J. Res. Natl. Inst. Stand. Technol.* **2012**, *117*, 1.
[327] E. V. Sacher, D. Parylene, *J. Appl. Polym. Sci.* **1983**, *28*, 1535.
[328] B. Rubehn, T. Stieglitz, *Biomaterials* **2010**, *31*, 3449.
[329] A. Souza, J. Ribeiro, F. Araújo, *J. Mech. Eng. Biomech.* **2019**, *4*, 1.
[330] E. Langereis, M. Creatore, S. B. S. Heil, M. C. M. van de Sanden, W. M. M. Kessels, *Appl. Phys. Lett.* **2006**, *89*, 081915.
[331] A. Bulusu, A. Singh, C. Y. Wang, A. Dindar, C. Fuentes-Hernandez, H. Kim, D. Cullen, B. Kippelen, S. Graham, *J. Appl. Phys.* **2015**, *118*, 085501.
[332] Z. Hu, J. Zhao, H. Guo, R. Li, M. Wu, J. Shen, Y. Wang, Z. Qiao, Y. Xu, G. Haugstad, D. An, Z. Xie, I. Kandela, K. R. Nandoliya, Y. Chen, Y. Yu, Q. Yuan, J. Hou, Y. Deng, A. H. AlDubayan, Q. Yang, L. Zeng, D. Lu, J. Koo, W. Bai, E. Song, S. Yao, C. Wolverton, Y. Huang, J. A. Rogers, *Adv. Mater.*, *n/a*, 2307782.
[333] J. Park, H. R. Yoon, M. A. Khan, S. Cho, M. M. Sung, *ACS Appl. Mater. Interfaces* **2020**, *12*, 8817.
[334] S. Majee, M. F. Cerqueira, D. Tondelier, B. Geffroy, Y. Bonnassieux, P. Alpuim, J. E. Bourée, *Prog. Org. Coat.* **2015**, *80*, 27.
[335] K. Kim, M. V. Gompel, K. Wu, G. Schiavone, J. Carron, F. Bourgeois, S. P. Lacour, Y. Leterrier, *Small n/a*, 2103039.
[336] K. Nanbakhsh, R. Ritasalo, W. A. Serdijn, V. Giagka, in *2020 IEEE 70th Electronic Components and Technology Conference (ECTC)*, **2020**, pp. 467–472, https://doi.org/10.1109/ECTC32862.2020.00081.
[337] Y. Huang, H. Li, T. Hu, J. Li, C. K. Yiu, J. Zhou, J. Li, X. Huang, K. Yao, X. Qiu, Y. Zhou, D. Li, B. Zhang, R. Shi, Y. Liu, T. H. Wong, M. Wu, H. Jia, Z. Gao, Z. Zhang, J. He, M. Zheng, E. Song, L. Wang, C. Xu, X. Yu, *Nano Lett.* **2022**, *22*, 5944.
[338] J. Koo, S. B. Kim, Y. S. Choi, Z. Xie, A. J. Bandodkar, J. Khalifeh, Y. Yan, H. Kim, M. K. Pezhouh, K. Doty, G. Lee, Y.-Y. Chen, S. M. Lee, D. D'Andrea, K. Jung, K. Lee, K. Li, S. Jo, H. Wang, J.-H. Kim, J. Kim, S.-G. Choi, W. J. Jang, Y. S. Oh, I. Park, S. S. Kwak, J.-H. Park, D. Hong, X. Feng, C.-H. Lee, et al., *Sci. Adv.* **2020**, *6*, eabb1093.

© 2024 The Author(s). Advanced Materials Technologies published by Wiley-VCH GmbH

2365709x, 0, Downloaded from https://onlinelibrary.wiley.com/doi/10.1002/admt.202400797 by University Of Oxford, Wiley Online Library on [19/11/2024]. See the Terms and Conditions (https://onlinelibrary.wiley.com/terms-and-conditions) on Wiley Online Library for rules of use; OA articles are governed by the applicable Creative Commons License

[339] D. Lim, I. Hong, S. U. Park, J. W. Chae, S. Lee, H. W. Baac, C. Shin, J. Lee, Y. Roh, C. Im, Y. Park, G. Lee, U. Kim, J.-S. Koh, D. Kang, S. Han, S. M. Won, *Adv. Funct. Mater.* **2022**, *32*, 2201854.
[340] M. Sang, K. Kim, J. Shin, K. J. Yu, *Adv. Sci.* **2022**, *9*, 2202980.
[341] S.-H. Ahn, J. Jeong, S. J. Kim, *Micromachines* **2019**, *10*, 508.
[342] J. Jiang, R. M. Nambisan, S. R. Green, Y. B. Gianchandani, *IEEE Trans. Biomed. Eng* **2018**, *66*, 2044.
[343] A. Sharma, L. Rieth, P. Tathireddy, R. Harrison, H. Oppermann, M. Klein, M. Töpper, E. Jung, R. Normann, G. Clark, F. Solzbacher, *Sens. Actuators Phys.* **2012**, *188*, 167.
[344] M. Mariello, K. Kim, K. Wu, S. P. Lacour, Y. Leterrier, *Adv. Mater.* **2022**, *1n/a*, 2201129.
[345] K. Wu, M. Mariello, Y. Leterrier, S. P. Lacour, *Adv. Mater.* **2024**, *n/a*, 2310201.
[346] E. Song, J. Li, J. A. Rogers, *APL Mater.* **2019**, *7*, 050902.
[347] S. Hu, H. Chen, S. Jia, X. Xiao, Y. Cao, W. Wang, *Microsyst. Technol.* **2021**, *27*, 2595.
[348] S. R. A. Ruth, M-.G. Kim, H. Oda, Z. Wang, Y. Khan, J. Chang, P. M. Fox, Z. Bao, *iScience* **2021**, *24*, 103079.
[349] R. Herbert, H.-R. Lim, B. Rigo, W.-H. Yeo, *Sci. Adv. 8*, eabm1175.
[350] S. Islam, X. Song, E. T. Choi, J. Kim, H. Liu, A. Kim, *IEEE Access* **2020**, *8*, 96340.
[351] P. Westerhoff, F. Graichen, A. Bender, A. Rohlmann, G. Bergmann, *Med. Eng. Phys.* **2009**, *31*, 207.
[352] J. Lee, S. J. Ihle, G. S. Pellegrino, H. Kim, J. Yea, C.-Y. Jeon, H.-C. Son, C. Jin, D. Eberli, F. Schmid, B. L. Zambrano, A. F. Renz, C. Forró, H. Choi, K.-I. Jang, R. Küng, J. Vörös, *Nat. Electron.* **2021**, *4*, 291.
[353] X. Ma, S. Ahadian, S. Liu, J. Zhang, S. Liu, T. Cao, W. Lin, D. Wu, N. R. de Barros, M. R. Zare, S. E. Diltemiz, V. Jucaud, Y. Zhu, S. Zhang, E. Banton, Y. Gu, K. Nan, S. Xu, M. R. Dokmeci, A. Khademhosseini, *Adv. Intell. Syst.* **2021**, *3*, 2000263.
[354] C. Yang, Q. Wu, J. Liu, J. Mo, X. Li, C. Yang, Z. Liu, J. Yang, L. Jiang, W. Chen, H.-J. Chen, J. Wang, X. Xie, *Nat. Commun.* **2022**, *13*, 2556.
[355] M. Abdul-Al, A. S. I. Amar, I. Elfergani, R. Littlehales, N. O. Parchin, Y.-A. Yasir, C. H. See, D. Zhou, Z. Z. Abidin, M. Alibakhshikenari, C. Zebiri, F. Elmegri, M. Abusitta, A. Ullah, F. M. A. Abdussalam, J. Rodriguez, N. J. McEwan, J. N. Noras, R. Hodgetts, R. A. Abd-Alhameed, *Electronics* **2022**, *11*, 511.
[356] T. S. Rappaport, *Wireless Communications: Principles and Practice*, Cambridge University Press, **2024**.
[357] R. Lemdiasov, A. Venkatasubramanian, R. Jegadeesan, in *Brain and Human Body Modeling 2020: Computational Human Models Presented at EMBC 2019 and the BRAIN Initiative® 2019 Meeting* (Eds: S. N. Makarov, G. M. Noetscher, A. Nummenmaa), Springer, Cham (CH) **2021**.
[358] X. Liu, H.-J. Chen, Y. Alfadhl, X. Chen, C. Parini, D. Wen, *J. Appl. Phys.* **2013**, *113*, 074902.
[359] K. R. Foster, R. Glaser, *Health Phys.* **2007**, *92*, 609.
[360] C. K. Chou, H. Bassen, J. Osepchuk, Q. Balzano, R. Petersen, M. Meltz, R. Cleveland, J. C. Lin, L. Heynick, *Bioelectromagnetics* **1996**, *17*, 195.
[361] C. M. Collins, Z. Wang, *Magn. Reson. Med.* **2011**, *65*, 1470.
[362] S. Pei, Z. Wanrong, H. Lu, J. Dongyue, X. Hongyun, *J. Semicond.* **2011**, *32*, 064011.
[363] J. Everard, *Fundamentals of RF Circuit Design with Low Noise Oscillators*, Wiley, Chichester, New York **2000**.
[364] J. Van Mulders, D. Delabie, C. Lecluyse, C. Buyle, G. Callebaut, L. Van der Perre, L. De Strycker, *Sensors* **2022**, *22*, 5573.
[365] Y. Özüpak, *Heliyon* **2024**, *10*, e27420.
[366] P. Jayathurathnage, A. Alphones, D. Vilathgamuwa, *IEEE Trans. Power Electron.* **2016**, *32*, 1.
[367] A. L. F. Stein, P. A. Kyaw, C. R. Sullivan, in *2017 IEEE 18th Workshop on Control and Modeling for Power Electronics (COMPEL)* **2017**, pp. 1–7, https://doi.org/10.1109/COMPEL.2017.8013323.
[368] Y. L. Wong, S. Shibui, M. Koga, S. Hayashi, S. Uchida, *Energies* **2022**, *15*, 3690.
[369] C. Algora, I. García, M. Delgado, R. Peña, C. Vázquez, M. Hinojosa, I. Rey-Stolle, *Joule* **2022**, *6*, 340.
[370] M. Zhao, T. Miyamoto, *Photonics* **2023**, *10*, 824.
[371] Z. Rong, M. Zhang, Y. Ning, W. Pang, *Sci. Rep.* **2022**, *12*, 1.
[372] A. Proto, L. Rufer, S. Basrour, M. Penhaker, *Micromachines* **2022**, *13*, 2127.
[373] B. Kar, U. Wallrabe, *Micromachines* **2020**, *11*, 355.
[374] H.-C. Song, S.-W. Kim, H. S. Kim, D.-G. Lee, C.-Y. Kang, S. Nahm, *Adv. Mater.* **2020**, *32*, 2002208.
[375] R. Xu, S. G. Kim, in *Proceedings of the PowerMEMS*, Atlanta, GA, USA **2012**.
[376] J. I. Roscow, H. Pearce, H. Khanbareh, S. Kar-Narayan, C. R. Bowen, *Eur. Phys. J. Spec. Top.* **2019**, *228*, 1537.
[377] D. B. Deutz, J.-A. Pascoe, B. Schelen, S. van der Zwaag, D. M. de Leeuw, P. Groen, *Mater. Horiz.* **2018**, *5*, 444.
[378] J. Peng, S. D. Kang, G. J. Snyder, *Sci. Adv.* **2017**, *3*, eaap8576.
[379] J. Shao, T. Jiang, W. Tang, X. Chen, L. Xu, Z. L. Wang, *Nano Energy* **2018**, *51*, 688.
[380] N. Hu, H. Cai, X. Dai, G. Chen, Y. Wang, D. Zhang, *Sol. Energy Mater. Sol. Cells* **2017**, *161*, 382.
[381] T. Kirchartz, P. Kaienburg, D. Baran, *J. Phys. Chem. C* **2018**, *122*, 5829.
[382] H. S. Kim, W. Liu, G. Chen, C.-W. Chu, Z. Ren, *Proc. Natl. Acad. Sci. USA* **2015**, *112*, 8205.
[383] G. J. Snyder, A. H. Snyder, *Energy Environ. Sci.* **2017**, *10*, 2280.
[384] K. Zhang, Y. Wang, Z. L. Wang, Y. Yang, *Nano Energy* **2019**, *55*, 534.
[385] H. Li, Y. Wang, K. Zhu, Z. Han, X. Wu, S. Wang, W. Zhang, W. Liu, *Adv. Sci.* **2023**, *10*, 2303695.
[386] H. M. Choe, J. H. Judy, A. V. D. Ziel, *Ferroelectrics* **1977**, 181.
[387] S. Patel, *J. Mater. Sci. Mater. Electron.* **2020**, *31*, 16708.
[388] A. N. M. Shahriyar Hossain, P. Mohseni, H. M. Lavasani, in *2022 IEEE Biomedical Circuits and Systems Conference (BioCAS)* **2022**, pp. 292–296, https://doi.org/10.1109/BioCAS54905.2022.9948595.
[389] M. Z. Asghar, S. A. Memon, J. Hämäläinen, *Sustainability* **2022**, *14*, 6356.
[390] B. Chatterjee, P. Mohseni, S. Sen, *Annu. Rev. Biomed. Eng.* **2023**, *25*, 101.
[391] A. K. RamRakhyani, G. Lazzi, in *Handbook of Biochips: Integrated Circuits and Systems for Biology and Medicine* (Ed: M. Sawan), Springer, New York, NY **2022** pp. 967–984.
[392] E. L. Gruenberg, *Handbook of Telemetry and Remote Control*, McGraw-Hill Inc, US **1967**.
[393] R. Krishan, M. Kaur, S. Mehta, *Innovative Smart Materials Used in Wireless Communication Technology*, IGI Global **2023**, https://services.igi-global.com/resolvedoi/resolve.aspx?
[394] M. R. Kattiakara Muni Samy, A. Gudipalli, *Meas. Sens.* **2023**, *28*, 100849.
[395] B. Kanaujia, S. K. Gupta, J. Kishor, D. Gangwar, *Printed Antennas: Theory and Design*, CRC Press, **2022**.
[396] B. Almohammed, A. Ismail, A. Sali, *Text. Res. J.* **2021**, *91*, 646.
[397] T. Whittaker, S. Zhang, A. Powell, C. J. Stevens, J. Y. C. Vardaxoglou, W. Whittow, *IEEE Antennas Propag. Mag.* **2023**, *65*, 10.
[398] D. F. Williams, *Biomaterials* **2008**, *29*, 2941.
[399] K. Bazaka, M. V. Jacob, *Electronics* **2013**, *2*, 1.
[400] Y. Chen, Y.-S. Kim, B. W. Tillman, W.-H. Yeo, Y. Chun, *Mater. Basel Switz.* **2018**, *11*, 522.
[401] C. J. Cyron, J. D. Humphrey, *Meccanica* **2017**, *52*, 645.
[402] A. Johnston, A. Callanan, *Biomimetics* **2023**, *8*, 205.
[403] D. Ambrosi, M. Ben Amar, C. J. Cyron, A. DeSimone, A. Goriely, J. D. Humphrey, E. Kuhl, *J. R. Soc. Interface* **2019**, *16*, 20190233.
[404] S. Bauer, P. Schmuki, K. von der Mark, J. Park, *Prog. Mater. Sci.* **2013**, *58*, 261.

© 2024 The Author(s). Advanced Materials Technologies published by Wiley-VCH GmbH

2365709x, 0, Downloaded from https://onlinelibrary.wiley.com/doi/10.1002/admt.202400797 by University Of Oxford, Wiley Online Library on [19/11/2024]. See the Terms and Conditions (https://onlinelibrary.wiley.com/terms-and-conditions) on Wiley Online Library for rules of use; OA articles are governed by the applicable Creative Commons License

[405] S. Choi, H. Lee, R. Ghaffari, T. Hyeon, D.-H. Kim, *Adv. Mater.* **2016**, *28*, 4203.
[406] J. Liu, H. Zheng, P. S. P. Poh, H.-G. Machens, A. F. Schilling, *Int. J. Mol. Sci.* **2015**, *16*, 15997.
[407] K. Sagdic, E. Fernández-Lavado, M. Mariello, O. Akouissi, S. P. Lacour, *MRS Bull.* **2023**, 495.
[408] M. C. Salvadori, A. R. Vaz, L. L. Melo, M. Cattani, *Surf. Rev. Lett.* **2003**, *10*, 571.
[409] M. A. Hopcroft, W. D. Nix, T. W. Kenny, *J. Microelectromechanical Syst.* **2010**, *19*, 229.
[410] W. Yang, Y. Gong, W. A. R. Li, *Front. Bioeng. Biotechnol.* **2021**, *8*.
[411] S. P. Lacour, S. Wagner, Z. Suo, *MRS Online Proc. Libr. OPL* **2003**, *795*, U6.9.
[412] N. Vachicouras, C. M. Tringides, P. B. Campiche, S. P. Lacour, *Extreme Mech. Lett.* **2017**, *15*, 63.
[413] Z. Jiang, N. Chen, Z. Yi, J. Zhong, F. Zhang, S. Ji, R. Liao, Y. Wang, H. Li, Z. Liu, Y. Wang, T. Yokota, X. Liu, K. Fukuda, X. Chen, T. Someya, *Nat. Electron.* **2022**, *5*, 784.
[414] S. Huang, Y. Liu, C. F. Guo, Z. Ren, *Adv. Electron. Mater.* **2017**, *3*, 1600534.
[415] S. Jeong, S. Heo, M. Kang, H.-J. Kim, *Mater. Des.* **2020**, *196*, 109178.
[416] Y. Ling, Q. Lyu, Q. Zhai, B. Zhu, S. Gong, T. Zhang, J. Dyson, W. Cheng, *ACS Sens.* **2020**, *5*, 3165.
[417] S. E. Shirzaei, C. Xu, C. Wang, Y. Song, J. Min, J. Tu, S. A. Solomon, J. Li, J. L. Banks, D. G. Armstrong, W. Gao, *Sci. Adv.* **2023**, *9*, eadf7388.
[418] J. Schulte, D. Ashouri, T. Stieglitz, *Adv. Funct. Mater.* **2024**, *34*, 2310130.
[419] M. Mueller, F. Köhler, J. S. Ordonez, T. Stieglitz, M. Schuettler, in *2014 IEEE 19th International Functional Electrical Stimulation Society Annual Conference (IFESS)* **2014**, pp. 1–4, https://doi.org/10.1109/IFESS.2014.7036753.
[420] S. Cohen, Surface electrode for electrical stimulation of tissue, *US20040162602A1* **2004**.
[421] C. Wang, C. Wang, Z. Huang, S. Xu, *Adv. Mater.* **2018**, *30*, 1801368.
[422] M. Maranha, A. F. Silva, P. A. Lopes, A. T. de Almeida, M. Tavakoli, *Adv. Sens. Res.* **2023**, *2*, 2200025.
[423] K. Khoshmanesh, S.-Y. Tang, J. Y. Zhu, S. Schaefer, A. Mitchell, K. Kalantar-zadeh, M. D. Dickey, *Lab Chip* **2017**, *17*, 974.
[424] M. D. Dickey, *ACS Appl. Mater. Interfaces* **2014**, *6*, 18369.
[425] Y. Deng, F. Bu, Y. Wang, P. S. Chee, X. Liu, C. Guan, *Npj Flex. Electron.* **2024**, *8*, 1.
[426] K. Park, S. Park, Y. Jo, S. A. Kim, T. Y. Kim, S. Kim, J. Seo, *Ind. Chem. Mater.* **2024**, *2*, 361.
[427] Y.-H. Wu, R.-M. Zhen, H.-Z. Liu, S.-Q. Liu, Z.-F. Deng, P.-P. Wang, S. Chen, L. Liu, *J. Mater. Chem. C* **2017**, *5*, 12483.
[428] K. N. Paracha, A. D. Butt, A. S. Alghamdi, S. A. Babale, P. J. Soh, *Sensors* **2020**, *20*, 177.
[429] S. Dash, C. Psomas, I. Krikidis, *Sci. Rep.* **2023**, *13*, 20551.
[430] J.-H. So, J. Thelen, A. Qusba, G. J. Hayes, G. Lazzi, M. D. Dickey, *Adv. Funct. Mater.* **2009**, *19*, 3632.
[431] A. Dey, R. Guldiken, G. Mumcu, *IEEE Trans. Antennas Propag.* **2016**, *64*, 2572.
[432] A. Hirsch, H. O. Michaud, A. P. Gerratt, S. de Mulatier, S. P. Lacour, *Adv. Mater.* **2016**, *28*, 4507.
[433] A. Hirsch, L. Dejace, H. O. Michaud, S. P. Lacour, *Acc. Chem. Res.* **2019**, *52*, 534.
[434] H. Chen, I. Furfaro, E. Fernández Lavado, S. P. Lacour, *Adv. Funct. Mater. n/a*, 2308698.
[435] R. Lin, H.-J. Kim, S. Achavananthadith, Z. Xiong, J. K. W. Lee, Y. L. Kong, J. S. Ho, *Nat. Commun.* **2022**, *13*, 2190.
[436] S. Guo, P. Wang, J. Zhang, W. Luan, Z. Xia, L. Cao, Z. He, *Front. Energy* **2019**, *13*, 474.
[437] K. Yamagishi, I. Kirino, I. Takahashi, H. Amano, S. Takeoka, Y. Morimoto, T. Fujie, *Nat. Biomed. Eng.* **2019**, *3*, 27.
[438] A. Romo-Gutiérrez, *MRS Bull.* **2023**, *48*, 704.
[439] J.-H. Fu, J.-Y. Gao, S. Chen, P. Qin, J.-T. Shi, J. Liu, *RSC Adv.* *9*, 35102.
[440] Q. Shen, M. Jiang, R. Wang, K. Song, M. H. Vong, W. Jung, F. Krisnadi, R. Kan, F. Zheng, B. Fu, P. Tao, C. Song, G. Weng, B. Peng, J. Wang, W. Shang, M. D. Dickey, T. Deng, *Science* **2023**, *379*, 488.
[441] A. Bianco, K. Kostarelos, M. Prato, *Chem. Commun.* **2011**, *47*, 10182.
[442] S. K. Smart, A. I. Cassady, G. Q. Lu, D. J. Martin, *Carbon* **2006**, *44*, 1034.
[443] V. Biju, *Chem. Soc. Rev.* **2014**, *43*, 744.
[444] S. Zhang, J. Pang, Y. Li, F. Yang, T. Gemming, K. Wang, X. Wang, S. Peng, X. Liu, B. Chang, H. Liu, W. Zhou, G. Cuniberti, M. H. Rümmeli, *Nano Res.* **2022**, *15*, 4613.
[445] L. Wang, S. Xie, Z. Wang, F. Liu, Y. Yang, C. Tang, X. Wu, P. Liu, Y. Li, H. Saiyin, S. Zheng, X. Sun, F. Xu, H. Yu, H. Peng, *Nat. Biomed. Eng.* **2020**, *4*, 159.
[446] H. Yang, Z. Qian, J. Wang, J. Feng, C. Tang, L. Wang, Y. Guo, Z. Liu, Y. Yang, K. Zhang, P. Chen, X. Sun, H. Peng, *Adv. Funct. Mater.* **2022**, *32*, 2204794.
[447] X. Jin, G. Li, T. Xu, L. Su, D. Yan, X. Zhang, *Biosens. Bioelectron.* **2022**, *196*, 113760.
[448] P. Gou, N. D. Kraut, I. M. Feigel, H. Bai, G. J. Morgan, Y. Chen, Y. Tang, K. Bocan, J. Stachel, L. Berger, M. Mickle, E. Sejdic, A. Star, *Sci. Rep.* **2014**, *4*, 4468.
[449] K. Okada, T. Horii, Y. Yamaguchi, K. Son, N. Hosoya, S. Maeda, T. Fujie, *ACS Appl. Mater. Interfaces* **2024**, *16*, 10427.
[450] M. Vafaiee, R. Mohammadpour, M. Vossoughi, E. Asadian, M. Janahmadi, P. Sasanpour, *Front. Bioeng. Biotechnol.* **2021**, 8.
[451] L. Lu, X. Fu, Y. Liew, Y. Zhang, S. Zhao, Z. Xu, J. Zhao, D. Li, Q. Li, G. B. Stanley, X. Duan, *Nano Lett.* **2019**, *19*, 1577.
[452] K. Wang, H. A. Fishman, H. Dai, J. S. Harris, *Nano Lett.* **2006**, *6*, 2043.
[453] E. Miyako, C. Hosokawa, M. Kojima, M. Yudasaka, R. Funahashi, I. Oishi, Y. Hagihara, M. Shichiri, M. Takashima, K. Nishio, Y. Yoshida, *Angew. Chem., Int. Ed.* **2011**, *50*, 12266.
[454] X. Li, H. Xiong, N. Rommelfanger, X. Xu, J. Youn, P. A. Slesinger, G. Hong, Z. Qin, *Matter* **2021**, *4*, 1484.
[455] E. E. Yildirim, L. A. Panes-Ruiz, P. Yemulwar, E. Cihan, B. Ibarlucea, G. Cuniberti, *MRS Bull.* **2023**, *48*, 1208.
[456] Meenakshi, S. K. Shukla, J. Narang, V. Kumar, P. Govender, A. Niv, C. M. Hussain, R. Wang, B. Mangla, R. S. Babu, *Chemosensors* **2020**, *8*, 45.
[457] R. Garg, D. S. Roman, Y. Wang, D. Cohen-Karni, T. Cohen-Karni, *Biophys. Rev.* **2021**, *2*,.
[458] Y. Xu, Q. Fei, M. Page, G. Zhao, Y. Ling, D. Chen, Z. Yan, *Nano Res.* **2021**, *14*, 3033.
[459] S. Patra, R. Choudhary, R. Madhuri, P. K. Sharma, in *Graphene Bioelectronics* (Ed: A. Tiwari), Elsevier, **2018**, pp. 307–338.
[460] Y.-T. Kwon, Y.-S. Kim, S. Kwon, M. Mahmood, H.-R. Lim, S.-W. Park, S.-O. Kang, J. J. Choi, R. Herbert, Y. C. Jang, Y.-H. Choa, W.-H. Yeo, *Nat. Commun.* **2020**, *11*, 3450.
[461] M. L. Mura, D. Cassioli, M. Shundalau, E. Cianca, P. Lamberti, *J. Phys. Conf. Ser.* **2024**, *2716*, 012045.
[462] T. Li, M. Qu, C. Carlos, L. Gu, F. Jin, T. Yuan, X. Wu, J. Xiao, T. Wang, W. Dong, X. Wang, Z.-Q. Feng, *Adv. Mater.* **2021**, *33*, 2006093.
[463] N. A. Kamel, *Biophys. Rev.* **2022**, *14*, 717.
[464] M. Ali, M. J. Bathaei, E. Istif, S. N. H. Karimi, L. Beker, *Adv. Healthcare Mater.* **2023**, *12*, 2300318.
[465] Z. L. Wang, J. Song, *Science* **2006**, *312*, 242.
[466] Z. Wang, *J. Phys. Condens. Matter* **2004**, *16*, R829.
[467] M. Acosta, N. Novak, V. Rojas, S. Patel, R. Vaish, J. Koruza, G. A. Rossetti, J. Rödel, *Appl. Phys. Rev.* **2017**, *4*, 041305.

© 2024 The Author(s). Advanced Materials Technologies published by Wiley-VCH GmbH

2365709x, 0, Downloaded from https://onlinelibrary.wiley.com/doi/10.1002/admt.202400797 by University Of Oxford, Wiley Online Library on [19/11/2024]. See the Terms and Conditions (https://onlinelibrary.wiley.com/terms-and-conditions) on Wiley Online Library for rules of use; OA articles are governed by the applicable Creative Commons License

[468] T. Gao, J. Liao, J. Wang, Y. Qiu, Q. Yang, M. Zhang, Y. Zhao, L. Qin, H. Xue, Z. Xiong, L. Chen, Q.-M. Wang, *J. Mater. Chem. A* **2015**, *3*, 9965.
[469] J. Gao, D. Xue, W. Liu, C. Zhou, X. Ren, *Actuators* **2017**, *6*, 24.
[470] M. Mariello, L. Fachechi, F. Guido, M. De Vittorio, *Nano Energy* **2021**, *83*, 105811.
[471] M. Mariello, T. W. A. Blad, V. M. Mastronardi, F. Madaro, F. Guido, U. Staufer, N. Tolou, M. De Vittorio, *Nano Energy* **2021**, *85*, 105986.
[472] M. Mariello, L. Fachechi, F. Guido, M. D. C. Vittorio, *Adv. Funct. Mater.* n/a, 2101047.
[473] A. Dangi, S. Agrawal, S.-R. Kothapalli, *Opt. Lett.* **2019**, *44*, 5326.
[474] G. Clementi, S. Margueron, M. A. Suarez, T. Baron, B. Dulmet, A. Bartasyte, *J. Phys. Conf. Ser.* **2019**, *1407*, 012039.
[475] H. Dong, W. Liu, Y. Li, X. Chen, D. Wang, *Adv. Electron. Mater.* **2023**, *9*, 2300469.
[476] A. Safari, M. Abazari, *IEEE Trans. Ultrason. Ferroelectr. Freq. Control* **2010**, *57*, 2165.
[477] P. Chakraborty, A. Karmakar, A. Saha, *Wirel. Pers. Commun.* **2024**, *134*, 1367.
[478] S. Narang, S. Bahel, *J. Ceram. Process. Res.* **2010**, *11*, 316.
[479] M. D. Hill, D. B. Cruickshank, I. A. MacFarlane, *Appl. Phys. Lett.* **2021**, *118*, 120501.
[480] M. T. Sebastian, R. Ubic, H. Jantunen, *Int. Mater. Rev.* **2015**, *60*, 392.
[481] C. Pang, C. Lee, K.-Y. Suh, *J. Appl. Polym. Sci.* **2013**, *130*, 1429.
[482] M. Tanaka, K. Sato, E. Kitakami, S. Kobayashi, T. Hoshiba, K. Fukushima, *Polym. J.* **2015**, *47*, 114.
[483] Q. Zhang, X. Liu, L. Duan, G. Gao, *J. Mater. Chem. A* **2021**, *9*, 1835.
[484] X. Zhang, N. Sheng, L. Wang, Y. Tan, C. Liu, Y. Xia, Z. Nie, K. Sui, *Mater. Horiz.* **2019**, *6*, 326.
[485] Y. Gao, S. Gu, F. Jia, G. Gao, *J. Mater. Chem. A* **2020**, *8*, 24175.
[486] Y. Gao, Y. Wang, Y. Dai, Q. Wang, P. Xiang, Y. Li, G. Gao, *Eur. Polym. J.* **2022**, *164*, 110981.
[487] Y. Zhang, S. Ye, L. Cao, Z. Lv, J. Ren, Z. Shao, Y. Yao, S. Ling, *Adv. Funct. Mater.* **2022**, *32*, 2200267.
[488] X. Fan, W. Nie, H. Tsai, N. Wang, H. Huang, Y. Cheng, R. Wen, L. Ma, F. Yan, Y. Xia, *Adv. Sci.* **2019**, *6*, 1900813.
[489] C. M. Proctor, J. Rivnay, G. G. Malliaras, *J. Polym. Sci. Part B Polym. Phys.* **2016**, *54*, 1433.
[490] M. J. Donahue, A. Sanchez-Sanchez, S. Inal, J. Qu, R. M. Owens, D. Mecerreyes, G. G. Malliaras, D. C. Martin, *Mater. Sci. Eng. R Rep.* **2020**, *140*, 100546.
[491] B. Lu, H. Yuk, S. Lin, N. Jian, K. Qu, J. Xu, X. Zhao, *Nat. Commun.* **2019**, *10*, 1043.
[492] M. Seiti, A. Giuri, C. E. Corcione, E. Ferraris, *Biomater. Adv.* **2023**, *154*, 213655.
[493] W. Zhang, Z. Su, X. Zhang, W. Wang, Z. Li, *VIEW* **2022**, *3*, 20220030.
[494] Y.-F. Wang, T. Sekine, Y. Takeda, K. Yokosawa, H. Matsui, D. Kumaki, T. Shiba, T. Nishikawa, S. Tokito, *Sci. Rep.* **2020**, *10*, 2467.
[495] M. Singh, S. S. Priyadarisini, J. R. Pradhan, S. Dasgupta, *Adv. Eng. Mater.* **2023**, *25*, 2300733.
[496] C. Liu, Y. Zhao, X. Cai, Y. Xie, T. Wang, D. Cheng, L. Li, R. Li, Y. Deng, H. Ding, G. Lv, G. Zhao, L. Liu, G. Zou, M. Feng, Q. Sun, L. Yin, X. Sheng, *Microsyst. Nanoeng.* **2020**, *6*, 64.
[497] J.-H. Bae, S.-H. Chang, *Funct. Compos. Struct.* **2019**, *1*, 012003.
[498] Y.-Y. Chiu, W.-Y. Lin, H.-Y. Wang, S.-B. Huang, M.-H. Wu, *Sens. Actuators Phys.* **2013**, *189*, 328.
[499] B. Fatma, S. Gupta, C. Chatterjee, R. Bhunia, V. Verma, A. Garg, *J. Mater. Chem. A* **2020**, *8*, 15023.
[500] K. Castkova, J. Kastyl, D. Sobola, J. Petrus, E. Stastna, D. Riha, P. Tofel, *Nanomaterials* **2020**, 10.
[501] X. Li, W. Yu, X. Gao, H. Liu, N. Han, X. Zhang, *Mater. Adv.* **2021**, *2*, 6011.
[502] Y. Tai, S. Yang, S. Yu, A. Banerjee, N. V. Myung, J. Nam, *Nano Energy* **2021**, *89*, 106444.
[503] S. G. Kirtania, A. W. Elger, M. R. Hasan, A. Wisniewska, K. Sekhar, T. Karacolak, P. K. Sekhar, *Micromachines* **2020**, *11*, 847.
[504] M. A. S. M. AL-Haddad, N. Jamel, A. N. Nordin, *J. Phys. Conf. Ser.* **2021**, *1878*, 012068.
[505] X. Pei, H. Zhang, Y. Zhou, L. Zhou, J. Fu, *Mater. Horiz.* **2020**, *7*, 1872.
[506] S. Choi, S. I. Han, D. Jung, H. J. Hwang, C. Lim, S. Bae, O. K. Park, C. M. Tschabrunn, M. Lee, S. Y. Bae, J. W. Yu, J. H. Ryu, S-.W. Lee, K. Park, P. M. Kang, W. B. Lee, R. Nezafat, T. Hyeon, D.-H. Kim, *Nat. Nanotechnol.* **2018**, *13*, 1048.
[507] Y. Cai, J. Qin, W. Li, A. Tyagi, Z. Liu, M. D. Hossain, H. Chen, J.-K. Kim, H. Liu, M. Zhuang, J. You, F. Xu, X. Lu, D. Sun, Z. Luo, *J. Mater. Chem. A* **2019**, *7*, 27099.
[508] S. Park, H. Yuk, R. Zhao, Y. S. Yim, E. W. Woldeghebriel, J. Kang, A. Canales, Y. Fink, G. B. Choi, X. Zhao, P. Anikeeva, *Nat. Commun.* **2021**, *12*, 3435.
[509] K. Kapat, Q. T. H. Shubhra, M. Zhou, S. Leeuwenburgh, *Adv. Funct. Mater.* **2020**, *30*, 1909045.
[510] S. Mishra, L. Unnikrishnan, S. K. Nayak, S. Mohanty, *Macromol. Mater. Eng.* **2019**, *304*,.
[511] K. Uchino, in *Advanced Piezoelectric Materials* (Ed: K. Uchino), Woodhead Publishing, **2010**, pp. 318–346.
[512] E. K. Akdogan, M. Allahverdi, A. Safari, *IEEE Trans. Ultrason. Ferroelectr. Freq. Control* **2005**, *52*, 746.
[513] J. Li, Y. Long, F. Yang, X. Wang, *Curr. Opin. Solid State Mater. Sci.* **2020**, *24*, 100806.
[514] T. Li, Z. Wei, F. Jin, Y. Yuan, W. Zheng, L. Qian, H. Wang, L. Hua, J. Ma, H. Zhang, H. Gu, M. G. Irwin, T. Wang, S. Wang, Z. Wang, Z.-Q. Feng, *Nat. Commun.* **2023**, *14*, 8386.
[515] G. D. Cha, D. Kang, J. Lee, D.-H. Kim, *Adv. Healthcare Mater.* **2019**, *8*, 1801660.
[516] M. Valko, K. Jomova, C. J. Rhodes, K. Kuča, K. Musílek, *Arch. Toxicol.* **2016**, *90*, 1.
[517] K. Jomova, M. Valko, *Toxicology* **2011**, *283*, 65.
[518] R. Li, L. Wang, D. Kong, L. Yin, *Bioact. Mater.* **2018**, *3*, 322.
[519] A. A. La Mattina, S. Mariani, G. Barillaro, *Adv. Sci. Weinh. Baden-Wurtt. Ger.* **2020**, *7*, 1902872.
[520] J. Koo, M. R. MacEwan, S.-K. Kang, S. M. Won, M. Stephen, P. Gamble, Z. Xie, Y. Yan, Y.-Y. Chen, J. Shin, N. Birenbaum, S. Chung, S. B. Kim, J. Khalifeh, D. V. Harburg, K. Bean, M. Paskett, J. Kim, Z. S. Zohny, S. M. Lee, R. Zhang, K. Luo, B. Ji, A. Banks, H. M. Lee, Y. Huang, W. Z. Ray, J. A. Rogers, *Nat. Med.* **2018**, *24*, 1830.
[521] D. Lu, T.-L. Liu, J.-K. Chang, D. Peng, Y. Zhang, J. Shin, T. Hang, W. Bai, Q. Yang, J. A. Rogers, *Adv. Mater.* **2019**, *31*, 1902739.
[522] D.-M. Lee, M. Kang, I. Hyun, B.-J. Park, H. J. Kim, S. H. Nam, H.-J. Yoon, H. Ryu, H.-M. Park, B.-O. Choi, S.-W. Kim, *Nat. Commun.* **2023**, *14*, 7315.
[523] L. Yin, H. Cheng, S. Mao, R. Haasch, Y. Liu, X. Xie, S.-W. Hwang, H. Jain, S.-K. Kang, Y. Su, R. Li, Y. Huang, J. A. Rogers, *Adv. Funct. Mater.* **2014**, *24*, 645.
[524] L. Wang, C. Lu, S. Yang, P. Sun, Y. Wang, Y. Guan, S. Liu, D. Cheng, H. Meng, Q. Wang, J. He, H. Hou, H. Li, W. Lu, Y. Zhao, J. Wang, Y. Zhu, Y. Li, D. Luo, T. Li, H. Chen, S. Wang, X. Sheng, W. Xiong, X. Wang, J. Peng, L. Yin, *Sci. Adv.* **2020**, *6*, eabc6686.
[525] J.-Y. Bae, E.-J. Gwak, G.-S. Hwang, H. W. Hwang, D.-J. Lee, J.-S. Lee, Y.-C. Joo, J.-Y. Sun, S. H. Jun, M.-R. Ok, J.-Y. Kim, S.-K. Kang, *Adv. Sci.* **2021**, *8*, 2004029.
[526] W. H. Lee, G. D. Cha, D.-H. Kim, *Curr. Opin. Biotechnol.* **2021**, *72*, 13.
[527] S. Li, D. Lu, S. Li, J. Liu, Y. Xu, Y. Yan, J. Z. Rodriguez, H. Bai, R. Avila, S. Kang, X. Ni, H. Luan, H. Guo, W. Bai, C. Wu, X. Zhou, Z. Hu, M.

© 2024 The Author(s). Advanced Materials Technologies published by Wiley-VCH GmbH

2365709x, 0, Downloaded from https://onlinelibrary.wiley.com/doi/10.1002/admt.202400797 by University Of Oxford, Wiley Online Library on [19/11/2024]. See the Terms and Conditions (https://onlinelibrary.wiley.com/terms-and-conditions) on Wiley Online Library for rules of use; OA articles are governed by the applicable Creative Commons License

A. Pet, C. W. Hammill, M. R. MacEwan, W. Z. Ray, Y. Huang, J. A. Rogers, *Sci. Adv.* **2024**, *10*, eadj0268.
[528] D.-H. Kim, J.-H. Ahn, W. M. Choi, H.-S. Kim, T.-H. Kim, J. Song, Y. Y. Huang, Z. Liu, C. Lu, J. A. Rogers, *Science* **2008**, *320*, 507.
[529] L. M. Jurkić, I. Cepanec, S. K. Pavelić, K. Pavelić, *Nutr. Metab.* **2013**, *10*, 2.
[530] J.-S. Shim, J. A. Rogers, S.-K. Kang, *Mater. Sci. Eng. R Rep.* **2021**, *145*, 100624.
[531] G. Pezzotti, E. Marin, T. Adachi, A. Rondinella, F. Boschetto, W. Zhu, N. Sugano, R. M. Bock, B. McEntire, S. B. Bal, *Sci. Rep.* **2017**, *7*, 44848.
[532] J. Shin, Y. Yan, W. Bai, Y. Xue, P. Gamble, L. Tian, I. Kandela, C. R. Haney, W. Spees, Y. Lee, M. Choi, J. Ko, H. Ryu, J.-K. Chang, M. Pezhouh, S.-K. Kang, S. M. Won, K. J. Yu, J. Zhao, Y. K. Lee, M. R. MacEwan, S.-K. Song, Y. Huang, W. Z. Ray, J. A. Rogers, *Nat. Biomed. Eng.* **2019**, *3*, 37.
[533] N. Lucas, C. Bienaime, C. Belloy, M. Queneudec, F. Silvestre, J.-E. Nava-Saucedo, *Chemosphere* **2008**, *73*, 429.
[534] A. Samir, F. H. Ashour, A. A. A. Hakim, M. Bassyouni, *Npj Mater. Degrad.* **2022**, *6*, 1.
[535] W. S. Pietrzak, D. Sarver, M. Verstynen, *Bone* **1996**, *19*, S109.
[536] Y. Li, W. Chen, L. Lu, *ACS Appl. Bio Mater.* **2021**, *4*, 122.
[537] K. Xu, S. Li, S. Dong, S. Zhang, G. Pan, G. Wang, L. Shi, W. Guo, C. Yu, J. Luo, *Adv. Healthcare Mater.* **2019**, *8*, e1801649.
[538] Y. S. Choi, J. Koo, Y. J. Lee, G. Lee, R. Avila, H. Ying, J. Reeder, L. Hambitzer, K. Im, J. Kim, K.-M. Lee, J. Cheng, Y. Huang, S.-K. Kang, J. A. Rogers, *Adv. Funct. Mater.* **2020**, *30*, 2000941.
[539] Y. S. Choi, Y.-Y. Hsueh, J. Koo, Q. Yang, R. Avila, B. Hu, Z. Xie, G. Lee, Z. Ning, C. Liu, Y. Xu, Y. J. Lee, W. Zhao, J. Fang, Y. Deng, S. M. Lee, A. Vázquez-Guardado, I. Stepien, Y. Yan, J. W. Song, C. Haney, Y. S. Oh, W. Liu, H.-J. Yoon, A. Banks, M. R. MacEwan, G. A. Ameer, W. Z. Ray, Y. Huang, T. Xie, et al., *Nat. Commun.* **2020**, *11*, 5990.
[540] H.-S. Kim, S. M. Yang, T.-M. Jang, N. Oh, H.-S. Kim, S.-W. Hwang, *Adv. Healthcare Mater.* **2018**, *7*, 1801071.
[541] S. Zhang, Z. Zhou, J. Zhong, Z. Shi, Y. Mao, T. H. Tao, *Adv. Sci.* **2020**, *7*, 1903802.
[542] S. M. Won, J. Koo, K. E. Crawford, A. D. Mickle, Y. Xue, S. Min, L. A. Mcilvried, Y. Yan, S. B. Kim, S. M. Lee, B. H. Kim, H. Jang, M. R. MacEwan, Y. Huang, R. W. Gereau IV, J. A. Rogers, *Adv. Funct. Mater.* **2018**, *28*, 1801819.
[543] M. Gao, Y. Yao, F. Yang, J. Ye, G. Liu, B. Wang, S. Liu, P. Wang, Y. Lu, *Device* **2023**, *1*, 100022.
[544] H. Kim, B. Rigo, G. Wong, Y. J. Lee, W.-H. Yeo, *Nano-Micro Lett.* **2023**, *16*, 52.
[545] K. J. Yu, D. Kuzum, S.-W. Hwang, B. H. Kim, H. Juul, N. H. Kim, S. M. Won, K. Chiang, M. Trumpis, A. G. Richardson, H. Cheng, H. Fang, M. Thompson, H. Bink, D. Talos, K. J. Seo, H. N. Lee, S.-K. Kang, J.-H. Kim, J. Y. Lee, Y. Huang, F. E. Jensen, M. A. Dichter, T. H. Lucas, J. Viventi, B. Litt, J. A. Rogers, *Nat. Mater.* **2016**, *15*, 782.
[546] K. Xie, S. Zhang, S. Dong, S. Li, C. Yu, K. Xu, W. Chen, W. guo, J. Luo, Z. Wu, *Sci. Rep.* **2017**, *7*, 7808.
[547] K. Keramatzadeh, A. Kiakojouri, M. S. Nahvi, Y. Khazaei, A. Feizi-nejad, M. H. Maghami, R. Mohammadi, M. Sharifshazileh, S. Nasiri, F. Akbari Boroumand, E. Nadimi, M. Rezaei, A. Shojaei, J. Mirnajafi-Zadeh, A. M. Sodagar, *Sci. Rep.* **2020**, *10*, 21261.
[548] J. Shin, Z. Liu, W. Bai, Y. Liu, Y. Yan, Y. Xue, I. Kandela, M. Pezhouh, M. R. MacEwan, Y. Huang, W. Z. Ray, W. Zhou, J. A. Rogers, *Sci. Adv.* **2019**, *5*, eaaw1899.
[549] G. L. Cerone, T. M. M. Vieira, A. Botter, M. Gazzoni, *Annu. Int. Conf. IEEE Eng. Med. Biol. Soc. IEEE Eng. Med. Biol. Soc. Annu. Int. Conf.* **2019**, *2019*, 3815.
[550] D. Andreu, B. Sijobert, M. Toussaint, C. Fattal, C. Azevedo-Coste, D. Guiraud, *Front. Neurosci.* **2020**, *14*, 117.
[551] L. Becerra-Fajardo, M. O. Krob, J. Minguillon, C. Rodrigues, C. Welsch, M. Tudela-Pi, A. Comerma, F. Oliveira Barroso, A. Schneider, A. Ivorra, *J. NeuroEngineering Rehabil.* **2022**, *19*, 57.
[552] J. S. Gewandter, E. Culakova, J. N. Davis, U. Gada, J. J. Guido, B. L. Burnette, J. D. Bearden, M. A. O'Rourke, K. M. Mustian, G. R. Morrow, K. A. Sluka, N. Mohile, *J. Clin. Oncol.* **2023**, *41*, e24134.
[553] M. Zhang, G. Yang, Z. Long, Y. Tang, D. Li, S. Liang, R. Lin, Z. Yang, H. Bao, L. Xing, X. Xue, Y. Zhan, Y. Xie, *Adv. Mater. Technol.* **2024**, *9*, 2301458.
[554] J. Kim, J. Jeon, J.-Y. Lee, B. Khoroldulam, S.-G. Choi, J.-Y. Bae, J. K. Hyun, S.-K. Kang, *Adv. Sci.* **2023**, *10*, 2302632.
[555] A. M. Rajnicek, N. Casañ-Pastor, *Biomater. Sci.* **2024**, 2180.
[556] J. K. Krauss, N. Lipsman, T. Aziz, A. Boutet, P. Brown, J. W. Chang, B. Davidson, W. M. Grill, M. I. Hariz, A. Horn, M. Schulder, A. Mammis, P. A. Tass, J. Volkmann, A. M. Lozano, *Nat. Rev. Neurol.* **2021**, *17*, 75.
[557] J. Li, Z. Che, X. Wan, F. Manshaii, J. Xu, J. Chen, *Biomaterials* **2024**, *304*, 122421.
[558] M. Sahin, V. Pikov, *Crit. Rev. Biomed. Eng.* **2011**, *39*, 63.
[559] M. Sahin, Y. Tie, *J. Neural Eng.* **2007**, *4*, 227.
[560] A. Wongsarnpigoon, W. M. Grill, *Conf. Proc. Annu. Int. Conf. IEEE Eng. Med. Biol. Soc. IEEE Eng. Med. Biol. Soc. Conf.* **2009**, *2009*, 634.
[561] S. Yun, C. S. Koh, J. Jeong, J. Seo, S.-H. Ahn, G. J. Choi, S. Shim, J. Shin, H. H. Jung, J. W. Chang, S. J. Kim, *Electronics* **2019**, *8*, 706.
[562] A. Burton, Z. Wang, D. Song, S. Tran, J. Hanna, D. Ahmad, J. Bakall, D. Clausen, J. Anderson, R. Peralta, K. Sandepudi, A. Benedetto, E. Yang, D. Basrai, L. E. Miller, M. C. Tresch, P. Gutruf, *Nat. Commun.* **2023**, *14*, 7887.
[563] M. Alpaugh, M. Saint-Pierre, M. Dubois, B. Aubé, D. Arsenault, J. Kriz, A. Cicchetti, F. Cicchetti, *Sci. Rep.* **2019**, *9*, 6444.
[564] D. Arsenault, J. Drouin-Ouellet, M. Saint-Pierre, P. Petrou, M. Dubois, J. Kriz, R. A. Barker, A. Cicchetti, F. Cicchetti, *J. Physiol.* **2015**, *593*, 2257.
[565] U. Topalovic, S. Barclay, C. Ling, A. Alzuhair, W. Yu, V. Hokhikyan, H. Chandrakumar, D. Rozgic, W. Jiang, S. Basir-Kazeruni, S. L. Maoz, C. S. Inman, M. Stangl, J. Gill, A. Bari, A. Fallah, D. Eliashiv, N. Pouratin, I. Fried, N. Suthana, D. Markovic, *Nat. Neurosci.* **2023**, *26*, 517.
[566] Y. Jiang, A. A. Trotsyuk, S. Niu, D. Henn, K. Chen, C.-C. Shih, M. R. Larson, A. M. Mermin-Bunnell, S. Mittal, J.-C. Lai, A. Saberi, E. Beard, S. Jing, D. Zhong, S. R. Steele, K. Sun, T. Jain, E. Zhao, C. R. Neimeth, W. G. Viana, J. Tang, D. Sivaraj, J. Padmanabhan, M. Rodrigues, D. P. Perrault, A. Chattopadhyay, Z. N. Maan, M. C. Leeolou, C. A. Bonham, S. H. Kwon, et al., *Nat. Biotechnol.* **2023**, *41*, 652.
[567] K. Yokoi, Y. Yasuda, A. Kanbe, T. Imura, S. Aoki, *Molecules* **2023**, *28*, 1433.
[568] A. Bansal, F. Yang, T. Xi, Y. Zhang, J. S. Ho, *Proc. Natl. Acad. Sci. USA* **2018**, *115*, 1469.
[569] K. Kim, I. S. Min, T. H. Kim, D. H. Kim, S. Hwang, K. Kang, K. Kim, S. Park, J. Lee, Y. U. Cho, J. W. Lee, W.-H. Yeo, Y. M. Song, Y. Jung, K. J. Yu, *Npj Flex. Electron.* **2023**, *7*, 1.
[570] W. S. Kim, M. I. Khot, H.-M. Woo, S. Hong, D.-H. Baek, T. Maisey, B. Daniels, P. L. Coletta, B.-J. Yoon, D. G. Jayne, S. I. Park, *Nat. Commun.* **2022**, *13*, 2178.
[571] M. Mariello, I. Eş, C. M. Proctor, *Adv. Healthcare Mater. n/a*, 2302969.
[572] J. Zhang, J. Xu, J. Lim, J. K. Nolan, H. Lee, C. H. Lee, *Adv. Healthcare Mater.* **2021**, *10*, e2100194.
[573] H. Lee, C. Song, Y. S. Hong, M. Kim, H. R. Cho, T. Kang, K. Shin, S. H. Choi, T. Hyeon, D.-H. Kim, *Sci. Adv.* **2017**, *3*, e1601314.

© 2024 The Author(s). Advanced Materials Technologies published by Wiley-VCH GmbH

2365709x, 0, Downloaded from https://onlinelibrary.wiley.com/doi/10.1002/admt.202400797 by University Of Oxford, Wiley Online Library on [19/11/2024]. See the Terms and Conditions (https://onlinelibrary.wiley.com/terms-and-conditions) on Wiley Online Library for rules of use; OA articles are governed by the applicable Creative Commons License

[574] H. Joo, Y. Lee, J. Kim, J.-S. Yoo, S. Yoo, S. Kim, A. K. Arya, S. Kim, S. H. Choi, N. Lu, H. S. Lee, S. Kim, S.-T. Lee, D.-H. Kim, *Sci. Adv.* **2021**, *7*, eabd4639.
[575] D. Wu, F. Fei, Q. Zhang, X. Wang, Y. Gong, X. Chen, Y. Zheng, B. Tan, C. Xu, H. Xie, W. Fang, Z. Chen, Y. Wang, *Sci. Adv.* **2022**, *8*, eabm3381.
[576] J. Liu, Z. Liu, X. Li, L. Zhu, G. Xu, Z. Chen, C. Cheng, Y. Lu, Q. Liu, *Biomed. Microdevices* **2020**, *22*, 53.
[577] P. J. van der Schaar, J. F. Dijksman, H. Broekhuizen-de Gast, J. Shimizu, N. van Lelyveld, H. Zou, V. Iordanov, C. Wanke, P. D. Siersema, *Gastrointest. Endosc.* **2013**, *78*, 520.
[578] V. Iacovacci, I. Tamadon, E. F. Kauffmann, S. Pane, V. Simoni, L. Marziale, M. Aragona, L. Cobuccio, M. Chiarugi, P. Dario, S. Del Prato, L. Ricotti, F. Vistoli, A. Menciassi, *Sci. Robot.* **2021**, *6*, eabh3328.
[579] T. Lin, P. Zou, R. Lin, H. Guan, Z. Fang, J. Chen, Z. Long, Y. Zhang, L. Xing, F. Qi, J. Lang, X. Xue, M. Chen, *Nano Energy* **2023**, *116*, 108826.
[580] I. Rosenthal, J. Z. Sostaric, P. Riesz, *Ultrason. Sonochem.* **2004**, *11*, 349.
[581] Y. Tufail, A. Yoshihiro, S. Pati, M. M. Li, W. J. Tyler, *Nat. Protoc.* **2011**, *6*, 1453.
[582] Y.-H. Hsiao, S.-J. Kuo, H.-D. Tsai, M.-C. Chou, G.-P. Yeh, *J. Cancer* **2016**, *7*, 225.
[583] Y.-F. Zhou, *World J. Clin. Oncol.* **2011**, *2*, 8.
[584] W. Legon, T. F. Sato, A. Opitz, J. Mueller, A. Barbour, A. Williams, W. J. Tyler, *Nat. Neurosci.* **2014**, *17*, 322.
[585] Y. Tufail, A. Matyushov, N. Baldwin, M. L. Tauchmann, J. Georges, A. Yoshihiro, S. I. H. Tillery, W. J. Tyler, *Neuron* **2010**, *66*, 681.
[586] E. Kim, J. Kum, S. H. Lee, H. Kim, *Front. Neurosci.* **2022**, *16*,.
[587] B. de Lucas, L. M. Pérez, A. Bernal, B. G. Gálvez, *PLoS One* **2021**, *16*, e0246261.
[588] A. Harrison, S. Lin, N. Pounder, Y. Mikuni-Takagaki, *Ultrasonics* **2016**, *70*, 45.
[589] H. Qin, Z. Luo, Y. Sun, Z. He, B. Qi, Y. Chen, J. Wang, C. Li, W. Lin, Z. Han, Y. Zhu, *Int. J. Biol. Sci.* **2023**, *19*, 1123.
[590] L. Jiang, Y. Yang, R. Chen, G. Lu, R. Li, J. Xing, K. K. Shung, M. S. Humayun, J. Zhu, Y. Chen, Q. Zhou, *Adv. Funct. Mater.* **2019**, *29*, 1902522.
[591] H. Hu, H. Huang, M. Li, X. Gao, L. Yin, R. Qi, R. S. Wu, X. Chen, Y. Ma, K. Shi, C. Li, T. M. Maus, B. Huang, C. Lu, M. Lin, S. Zhou, Z. Lou, Y. Gu, Y. Chen, Y. Lei, X. Wang, R. Wang, W. Yue, X. Yang, Y. Bian, J. Mu, G. Park, S. Xiang, S. Cai, P. W. Corey, et al., *Nature* **2023**, *613*, 667.
[592] C. M. Boutry, L. Beker, Y. Kaizawa, C. Vassos, H. Tran, A. C. Hinckley, R. Pfattner, S. Niu, J. Li, J. Claverie, Z. Wang, J. Chang, P. M. Fox, Z. Bao, *Nat. Biomed. Eng.* **2019**, *3*, 47.
[593] B. Rigo, A. Bateman, J. Lee, H. Kim, Y. Lee, L. Romero, Y. C. Jang, R. Herbert, W.-H. Yeo, *Biosens. Bioelectron.* **2023**, *241*, 115650.
[594] Q. Yang, T. Wei, R. T. Yin, M. Wu, Y. Xu, J. Koo, Y. S. Choi, Z. Xie, S. W. Chen, I. Kandela, S. Yao, Y. Deng, R. Avila, T.-L. Liu, W. Bai, Y. Yang, M. Han, Q. Zhang, C. R. Haney, K. Benjamin Lee, K. Aras, T. Wang, M.-H. Seo, H. Luan, S. M. Lee, A. Brikha, N. Ghoreishi-Haack, L. Tran, I. Stepien, F. Aird, et al., *Nat. Mater.* **2021**, *20*, 1559.
[595] P. Brusini, M. L. Salvetat, M. Zeppieri, *J. Clin. Med.* **2021**, *10*, 3860.
[596] J. O. Lee, H. Park, J. Du, A. Balakrishna, O. Chen, D. Sretavan, H. Choo, *Microsyst. Nanoeng.* **2017**, *3*, 1.
[597] J. Zhang, K. Kim, H. J. Kim, D. Meyer, W. Park, S. A. Lee, Y. Dai, B. Kim, H. Moon, J. V. Shah, K. E. Harris, B. Collar, K. Liu, P. Irazoqui, H. Lee, S. A. Park, P. S. Kollbaum, B. W. Boudouris, C. H. Lee, *Nat. Commun.* **2022**, *13*, 5518.
[598] I. E. Araci, B. Su, S. R. Quake, Y. Mandel, *Nat. Med.* **2014**, *20*, 1074.
[599] T. Y. Kim, J. W. Mok, S. H. Hong, S. H. Jeong, H. Choi, S. Shin, C.-K. Joo, S. K. Hahn, *Nat. Commun.* **2022**, *13*, 6801.
[600] A. K. Locke, A. K. Means, P. Dong, T. J. Nichols, G. L. Coté, M. A. Grunlan, *ACS Appl. Bio Mater.* **2018**, *1*, 1319.
[601] W. Bai, J. Shin, R. Fu, I. Kandela, D. Lu, X. Ni, Y. Park, Z. Liu, T. Hang, D. Wu, Y. Liu, C. R. Haney, I. Stepien, Q. Yang, J. Zhao, K. R. Nandoliya, H. Zhang, X. Sheng, L. Yin, K. MacRenaris, A. Brikha, F. Aird, M. Pezhouh, J. Hornick, W. Zhou, J. A. Rogers, *Nat. Biomed. Eng.* **2019**, *3*, 644.
[602] V. Kalidasan, X. Yang, Z. Xiong, R. R. Li, H. Yao, H. Godaba, S. Obuobi, P. Singh, X. Guan, X. Tian, S. A. Kurt, Z. Li, D. Mukherjee, R. Rajarethinam, C. S. Chong, J.-W. Wang, P. L. R. Ee, W. Loke, B. C. K. Tee, J. Ouyang, C. J. Charles, J. S. Ho, *Nat. Biomed. Eng.* **2021**, *5*, 1217.
[603] J. N. Wong, J. R. Walter, E. C. Conrad, D. R. Seshadri, J. Y. Lee, H. Gonzalez, W. Reuther, S. J. Hong, N. Pini, L. Marsillio, K. Moskalyk, M. Vicenteno, E. Padilla, O. Gann, H. U. Chung, D. Ryu, C. du Plessis, H. J. Odendaal, W. P. Fifer, J. Y. Wu, S. Xu, *PLOS Digit. Health* **2023**, *2*, e0000291.
[604] Point-of-Care EEG | Ceribell, https://ceribell.com/product/point-of-care-eeg.
[605] *EPILOG*, https://www.epilog.care/.
[606] M. A. Frankel, M. J. Lehmkuhle, M. C. Spitz, B. J. Newman, S. V. Richards, A. M. Arain, *Front. Neurol.* **2021**, *12*, 728484.
[607] I. Epitel, Assessment of Remote EEG Monitoring (REMI-EEG) in Pediatric Emergency and Adult Critical Care Units, **2024**, https://clinicaltrials.gov/study/NCT05818930.
[608] X. Cai, H. Zhang, P. Wei, Q. Liu, D. Sheng, Z. Li, B. Zhang, G. Tang, W. Zhao, Z. Ye, Z. Xue, Y. Xie, Y. Dai, C. Wang, Y. Wang, X. Fu, L. Yin, H. Peng, H. Ding, G. Zhao, X. Sheng, *Nat. Photonics* **2024**, *18*, 492.
[609] T. Vuorinen, K. Noponen, A. Vehkaoja, T. Onnia, E. Laakso, S. Leppänen, K. Mansikkamäki, T. Seppänen, M. Mäntysalo, *Adv. Mater. Technol.* **2019**, *4*, 1900246.
[610] A. Kiourti, Z. Wang, C. Lee, H. Scwerdt, J. Chae, J. L. Volakis, in *The 8th European Conference on Antennas and Propagation (EuCAP 2014)* **2014**, pp. 3452–3453, https://doi.org/10.1109/EuCAP.2014.6902571.
[611] A. Bagheri, S. R. I. Gabran, M. T. Salam, J. L. Perez Velazquez, R. R. Mansour, M. M. A. Salama, R. Genov, in *2012 IEEE Biomedical Circuits and Systems Conference (BioCAS)* **2012**, pp. 184–187, https://doi.org/10.1109/BioCAS.2012.6418466.
[612] B. N. Jensen, Y. Wang, A. Le Friec, S. Nabavi, M. Dong, D. Seliktar, M. Chen, *Npj Flex. Electron.* **2023**, *7*, 1.
[613] A. Burton, S. M. Won, A. K. Sohrabi, T. Stuart, A. Amirhossein, J. U. Kim, Y. Park, A. Gabros, J. A. Rogers, F. Vitale, A. G. Richardson, P. Gutruf, *Microsyst. Nanoeng.* **2021**, *7*, 1.
[614] M. M. Samani, A. Mahnam, N. Hosseini, *J. Med. Signals Sens.* **2014**, *4*, 94.
[615] M. Capogrosso, T. Milekovic, D. Borton, F. Wagner, E. M. Moraud, J.-B. Mignardot, N. Buse, J. Gandar, Q. Barraud, D. Xing, E. Rey, S. Duis, Y. Jianzhong, W. K. D. Ko, Q. Li, P. Detemple, T. Denison, S. Micera, E. Bezard, J. Bloch, G. Courtine, *Nature* **2016**, *539*, 284.
[616] H. Lorach, A. Galvez, V. Spagnolo, F. Martel, S. Karakas, N. Intering, M. Vat, O. Faivre, C. Harte, S. Komi, J. Ravier, T. Collin, L. Coquoz, I. Sakr, E. Baaklini, S. D. Hernandez-Charpak, G. Dumont, R. Buschman, N. Buse, T. Denison, I. van Nes, L. Asboth, A. Watrin, L. Struber, F. Sauter-Starace, L. Langar, V. Auboiroux, S. Carda, S. Chabardes, T. Aksenova, et al., *Nature* **2023**, *618*, 126.
[617] Q. Xu, D. Hu, B. Duan, J. He, *IEEE Trans. Neural Syst. Rehabil. Eng. Publ. IEEE Eng. Med. Biol. Soc.* **2015**, *23*, 683.
[618] H. Guan, P. Zou, R. Lin, L. Xiao, Z. Fang, J. Chen, T. Lin, Y. Wang, Y. Peng, T. Zhong, B. Zhang, J. Lang, Y. Zhang, L. Xing, M. Chen, X. Xue, *Nano Energy* **2023**, *105*, 108002.
[619] S.-H. Jeong, M.-G. Lee, C.-C. Kim, J. Park, Y. Baek, B. I. Park, J. Doh, J.-Y. Sun, *Mater. Horiz.* **2023**, *10*, 2215.

© 2024 The Author(s). Advanced Materials Technologies published by Wiley-VCH GmbH

2365709x, 0, Downloaded from https://onlinelibrary.wiley.com/doi/10.1002/admt.202400797 by University Of Oxford, Wiley Online Library on [19/11/2024]. See the Terms and Conditions (https://onlinelibrary.wiley.com/terms-and-conditions) on Wiley Online Library for rules of use; OA articles are governed by the applicable Creative Commons License

[620] D. B. L. Teh, A. Bansal, C. Chai, T. B. Toh, R. A. J. Tucker, G. G. L. Gammad, Y. Yeo, Z. Lei, X. Zheng, F. Yang, J. S. Ho, N. Bolem, B. C. Wu, M. K. Gnanasammandhan, L. Hooi, G. S. Dawe, C. Libedinsky, W.-Y. Ong, B. Halliwell, E. K.-H. Chow, K.-L. Lim, Y. Zhang, B. K. Kennedy, *Adv. Mater.* **2020**, *32*, 2001459.
[621] *Plexon*. https://plexon.com/products/helios-wireless-optogenetic-system/.
[622] C. Kathe, F. Michoud, P. Schönle, A. Rowald, N. Brun, J. Ravier, I. Furfaro, V. Paggi, K. Kim, S. Soloukey, L. Asboth, T. H. Hutson, I. Jelescu, A. Philippides, N. Alwahab, J. Gandar, D. Huber, C. I. De Zeeuw, Q. Barraud, Q. Huang, S. P. Lacour, G. Courtine, *Nat. Biotechnol.* **2022**, *40*, 198.
[623] Y. Yang, M. Wu, A. Vázquez-Guardado, A. J. Wegener, J. G. Grajales-Reyes, Y. Deng, T. Wang, R. Avila, J. A. Moreno, S. Minkowicz, V. Dumrongprechachan, J. Lee, S. Zhang, A. A. Legaria, Y. Ma, S. Mehta, D. Franklin, L. Hartman, W. Bai, M. Han, H. Zhao, W. Lu, Y. Yu, X. Sheng, A. Banks, X. Yu, Z. R. Donaldson, R. W. Gereau, C. H. Good, Z. Xie, et al., *Nat. Neurosci.* **2021**, *24*, 1035.
[624] J. Park, K. Kim, Y. Kim, T. S. Kim, I. S. Min, B. Li, Y. U. Cho, C. Lee, J. Y. Lee, Y. Gao, K. Kang, D. H. Kim, W. J. Choi, H.-B. Shin, H. K. Kang, Y. M. Song, H. Cheng, I.-J. Cho, K. J. Yu, et al., *Sci. Adv.* **2023**, *9*, eadi8918.
[625] J. Ausra, M. Wu, X. Zhang, A. Vázquez-Guardado, P. Skelton, R. Peralta, R. Avila, T. Murickan, C. R. Haney, Y. Huang, J. A. Rogers, Y. Kozorovitskiy, P. Gutruf, *Proc. Natl. Acad. Sci* **2021**, *118*, e2025775118.
[626] G.-H. Lee, C. Jeon, J. W. Mok, S. Shin, S.-K. Kim, H. H. Han, S.-J. Kim, S. H. Hong, H. Kim, C.-K. Joo, J.-Y. Sim, S. K. Hahn, *Adv. Sci.* **2022**, *9*, 2103254.
[627] A. L. Carlson, J. L. Sherr, D. I. Shulman, S. K. Garg, R. Pop-Busui, B. W. Bode, D. R. Lilenquist, R. L. Brazg, K. B. Kaiserman, M. S. Kipnes, J. R. Thrasher, J. H. C. Reed, R. H. Slover, A. Philis-Tsimikas, M. Christiansen, B. Grosman, A. Roy, M. Vella, R. A. M. Jonkers, X. Chen, J. Shin, T. L. Cordero, S. W. Lee, A. S. Rhinehart, R. A. Vigersky, *Diabetes Technol. Ther.* **2022**, *24*, 178.
[628] *Medtronic Diabetes*, **2021**, https://www.medtronicdiabetes.com/products/inpen-smart-insulin-pen-system.
[629] E. Söderlind, B. Abrahamsson, F. Erlandsson, C. Wanke, V. Iordanov, C. von Corswant, *J. Controlled Release* **2015**, *217*, 300.
[630] S. C. Bain, *Eur. Endocrinol.* **2017**, *13*, 13.
[631] D. H. Keum, S.-K. Kim, J. Koo, G.-H. Lee, C. Jeon, J. W. Mok, B. H. Mun, K. J. Lee, E. Kamrani, C.-K. Joo, S. Shin, J.-Y. Sim, D. Myung, S. H. Yun, Z. Bao, S. K. Hahn, *Sci. Adv.* **2020**, *6*, eaba3252.
[632] G. Xu, Y. Lu, C. Cheng, X. Li, J. Xu, Z. Liu, J. Liu, G. Liu, Z. Shi, Z. Chen, F. Zhang, Y. Jia, D. Xu, W. Yuan, Z. Cui, S. S. Low, Q. Liu, *Adv. Funct. Mater.* **2021**, *31*, 2100852.
[633] Y. Zhang, F. Liu, Y. Zhang, J. Wang, D. D'Andrea, J. B. Walters, S. Li, H.-J. Yoon, M. Wu, S. Li, Z. Hu, T. Wang, J. Choi, K. Bailey, E. Dempsey, K. Zhao, A. Lantsova, Y. Bouricha, I. Huang, H. Guo, X. Ni, Y. Wu, G. Lee, F. Jiang, Y. Huang, C. K. Franz, J. A. Rogers, *Proc. Natl. Acad. Sci* **2023**, *120*, e2217734120.
[634] M. L. Wang, P. Yeon, C. F. Chamberlayne, M. Mofidfar, H. Xu, J. P. Annes, R. N. Zare, A. Arbabian, in *2021 IEEE Biomedical Circuits and Systems Conference (BioCAS)* **2021**, pp. 1–4, https://doi.org/10.1109/BioCAS49922.2021.9644991.
[635] X. Luo, Q. Yu, L. Yang, Y. W. Cui, *ACS Sens.* **2023**, *8*, 1710.
[636] X. Li, X. Huang, J. Mo, H. Wang, Q. Huang, C. Yang, T. Zhang, H.-J. Chen, T. Hang, F. Liu, L. Jiang, Q. Wu, H. Li, N. Hu, X. Xie, *Adv. Sci.* **2021**, *8*, 2100827.
[637] E. Kim, J. Sanchez-Casanova, E. Anguluan, H. Kim, J. G. Kim, *Annu. Int. Conf. IEEE Eng. Med. Biol. Soc. IEEE Eng. Med. Biol. Soc. Annu. Int. Conf.* **2019**, *2019*, 6282.
[638] E. Kim, E. Anguluan, J. Kum, J. Sanchez-Casanova, T. Y. Park, J. G. Kim, H. Kim, *IEEE Trans. Biomed. Eng.* **2021**, *68*, 2195.
[639] J.-É. S. Kenny, *J. Cardiothorac. Vasc. Anesth.* **2021**, *35*, 1509.
[640] M. Di Rienzo, G. Rizzo, Z. M. Işilay, P. Lombardi, *Sensors* **2020**, *20*, 680.
[641] Q. Zheng, H. Zhang, B. Shi, X. Xue, Z. Liu, Y. Jin, Y. Ma, Y. Zou, X. Wang, Z. An, W. Tang, W. Zhang, F. Yang, Y. Liu, X. Lang, Z. Xu, Z. Li, Z. L. Wang, *ACS Nano* **2016**, *10*, 6510.
[642] My Heart Monitor – Philips BioTel Heart, https://www.myheartmonitor.com/
[643] R. John, S. Vijayaraghavan, R. Pradeep, in *2019 International Conference on Communication and Electronics Systems (ICCES)* **2019**, pp. 750–756, https://doi.org/10.1109/ICCES45898.2019.9002563.
[644] S. Murali, N. Brugger, F. Rincon, M. Mashru, S. Cook, J.-J. Goy, *Front. Cardiovasc. Med.* **2020**, *7*,.
[645] H. Zhu, H. Yang, L. Zhan, Y. Chen, J. Wang, F. Xu, *ACS Sens.* **2022**, *7*, 3014.
[646] M. H. M. Kouhani, J. Wu, A. Tavakoli, A. J. Weber, W. Li, *Lab Chip* **2020**, *20*, 332.
[647] H. Yang, H. Zhu, H. Liu, Z. Mao, J. Luo, S. Zhu, Hu, S. Yuan, F. Xu, *Adv. Funct. Mater. n/a*, 2400722.
[648] A. Iqbal, P. R. Sura, M. Al-Hasan, I. B. Mabrouk, T. A. Denidni, *Sci. Rep.* **2022**, *12*, 13689.
[649] M. Haerinia, R. Shadid, *Signals* **2020**, *1*, 209.
[650] M. J. Karimi, A. Schmid, C. Dehollain, *IEEE Sens. J.* **2021**, *21*, 7145.
[651] B. D. Nelson, S. S. Karipott, Y. Wang, K. G. Ong, *Sensors* **2020**, *20*, 4604.
[652] K. Dehghan, O. Shoaei, S. Jafarabadi Ashtiani, *IEEE Trans. Circuits Syst. II Express Briefs* **2022**, *69*, 2692.
[653] H. Zhu, M. Tahir, X. Wu, S. Hu, *Energies* **2024**, *17*, 731.
[654] W. Liao, J. Shi, J. Wang, *IET Microw. Antennas Propag.* **2017**, *11*, 330.
[655] Y. M. Roshan, E. J. Park, *IET Power Electron* **2017**, *10*, 931.
[656] Z. Xu, E. Rodriguez-Villegas, *IEEE Trans. Biomed. Circuits Syst.* **2024**, *18*, 460.
[657] N. Dobrostomat, G. Turcan, M. Neag, in *2014 International Semiconductor Conference (CAS)* **2014**, pp. 259–262, https://doi.org/10.1109/SMICND.2014.6966453.
[658] S. Nguyen, C. Duong, R. Amirtharajah, in *2021 IEEE Wireless Power Transfer Conference (WPTC)* **2021**, pp. 1–4, https://doi.org/10.1109/WPTC51349.2021.9458174.
[659] S. Warren, B. Natarajan, in *Wearable Monitoring Systems* (Eds: A. Bonfiglio, D. De Rossi), Springer US, Boston, MA **2011**, pp. 51–80.
[660] P. J. Soh, G. A. E. Vandenbosch, M. Mercuri, D. M. M.-P. Schreurs, *IEEE Microw. Mag.* **2015**, *16*, 55.
[661] T. Liang, Y. J. Yuan, *IEEE Sens. J.* **2016**, *16*, 8186.
[662] V. Custodio, F. J. Herrera, G. López, J. I. Moreno, *Sensors* **2012**, *12*, 13907.
[663] M. Ghamari, H. Arora, R. S. Sherratt, W. Harwin, in *2015 International Conference on Computer, Communications, and Control Technology (I4CT)* **2015**, pp. 1–6, https://doi.org/10.1109/I4CT.2015.7219525.
[664] M. Yuan, R. Das, E. McGlynn, R. Ghannam, Q. H. Abbasi, H. Heidari, *IEEE Sens. J.* **2021**, *21*, 12484.
[665] M. Zada, I. A. Shah, A. Basir, H. Yoo, *IEEE Trans. Antennas Propag.* **2022**, *70*, 2990.
[666] J. Pandey, Y.-T. Liao, A. Lingley, B. Parviz, B. Otis, in *2009 IEEE Biomedical Circuits and Systems Conference* **2009**, pp. 125–128, https://doi.org/10.1109/BIOCAS.2009.5372069.
[667] T. Takamatsu, Y. Sijie, F. Shujie, L. Xiaohan, T. Miyake, *Adv. Funct. Mater.* **2020**, *30*, 1906225.
[668] T. Takamatsu, Y. Chen, T. Yoshimasu, M. Nishizawa, T. Miyake, *Adv. Mater. Technol.* **2019**, *4*, 1800671.

© 2024 The Author(s). Advanced Materials Technologies published by Wiley-VCH GmbH

2365709x, 0, Downloaded from https://onlinelibrary.wiley.com/doi/10.1002/admt.202400797 by University Of Oxford, Wiley Online Library on [19/11/2024]. See the Terms and Conditions (https://onlinelibrary.wiley.com/terms-and-conditions) on Wiley Online Library for rules of use; OA articles are governed by the applicable Creative Commons License

[669] M. Yuan, R. Das, R. Ghannam, Y. Wang, J. Reboud, R. Fromme, F. Moradi, H. Heidari, *Adv. Intell. Syst.* **2020**, *2*, 1900190.
[670] H. Yao, Y. Liao, A. R. Lingley, A. Afanasiev, I. Lähdesmäki, B. P. Otis, B. A. Parviz, *J. Micromechanics Microengineering* **2012**, *22*, 075007.
[671] C.-P. Chang, W.-W. Yen, P. C.-P. Chao, *Microsyst. Technol.* **2021**, *27*, 2303.
[672] J. Kim, H. Kim, D. Kim, H-.J. Park, K. Ban, S. Ahn, S-.M. Park, *Energies* **2020**, *13*, 905.
[673] X. Huang, Y. Liu, G. W. Kong, J. H. Seo, Y. Ma, K.-I. Jang, J. A. Fan, S. Mao, Q. Chen, D. Li, H. Liu, C. Wang, D. Patnaik, L. Tian, G. A. Salvatore, X. Feng, Z. Ma, Y. Huang, J. A. Rogers, *Microsyst. Nanoeng* **2016**, *2*, 1.
[674] S. R. Krishnan, C.-J. Su, Z. Xie, M. Patel, S. R. Madhvapathy, Y. Xu, J. Freudman, B. Ng, S. Y. Heo, H. Wang, T. R. Ray, J. Leshock, I. Stankiewicz, X. Feng, Y. Huang, P. Gutruf, J. A. Rogers, *Small* **2018**, *14*, 1803192.
[675] M. Shi, H. Wu, J. Zhang, M. Han, B. Meng, H. Zhang, *Nano Energy* **2017**, *32*, 479.
[676] Y.-G. Park, S. Lee, J.-U. Park, *Sensors* **2019**, *19*, 4353.
[677] S. Amendola, C. Occhiuzzi, C. Miozzi, S. Nappi, F. Amato, F. Camera, G. Marrocco, in *Wearable Sensors*, 2nd ed. (Ed: E. Sazonov), Academic Press, Oxford **2021**, pp. 133–161.
[678] E. Kar, P. Ghosh, S. Pratihar, M. Tavakoli, S. Sen, *ACS Appl. Mater. Interfaces* **2023**, *15*, 20372.
[679] S. Kim, S. Park, J. Choi, W. Hwang, S. Kim, I.-S. Choi, H. Yi, R. Kwak, *Nat. Commun.* **2022**, *13*, 6705.
[680] G.-S. Byun, *Electronics* **2022**, *11*, 4197.
[681] A. Abid, J. M. O'Brien, T. Bensel, C. Cleveland, L. Booth, B. R. Smith, R. Langer, G. Traverso, *Sci. Rep.* **2017**, *7*, 46745.
[682] A. Iqbal, M. Al-Hasan, I. B. Mabrouk, T. A. Denidni, *IEEE Trans. Antennas Propag.* **2022**, *70*, 9819.
[683] Y. Meng, G. Yan, P. Jiang, K. Zhao, W. Wang, F. Chen, H. Zhuang, *Sens. Actuators Phys.* **2021**, *321*, 112413.
[684] A. Kiourti, K. A. Psathas, K. S. Nikita, *Bioelectromagnetics* **2014**, *35*, 1.
[685] A. Kiourti, R. M. Shubair, in *2017 IEEE International Symposium on Antennas and Propagation & USNC/URSI National Radio Science Meeting* **2017**, pp. 1677–1678, https://doi.org/10.1109/APUSNCURSINRSM.2017.8072881.
[686] A. Kiourti, K. S. A. Nikita, *IEEE Trans. Biomed. Eng.* **2017**, *64*, 1422.
[687] L. Lu, G. Yan, K. Zhao, F. Xu, *IEEE Sens. J.* **2015**, *15*, 3524.
[688] A. Javan-Khoshkholgh, A. Farajidavar, *IEEE J. Electromagn. RF Microw. Med. Biol.* **2022**, *6*, 3.



Massimo Mariello holds a B.Sc. in industrial engineering (2015), and an M.Sc. (2017) and a Ph..D (2021) in materials engineering and nanotechnology at the Università del Salento and at the Center for Biomolecular Nanotechnologies (CBN), Istituto Italiano di Tecnologia (IIT). He worked on flexible piezo-triboelectric nanogenerators for biosensing and energy harvesting. In 2021 he joined the école Polytechnique Fédérale de Lausanne (EPFL) as postdoctoral scientist, working on implantable neuroprostheses and thin-film encapsulations. His research involves microfabricated devices, soft (bio)materials, translational medicine. He joined the University of Oxford (IBME) in June 2023 as senior Postdoctoral Research Associate to develop electronically-controlled drug-delivery bioelectronics.



Christopher Proctor is an associate professor in Bioelectronics and BBSRC David Phillips Fellow at Oxford University. Chris received a B.Sc. in interdisciplinary physics from the University of Michigan. Following 2 years as a general scientist at the U.S. Nuclear Regulatory Commission, he earned a Ph.D. in materials from UCSB where he investigated organic photovoltaics. Subsequently, Chris was a Whitaker International postdoc fellow and developed implantable bioelectronics for treating neurological disorders at the Ecole des Mines de St-Etienne. He then joined the University of Cambridge as Borysiewicz Biomedical Sciences Fellow, and group leader in 2020 before moving to Oxford in 2022.

© 2024 The Author(s). Advanced Materials Technologies published by Wiley-VCH GmbH

2365709x, 0, Downloaded from https://onlinelibrary.wiley.com/doi/10.1002/admt.202400797 by University Of Oxford, Wiley Online Library on [19/11/2024]. See the Terms and Conditions (https://onlinelibrary.wiley.com/terms-and-conditions) on Wiley Online Library for rules of use; OA articles are governed by the applicable Creative Commons License